

**EFFECTS OF CALCITRIOL ON THE CROSSTALK BETWEEN  
MACROPHAGES AND HUMAN ADIPOCYTES**

Thesis submitted in accordance with the requirements of the University of  
Liverpool for the degree of Master of Philosophy

by

Cherlyn Ding

October 2011

## ABSTRACT

Macrophage-infiltration of adipocytes in obesity provides an important mechanistic link that may explain the increase in inflammatory mediators produced by adipose tissue. Elucidating the crosstalk mechanisms between macrophages and adipocytes is important as adipose tissue has been shown to be the linchpin linking inflammation and insulin resistance. Growing evidence suggests that vitamin D exerts immunomodulatory effects and adipose tissue could be a target for its action. This study investigated the role of vitamin D<sub>3</sub> (calcitriol) in alleviating inflammation mediators expressed and released by human adipocytes under the basal and stimulated conditions. The study also examined the effect of calcitriol on monocyte migration as well as on the NF-κB and MAPK signalling pathways.

A simulated model of adipocyte inflammation was created by incubating adipocytes with macrophage-conditioned (MC) medium, and this model was then used to study the effect of vitamin D. High dose calcitriol (10<sup>-8</sup>M) decreased the basal levels of MCP-1 and IL-6 released by adipocytes. Pretreatment with calcitriol (10<sup>-8</sup>M) reduced the rise in protein levels of MCP-1 and IL-6 released by adipocytes after stimulation with MC medium. Calcitriol (10<sup>-8</sup>M) also decreased IL-6 release but it had no effect on MCP-1 production by adipocytes stimulated with TNF-α. Upon MC medium stimulation, calcitriol (10<sup>-8</sup>M) partially reversed the decrease in gene expression of adiponectin and ZAG although the release of adiponectin or ZAG by adipocytes was unaffected. In addition, calcitriol (10<sup>-11</sup>M and 10<sup>-8</sup>M) supplementation decreased THP-1 macrophage migration although it did not reverse the effects of MC medium or TNF-α. Furthermore, calcitriol increased the basal protein abundance of NF-κB IκBα and reversed the inhibitory effect of MC medium on IκBα. Calcitriol supplementation also decreased both basal and MC medium stimulated protein abundance of phosphorylated NF-κB p65 as well as basal and MC medium stimulated levels of phosphorylated p38 MAPK.

In conclusion, this study has shown that MC medium potently stimulated inflammatory responses in human adipocytes. Calcitriol supplementation was able to reduce the basal and stimulated production of the proinflammatory mediators by adipocytes. Calcitriol also led to a decrease in chemoattractant ability of adipocytes. In addition, calcitriol exhibited an inhibitory effect on the activation of the NF-κB and MAPK signalling pathways. These results suggest that calcitriol may have a beneficial effect in protecting against adipose tissue inflammation induced by the crosstalk between macrophages and adipocytes.

## **ACKNOWLEDGEMENTS**

I would like to express my gratitude towards my supervisors Dr Chen Bing and Dr Frank McArdle for the opportunity to research under their guidance.

I thank my mentor Dr Dan Gao for providing technical and moral support which were most helpful during the course of my research.

I would also like to thank the staff associated with the Department of Obesity and Endocrinology in the Institute of Aging and Chronic Diseases, University of Liverpool for valuable advice and technical assistance.

Last but not least, I thank my parents, family and loved ones for their unwavering love and support.

## TABLE OF CONTENTS

<b>LIST OF TABLES</b> .....	<i>iv</i>
<b>LIST OF FIGURES</b> .....	<i>v</i>
<b>ABBREVIATIONS</b> .....	<i>vii</i>
<b>CHAPTER 1 INTRODUCTION</b> .....	<b>1</b>
<b>1.1 THE ADIPOSE ORGAN</b> .....	<b>2</b>
1.1.1 ADIPOSE TISSUE ANATOMY.....	2
1.1.2 ADIPOSE TISSUE FUNCTION.....	9
1.1.3 ADIPOSE TISSUE ALTERATION IN OBESITY.....	13
1.1.4 ADIPOKINES IN INFLAMMATION.....	15
1.1.5 DYSREGULATION OF ADIPOKINES IN OBESITY.....	17
1.1.6 THE ADIPOCYTE AS A MODEL SYSTEM.....	21
<b>1.2 THE VITAMIN D SYSTEM</b> .....	<b>24</b>
1.2.1 CALCITRIOL, VDR AND THE FUNCTION OF VDR IN SIGNALLING AND TRANSCRIPTION.....	25
1.2.2 IMMUNOMODULATING EFFECTS OF VITAMIN D OR VDR ACTIVATION.....	29
1.2.3 VITAMIN D AND OBESITY.....	30
<b>1.3 AIMS OF THE STUDY</b> .....	<b>32</b>
<b>CHAPTER 2 MATERIALS AND METHODS</b> .....	<b>34</b>
<b>2.1 REAGENTS AND EQUIPMENT</b> .....	<b>35</b>
<b>2.2 CELL CULTURE</b> .....	<b>41</b>
2.2.1 THP-1 MONOCYTES CULTURE AND PREPARATION OF MACROPHAGE- CONDITIONED MEDIUM.....	41
2.2.2 CULTURE AND DIFFERENTIATION OF HUMAN PREADIPOCYTES.....	43
<b>2.3 CELL CULTURE TREATMENT</b> .....	<b>46</b>
2.3.1 MACROPHAGE-INDUCED INFLAMMATION IN ADIPOCYTES.....	46
2.3.2 EFFECTS OF VITAMIN D ON MACROPHAGE-INDUCED INFLAMMATORY RESPONSE IN ADIPOCYTES.....	47
2.3.3 EFFECT OF VITAMIN D ON TNF- $\alpha$ INDUCED INFLAMMATORY RESPONSE IN ADIPOCYTES.....	47
<b>2.4 CELL AND MEDIA COLLECTION</b> .....	<b>48</b>
2.4.1 CELL CULTURE MEDIUM COLLECTION.....	48
2.4.2 TRIZOL® COLLECTION FOR TOTAL RNA ANALYSIS.....	49
2.4.3 CELL LYSATE COLLECTION.....	50
<b>2.5 TOTAL RNA ISOLATION</b> .....	<b>52</b>
2.5.1 PRINCIPLES.....	52
2.5.3 METHOD.....	54
2.5.4 RNA QUANTIFICATION.....	55
<b>2.6 REVERSE-TRANSCRIPTION POLYMERASE CHAIN REACTION</b> .....	<b>56</b>
2.6.1 FIRST-STRAND CDNA SYNTHESIS.....	56
<b>2.7 REAL-TIME POLYMERASE CHAIN REACTION (RT-QPCR)</b> .....	<b>59</b>
2.7.1 TAQMAN SYSTEM PRINCIPLES.....	59
2.7.2 SYBR GREEN PRINCIPLES.....	60



2.7.3	PREPARATION OF 96 WELL PLATES FOR REAL-TIME PCR.....	63
2.7.4	ANALYSIS OF REAL-TIME PCR DATA.....	66
2.7.5	PRIMER AND PROBE SEQUENCES.....	67
<b>2.8</b>	<b>ENZYME-LINKED IMMUNOSORBENT ASSAY (ELISA).....</b>	<b>69</b>
2.8.1	ELISA PRINCIPLES.....	69
2.8.2	METHOD.....	72
<b>2.9</b>	<b>PROTEIN DETECTION USING WESTERN BLOTTING.....</b>	<b>77</b>
2.9.1	WESTERN BLOTTING PRINCIPLES.....	77
2.9.2	PROTEIN QUANTIFICATION BY THE BICINCHONINIC ACID METHOD.....	78
2.9.4	SODIUM DODECYL SULPHATE POLYACRYLAMIDE GEL ELECTROPHORESIS (SDS-PAGE).....	81
2.9.5	ELECTROBLOTTING.....	84
2.9.6	IMMUNOLOGICAL DETECTION OF PROTEINS.....	85
2.9.7	RELATIVE QUANTITATION OF PROTEINS.....	87
<b>2.10</b>	<b>CYTOTOXICITY TESTS.....</b>	<b>88</b>
2.10.1	LDH ASSAY.....	88
<b>2.11</b>	<b>TRANSMIGRATION ASSAY.....</b>	<b>89</b>
2.11.1	PRINCIPLES.....	89
2.11.2	METHOD.....	90
<b>2.12</b>	<b>STATISTICAL ANALYSIS.....</b>	<b>91</b>
<b>CHAPTER 3</b>	<b><i>MACROPHAGE-INDUCED INFLAMMATORY RESPONSE IN HUMAN PRIMARY ADIPOCYTES.....</i></b>	<b>92</b>
<b>3.1</b>	<b>INTRODUCTION.....</b>	<b>93</b>
<b>3.2</b>	<b>CHANGES IN PROINFLAMMATORY MEDIATOR PRODUCTION BY HUMAN PRIMARY ADIPOCYTES STIMULATED BY MACROPHAGE-SECRETED FACTORS.....</b>	<b>95</b>
3.2.1	GENE EXPRESSION AND SECRETION OF MCP-1, IL-6 AND IL-1 $\beta$ BY ADIPOCYTES STIMULATED WITH MACROPHAGE-CONDITIONED MEDIUM OR TNF- $\alpha$ .....	95
3.2.2	PROTEIN SECRETION OF MCP-1 AND IL-6 BY ADIPOCYTES STIMULATED WITH MACROPHAGE-CONDITIONED MEDIUM OR TNF- $\alpha$ .....	98
<b>3.3</b>	<b>EFFECTS OF MACROPHAGE-SECRETED FACTORS ON ADIPOKINE PRODUCTION BY HUMAN PRIMARY ADIPOCYTES.....</b>	<b>100</b>
3.3.1	GENE EXPRESSION OF ADIPONECTIN AND ZAG.....	100
3.3.3	ADIPONECTIN AND ZAG PRODUCTION BY ADIPOCYTES STIMULATED WITH 25% MC MEDIUM OR TNF- $\alpha$ .....	103
<b>3.4</b>	<b>ACTIVATION OF NF-<math>\kappa</math>B AND MAPK SIGNALLING PATHWAYS IN ADIPOCYTES BY MACROPHAGE-CONDITIONED MEDIUM.....</b>	<b>105</b>
3.4.1	PROTEIN ABUNDANCE OF I $\kappa$ B $\alpha$ IS DECREASED AND PHOSPHORYLATED NF- $\kappa$ B P65 INCREASED IN ADIPOCYTES TREATED WITH 25% MC MEDIUM.....	105
3.4.2	MC MEDIUM INCREASES PROTEIN ABUNDANCE OF PHOSPHORYLATED P38 MAPK IN ADIPOCYTES.....	106
<b>CHAPTER 4</b>	<b><i>THE EFFECTS OF CALCITRIOL SUPPLEMENTATION ON INFLAMMATORY RESPONSE IN HUMAN PRIMARY ADIPOCYTES... 110</i></b>	
<b>4.1</b>	<b>INTRODUCTION.....</b>	<b>111</b>
<b>4.2</b>	<b>THE EFFECTS OF CALCITRIOL ON THE PRODUCTION OF PROINFLAMMATORY MEDIATORS BY ADIPOCYTES.....</b>	<b>111</b>

4.2.1	CALCITRIOL HAS NO EFFECT ON BASAL EXPRESSION OF GENES RELATED TO INFLAMMATION.....	111
4.2.2	CALCITRIOL DECREASES BASAL PRODUCTION OF MCP-1 AND IL-6 BY ADIPOCYTES.....	112
4.2.3	EFFECT OF CALCITRIOL ON GENE EXPRESSION OF PROINFLAMMATORY MEDIATORS IN ADIPOCYTES WITH PROINFLAMMATORY STIMULATION.....	115
<b>4.3</b>	<b>THE EFFECTS OF CALCITRIOL ON THE PRODUCTION OF THE ADIPOKINES, ADIPONECTIN AND ZAG, BY HUMAN ADIPOCYTES.....</b>	<b>120</b>
4.3.1	CALCITRIOL INCREASES BASAL ADIPONECTIN AND ZAG TRANSCRIPTION IN ADIPOCYTES WITH MC MEDIUM STIMULATION.....	120
4.3.2	EFFECTS OF CALCITRIOL ON BASAL ADIPONECTIN AND ZAG PRODUCTION BY ADIPOCYTES.....	120
4.3.3	EFFECTS OF CALCITRIOL ON GENE EXPRESSION OF ADIPONECTIN AND ZAG IN ADIPOCYTES STIMULATED WITH MC MEDIUM.....	121
4.3.4	EFFECTS OF CALCITRIOL ON ADIPONECTIN AND ZAG RELEASE BY ADIPOCYTES STIMULATED WITH MC MEDIUM.....	121
<b>4.4</b>	<b>THE EFFECTS OF CALCITRIOL ON THE INTRACELLULAR SIGNALLING INVOLVED IN INFLAMMATORY RESPONSE IN HUMAN ADIPOCYTES.....</b>	<b>127</b>
4.4.1	CALCITRIOL SUPPLEMENTATION REVERSES THE EFFECTS OF MC MEDIUM ON I $\kappa$ B $\alpha$ , PHOSPHORYLATED NF- $\kappa$ B P65 AND PHOSPHORYLATED P38 MAPK IN ADIPOCYTES.....	127
<b>4.6</b>	<b>THE EFFECTS OF CALCITRIOL ON MONOCYTE MIGRATION.....</b>	<b>132</b>
4.6.1	CALCITRIOL SUPPLEMENTATION DECREASES THP-1 MONOCYTE MIGRATION..	132
4.6.2	EFFECTS OF CALCITRIOL SUPPLEMENTATION ON THP-1 CELL MIGRATION BY ADIPOCYTES STIMULATED WITH MC MEDIUM.....	132
4.6.3	CALCITRIOL SUPPLEMENTATION DOES NOT DECREASE THP-1 MONOCYTE MIGRATION BY ADIPOCYTES STIMULATED WITH TNF- $\alpha$ .....	133
<b>4.7</b>	<b>THE EFFECTS OF CALCITRIOL ON GENE EXPRESSION OF VDR IN HUMAN ADIPOCYTES.....</b>	<b>137</b>
4.7.1	CALCITRIOL ENHANCES VDR GENE TRANSCRIPTION.....	137
<b>4.8</b>	<b>CYTOTOXICITY ASSESSMENT.....</b>	<b>140</b>
<b>CHAPTER 5</b>	<b>DISCUSSION AND CONCLUSION.....</b>	<b>142</b>
<b>5.1</b>	<b>INTRODUCTION.....</b>	<b>143</b>
<b>5.2</b>	<b>MACROPHAGE-PRODUCED FACTORS INDUCE INFLAMMATORY RESPONSES IN HUMAN ADIPOCYTES.....</b>	<b>144</b>
<b>5.3</b>	<b>CALCITRIOL PROMOTES ANTI-INFLAMMATORY ACTIVITY IN ADIPOCYTES.....</b>	<b>148</b>
<b>5.4</b>	<b>LIMITATIONS OF THE STUDY AND FUTURE WORK.....</b>	<b>152</b>
<b>5.5</b>	<b>CONCLUSION.....</b>	<b>158</b>
	<b>REFERENCES.....</b>	<b>160</b>

## LIST OF TABLES

TABLE 2.1 CHEMICAL REAGENTS .....	35
TABLE 2.2 COMMERCIAL KITS .....	37
TABLE 2.3 EQUIPMENT.....	37
TABLE 2.4 SOFTWARE .....	38
TABLE 2.5 SUPPLIERS' ADDRESSES AND URLS .....	39
TABLE 2.6 PRIMER AND PROBE SEQUENCES OF HUMAN TARGET GENES .....	68
TABLE 2.7 ANTIBODY AND STANDARD CONCENTRATIONS USED FOR ELISA.....	75
TABLE 2.8 ANTIBODY DILUTIONS AND CONDITIONS USED FOR WESTERN BLOTS.....	87

## LIST OF FIGURES

FIGURE 1.1 WHITE ADIPOCYTE AND BROWN ADIPOCYTE .....	8
FIGURE 2.1 ISOLATION OF RNA FROM TRIZOL® EXTRACTS .....	53
FIGURE 2.2 FIRST-STRAND cDNA SYNTHESIS .....	58
FIGURE 2.3 AMPLIFICATION PLOT .....	62
FIGURE 2.4 SCHEMATIC DIAGRAM OF ELISA .....	71
FIGURE 2.5 STANDARD CURVE GENERATION FOR BICINCHONINIC ACID METHOD .....	80
FIGURE 3.1 GENE EXPRESSION OF MCP-1, IL-6 AND IL-1 $\beta$ IN ADIPOCYTES STIMULATED WITH 25% MC MEDIUM OR TNF- $\alpha$ .....	97
FIGURE 3.2 MCP-1 AND IL-6 RELEASE BY ADIPOCYTES STIMULATED WITH 25% MC MEDIUM ...	99
FIGURE 3.3 RELATIVE EXPRESSION OF ADIPONECTIN AND ZAG mRNA IN ADIPOCYTES STIMULATED WITH 25% MC OR TNF- $\alpha$ .....	102
FIGURE 3.4 ADIPONECTIN AND ZAG PRODUCTION BY HUMAN PRIMARY ADIPOCYTES .....	104
FIGURE 3.5 I $\kappa$ B $\alpha$ PROTEIN EXPRESSION IN HUMAN PRIMARY ADIPOCYTES STIMULATED WITH 25% MC MEDIUM.....	107
FIGURE 3.6 PHOSPHORYLATED NF- $\kappa$ B p65 PROTEIN EXPRESSION IN HUMAN PRIMARY ADIPOCYTES STIMULATED WITH 25% MC MEDIUM.....	108
FIGURE 3.7 PHOSPHORYLATED p38 MAPK PROTEIN EXPRESSION IN HUMAN PRIMARY ADIPOCYTES STIMULATED WITH 25% MC MEDIUM.....	109
FIGURE 4.1 GENE EXPRESSION OF PROINFLAMMATORY MEDIATORS IN ADIPOCYTES PRETREATED WITH CALCITRIOL.....	113
FIGURE 4.2 MCP-1 AND IL-6 PRODUCTION BY ADIPOCYTES PRETREATED WITH CALCITRIOL....	114
FIGURE 4.3 GENE EXPRESSION OF MCP-1, IL-6 AND IL-1 $\beta$ IN CALCITRIOL-SUPPLEMENTED ADIPOCYTES STIMULATED WITH 25% MC MEDIUM.....	117
FIGURE 4.4 MCP-1 AND IL-6 CONCENTRATION IN MEDIUM OF CALCITRIOL-SUPPLEMENTED ADIPOCYTES STIMULATED WITH 25% MC MEDIUM AND TNF- $\alpha$ .....	119
FIGURE 4.5 GENE EXPRESSION OF ADIPONECTIN AND ZAG IN ADIPOCYTES TREATED WITH CALCITRIOL .....	123
FIGURE 4.6 ADIPONECTIN AND ZAG PRODUCTION BY ADIPOCYTES TREATED WITH CALCITRIOL .....	124
FIGURE 4.7 GENE EXPRESSION OF ADIPONECTIN AND ZAG IN CALCITRIOL SUPPLEMENTED ADIPOCYTES STIMULATED WITH 25% MC MEDIUM.....	125
FIGURE 4.8 ADIPONECTIN AND ZAG RELEASE FROM CALCITRIOL-SUPPLEMENTED ADIPOCYTES STIMULATED WITH 25% MC MEDIUM.....	126
FIGURE 4.9 I $\kappa$ B $\alpha$ PROTEIN EXPRESSION IN HUMAN ADIPOCYTES SUPPLEMENTED WITH CALCITRIOL .....	129
FIGURE 4.10 PHOSPHORYLATED NF- $\kappa$ B p65 PROTEIN EXPRESSION IN HUMAN ADIPOCYTES SUPPLEMENTED WITH CALCITRIOL .....	130
FIGURE 4.11 PHOSPHORYLATED p38 MAPK PROTEIN EXPRESSION IN HUMAN ADIPOCYTES SUPPLEMENTED WITH CALCITRIOL .....	131
FIGURE 4.12 THP-1 MONOCYTE TRANSMIGRATION BY THE MEDIUM OF CALCITRIOL-SUPPLEMENTED ADIPOCYTES.....	134
FIGURE 4.13 THP-1 MONOCYTE TRANSMIGRATION BY THE MEDIUM OF ADIPOCYTES STIMULATED WITH MC MEDIUM .....	135
FIGURE 4.14 THP-1 MONOCYTE TRANSMIGRATION BY THE MEDIUM OF ADIPOCYTES STIMULATED WITH TNF- $\alpha$ .....	136
FIGURE 4.15 VDR GENE EXPRESSION IN MC MEDIUM AND TNF- $\alpha$ STIMULATED ADIPOCYTES ..	139
FIGURE 4.16 LDH RELEASE FROM HUMAN ADIPOCYTES .....	141

FIGURE 5.1 GLUT-4 MRNA EXPRESSION IN CALCITRIOL-SUPPLEMENTED ADIPOCYTES.....	155
FIGURE 5.2 GLUT-4 PROTEIN PRODUCTION IN CALCITRIOL-SUPPLEMENTED ADIPOCYTES.....	156
FIGURE 5.3 IR $\beta$ EXPRESSION IN HUMAN PRIMARY ADIPOCYTES SUPPLEMENTED WITH CALCITRIOL INCUBATED WITH 25% MC MEDIUM.....	157

## ABBREVIATIONS

<b>1,25 MARRS</b>	Vitamin D Membrane-associated rapid response steroid hormone binding protein
<b>AF-1</b>	Activation function 1
<b>AF-2</b>	Activation function 2
<b>ANOVA</b>	Analysis of variance between groups
<b>ATGL</b>	Adipose triglyceride lipase
<b>ATP</b>	Adenosine-5'-triphosphate
<b>BAT</b>	Brown adipose tissue
<b>BSA</b>	Bovine serum albumin
<b>CD</b>	Cluster of differentiation
<b>cDNA</b>	Complementary deoxyribonucleic acid
<b>COX-2</b>	Cyclooxygenase-2
<b>CRP</b>	C-reactive protein
<b>CYP27B1</b>	Cytochrome P450, subfamily XXVIIB
<b>DBD</b>	DNA-binding domain
<b>DNA</b>	Deoxyribonucleic acid
<b>ECM</b>	Extracellular matrix
<b>ELISA</b>	Enzyme-linked immunosorbent assay
<b>ER</b>	Endoplasmic reticulum
<b>FAS</b>	Fatty acid synthase
<b>FFA</b>	Free fatty acid
<b>GLUT-1</b>	Glucose transporter 1

<b>GLUT-4</b>	Glucose transporter 4
<b>GPCR</b>	G-protein-coupled receptor
<b>HRP</b>	Horseradish peroxidase
<b>HSL</b>	Hormone sensitive lipase
<b>ICAM-1</b>	Intracellular adhesion molecule-1
<b>IFN-<math>\gamma</math></b>	Interferon-gamma
<b>IL-1<math>\beta</math></b>	Interleukin-1 beta
<b>IL-6</b>	Interleukin-6
<b>iNOS</b>	Inducible nitric oxide synthase
<b>IR<math>\beta</math></b>	Insulin receptor beta subunit
<b>IRS-1</b>	Insulin-receptor substrate 1
<b>IRS-2</b>	Insulin-receptor substrate 2
<b>I<math>\kappa</math>B<math>\alpha</math></b>	Nuclear factor of kappa light polypeptide gene enhancer in B-cells inhibitor, alpha
<b>JAK/STAT</b>	Janus Kinase / Signal Transducer and Activator of Transcription
<b>LBD</b>	Ligand-binding domain
<b>LDH</b>	Lactate dehydrogenase
<b>LH</b>	Luteinizing hormone
<b>LPL</b>	Lipoprotein lipase
<b>LPS</b>	Lipopolysaccharide
<b>MAC-1</b>	Macrophage-1 antigen
<b>MAPK</b>	Mitogen-activated protein kinase
<b>MC</b>	Macrophage-conditioned

<b>MCP-1</b>	Monocyte chemoattractant protein-1
<b>MMP</b>	Matrix metalloproteinases
<b>mRNA</b>	Messenger ribonucleic acid
<b>NF-<math>\kappa</math>B</b>	Nuclear Factor kappa-light-chain-enhancer of activated B cells
<b>OD</b>	Optical density
<b>PAI-1</b>	Plasminogen activator inhibitor-1
<b>PBS</b>	Phosphate buffered saline
<b>PCR</b>	Polymerase chain reaction
<b>PI3-K</b>	Phosphatidylinositol 3-kinase
<b>PKC</b>	Protein kinase C
<b>PPAR-<math>\gamma</math></b>	Proliferation-activated receptor-gamma
<b>ROS</b>	Reactive oxygen species
<b>RPMI-1640</b>	Roswell Park Memorial Institute-1640
<b>RT</b>	Reverse transcription
<b>RT-PCR</b>	Real time polymerase chain reaction
<b>RXR</b>	Retinoid X receptor
<b>SAA</b>	Serum amyloid A
<b>SD</b>	Standard deviation
<b>SOCS-3</b>	Suppressor of cytokine signalling-3
<b>Sp1</b>	Specificity Protein-1
<b>ssDNA</b>	Single-stranded deoxyribonucleic acid
<b>SVF</b>	Stromal vascular fraction
<b>TGF-<math>\beta</math></b>	Transforming growth factor beta



<b>THP-1</b>	Human acute monocytic leukaemia cell line
<b>TLR-4</b>	Toll-like receptor-4
<b>TNF-<math>\alpha</math></b>	Tumour necrosis factor-alpha
<b>TSH</b>	Thyroid stimulating hormone
<b>UCP-1</b>	Uncoupling protein-1
<b>UPR</b>	Unfolded protein response
<b>UV</b>	Ultraviolet
<b>VCAM-1</b>	Vascular cell adhesion protein 1
<b>VDR</b>	Vitamin D receptor
<b>VDRE</b>	Vitamin D response element
<b>VLDL</b>	Very low density lipoprotein
<b>WAT</b>	White adipose tissue
<b>ZAG</b>	Zinc-alpha-2-glycoprotein
<b><math>\beta</math>3AR</b>	$\beta$ 3 adrenergic receptor

# **Chapter 1**

## **Introduction**

## **1.1 The Adipose Organ**

### **1.1.1 Adipose tissue anatomy**

As defined by Cinti (2009), an organ is defined as an anatomically dissectible structure with a discrete gross anatomy comprising at least two different tissues. The adipose organ is made up of adipocytes suspended as white adipose tissue (WAT) and brown adipose tissue (BAT) in intermingled in a stromal vascular fraction (SVF) in a connective tissue matrix of collagen, vascular and nerve tissue. Although the gross anatomy of the human adipose organ has never been described in detail, it is understood to be composed of several subcutaneous, visceral and intermuscular depots. Much of our understanding is based on the morphological similarities between humans and rodents. The subcutaneous depot is in continuity with dermal adipose tissue, not confined to specific areas and presents as a continuous layer beneath the skin. Mammary and gluteo-femoral subcutaneous adipose tissue tends to be more developed in females compared to males (Cinti, 2006). Visceral depots in humans correspond to those in rodents, mainly locating at the thorax and abdomen cavities. Recent observations suggest that the omental depot is particularly well developed in humans compared to the relatively small omental depot in mice. Periepididymal adipose tissue, found in rodents, is not present in humans. Human adipose tissue exhibits greater complexity; variable amounts of adipocytes can be found in the parotid, parathyroid, bone marrow, pancreas, thymus, lymph nodes and other minor locations. The weight of the human adipose organ of lean adults is about 8–18% of the

body weight in males and 14–28% in females (Cinti, 2009). Adipose tissue turnover in humans is dynamic and approximated at 10% annually for all humans.

Classically, adipose tissue functions primarily as a fat depot for the body and stores energy in the form of triglycerides. As such, approximately 90% of the adipocyte is made up of triglycerides, with the remaining 10% consisting of cytoplasm, mitochondria, nucleus and other organelles (Björntorp and Ostman, 1971).

#### *1.1.1.1 White adipose tissue*

WAT is mainly found in the subcutaneous and visceral depots in humans, mice and rats and is known to function as a long-term fuel repository for the organism as a whole, with a considerable caloric value compared to carbohydrates (39.1 KJ/g to 15.4-17.5KJ/g). It is the main form of energy storage, comprising 20 to 25% of the body weight in humans because of its low water content (Trayhurn, 2007). From the evolutionary standpoint, water content associated with the storage of carbohydrates as an energy source is disadvantageous as it would render terrestrial mammals immobile - hence the preferential storage of lipids. The white adipocyte is typically white in appearance and are typically unilocular, with a single large lipid droplet comprising >90% of the cell's volume (Figure 1.1). It is present in WAT is found throughout the body, with the largest depots found in subcutaneously and surrounding the viscera. White adipocytes have a fairly variable size throughout the body which depends largely on the amount of lipid storage. Electron microscopic examination shows no distinct structure separating it from the thin rim of cytoplasm, although perilipin is generally known to exist at the periphery (Blanchette-

Mackie, 1995; Greenberg, 1991). WAT mitochondria are thin and elongated, with randomly oriented cristae. A distinct basal membrane surrounds the adipocyte and several caveolae can be found on the outer surface.

#### *1.1.1.2 Brown adipose tissue*

Brown adipose tissue is found integrated within WAT depots and functions as a heat producer through non-shivering thermogenesis. Physically it contrasts well with WAT, characterised by the brown adipocyte's brown colour and multilocular appearance. It is characterised by high tissue vascularisation in BAT contributing to its brown appearance. Brown adipocytes are mostly polygonal and possess variable diameters ranging from 15 to 50  $\mu\text{m}$  (Cinti, 2009). The subcutaneous interscapular brown adipose tissue depot has been well-studied in rodents. Activation is facilitated by postganglionic sympathetic nerves that unilaterally innervate the two interscapular brown adipose tissue lobes and forms a dense network of unmyelinated fibres which reaches virtually every cells by noradrenaline release through varicosities (De Matteis *et al.* 1998). This innervations is essential for the thermogenic ability of brown adipose tissue. Parasympathetic innervations in BAT is generally absent with the exception of pericardial and mediastinal BAT (Giordano *et al.* 2004; Schafer *et al.*, 1998).

In addition, BAT possess type II thyroxine-5'deiodinase that generates a high triiodothyronine concentration within the tissue. BAT also harbours abundant mitochondria, distinguished ultrastructurally by the discovery of densely packed cristae (Né Chad, 1986). The difference in cristae morphology within BAT mitochondria is

indicative of its high energy dissipation role as these characteristics are usually associated with energy demanding processes e.g. cardiac myocytes. Perhaps the most unique feature of BAT is its expression of Uncoupling protein-1 (UCP1), a 32-kDa protein embedded within the inner mitochondrial membrane. UCP-1 functions to uncouple mitochondrial respiration, giving BAT its ability to generate energy from the stored fatty acids independent of ADP availability. UCP1 can be found exclusively in brown adipocytes although there have been accounts of low-level UCP-1 expression in thymocytes (Carroll *et al.*, 2004). Upon exposure to cold temperatures, thermoceptors elicit subcutaneous thermal afferent signals which are then transmitted to the brain, resulting in non-shivering thermogenesis in BAT (Morrison, 2004). Neuronal studies on the thermal somatosensory reflex suggest that peripheral thermoceptors transmit cold sensation through afferent neuronal projections to the preoptic area (POA) in the rostral hypothalamus (Morrison *et al.* 2008). When thermoneutrality is reached, efferent inhibitory neurons originating from the POA to the dorsal medial hypothalamus and the brain stem tonically block sympathetic outflow to BAT (Nakamura and Morrison, 2008). Brown fat has been shown to counteract obesity and metabolic disease in studies (Lowell *et al.*, 1993). Specifically, rodent studies have shown that mice with higher amounts of brown fat gain less weight, have greater insulin-sensitivity and lower levels of serum free fatty acids (Kopecky *et al.*, 1995, 1996; Cederberg *et al.*, 2001).

#### *1.1.1.3 Brite cells*

In recent years, “brite” or “beige” cells have been identified, which are postulated to be the intermediates of white and brown adipocytes (Ishibashi and Seale, 2010). These cells

are derived from a different cell lineage than native BAT, but possess the ability to generate heat by mitochondrial uncoupling similar to BAT cells. Prolonged exposure to cold or  $\beta_3$ -adrenergic agonists in white adipose tissue can cause tissue transdifferentiation to beige *adipose* tissue (Seale *et al.*, 2009). Rodent studies have shown that white adipocytes in mice increase expression of the enzyme cyclooxygenase-2 (COX-2) in response to cold temperatures or  $\beta_3$ -adrenergic agonists, which consequently produces prostaglandins (Vegiopoulos *et al.*, 2010). Prostaglandins produced by white fat cells or from the circulation stimulate the formation of thermogenic beige cells in white fat. It is not clear if beige cells arise from unique precursor cells or by transdifferentiation of white fat cells (Vegiopoulos *et al.*, 2010). Overexpression of COX-2 induced ectopic beige fat development and showed a 20% reduction in body weight correlating with a severe reduction in body fat content. Oxygen consumption and body temperature has been shown to increase in transgenic mice overexpressing COX-2, reflecting a significant elevation of the resting metabolic rate. Plasma free fatty acid and glycerol levels were also lower in the transgenic mice (Vegiopoulos *et al.*, 2010). The current evidence suggests that beige fat development via the COX-2-prostaglandin pathway contributes positively to adaptive thermogenesis and energy homeostasis.

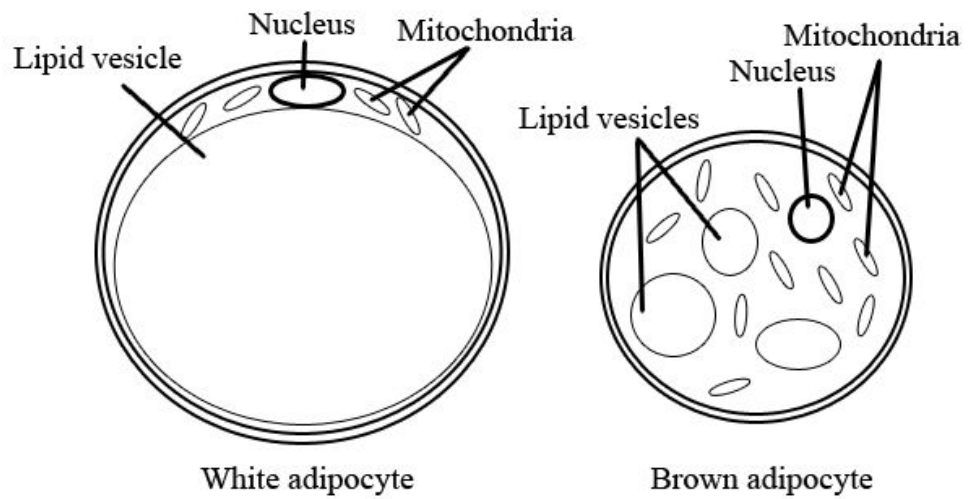
#### *1.1.1.4 Stromal vascular fraction*

Non-adipocyte cells make up the SVF in adipose tissue. It consists of its constituent cells, sympathetic nerves, connective tissue and extracellular matrix. Collagen, elastic fibres and resident fibroblasts maintain the integrity of the ECM, creating a define tissue mass

and the boundaries of individual adipose tissue depots. The stromal vascular fraction (SVF) is a dynamic site of activity because of its known cellular constituents, namely the mesenchymal stem cells (MSC), T regulatory cells, endothelial precursor cells, macrophages and preadipocytes (Riordan *et al.*, 2009). The SVF within various adipose tissue depots are known to harbour different proteomic profiles, establishing the distinction of characteristics between visceral adipose tissue and subcutaneous tissue and contributing to their differential metabolic properties. For example, Peinado *et al.* (2010) identified 24 genes differentially expressed in the SVF of VAT and ScAT. TBX15 (Gesta, 2011) was found to be higher in visceral SVF compared to subcutaneous SVF, while Krüppel-like factor 4 and CAV-1 has recently been discovered to be downregulated in obesity and in lower quantities in visceral tissue SVF (Liao *et al.*, 2011). Complement components C2, C3, C4, C7, and Factor B had higher expression in omental compared with subcutaneous adipose tissue.



**Figure 1.1 White adipocyte and brown adipocyte**



WAT cells are characterised by a single large lipid vacuole and while the brown fat cell is characterised by numerous smaller lipid vacuoles and the presence of numerous mitochondria. Unilocular cells usually range from 25-200 microns in diameter, while multilocular cells are about 60 microns in diameter.

### **1.1.2 Adipose tissue function**

Adipose tissue is classically understood to function as energy storage depots in the form of fatty acids, so as to ensure adequate energy availability in between meals. It is also known to function as cushioning and insulation for the body. Most of its classical functions depend largely on WAT which is found in greater abundance within the adipose organ. Both BAT and WAT are similar with regard to its highly specialised biochemical functions, which include lipogenesis and lipolysis (Lowell and Flier, 1997). In the formation of triglycerides within an adipocyte, lipids are presented to the cell in the form of chylomicrons and VLDL cholesterol. Lipoprotein Lipase (LPL) present within the adipocyte breaks down the triglyceride contents of chylomicrons and VLDL cholesterol for incorporation into the adipocyte (Large *et al.*, 2004). Hormone-sensitive lipase (HSL) triggers the breaking down the triglycerides within the adipocyte in response to hormonal signals such as corticotrophin, adrenaline, noradrenaline, TSH, Prolactin, LH and glucagon (Rodbell *et al.*, 1970). Beyond its role in physical protection and energy regulation and conservationism, adipose tissue has been known for its role in steroid conversion as well as a secretory source of various bioactive substances. Its resultant designation as an endocrine organ comes with the discovery of heterogeneity of adipose tissue which come together to serve its multitude of functions.

#### *1.1.2.1 Heterogeneity of adipose tissue*

Although the cells of the adipose organ share common characteristics, the protean nature of the adipose organ is due to its variability at its levels of organization. At the cellular

level, white and brown adipocytes have opposite functions attributable to their intracellular makeup, giving them the respective roles of storing and dissipating energy. This attribute partly gives it the ability to act as a buffer for the flux of fatty acids in the circulation during the postprandial period, and emulates the role of the liver and skeletal muscles in buffering postprandial glucose fluxes (Frayn, 2002). The cells of adipose tissue are also known for its plasticity. Adipocytes demonstrate a formidable ability to enlarge reversibly and transdifferentiate macroscopically between BAT and WAT during development (Cinti, 2009). Its physical changes are often coupled with functional changes e.g. greater leptin secretion and higher free fatty acid output in hypertrophy. This seems to play a part in acclimatization and adaptation to environmental changes e.g. temperature fluctuations, pregnancy/lactation, obesity, fasting, and calorie restrictions (Cinti, 2009). SVF preadipocytes also show multiple differentiation potentials including osteogenic, chondrogenic, myogenic and neurogenic lineages (Prunet-Marcassus *et al.*, 2006).

At the tissular level, the differences in locale and cellular morphology of adipose tissue cells determine the differences between adipose tissue function. Adipocyte size tends to be larger in subcutaneous depots compared to omental depots (Ostman *et al.* 1979; Rebuffe-Scrive *et al.*, 1989; Reynisdottir *et al.*, 1997). Lowered basal lipolysis, coupled with an increased sensitivity to insulinic anti-lipolytic activity is also more frequently associated with subcutaneous depots rather than visceral fat (Arner, 1995). These features seem to relate to their respective functions, whereby a greater surface area to volume ratio and a lesser metabolically active state in subcutaneous depots helps it to fulfil its

energy storage and lipid buffering capabilities. The richer vascularity and innervation of visceral adipose tissue and added portal drainage may be related to its function to provide direct hepatic access to FFAs and cortisolic functions in the liver. However, there is some evidence to suggest that adipocyte lipolysis may be more related to adipocyte size than regional origin (Edens *et al.*, 1993; Farnier *et al.*, 2003; Tchernof *et al.*, 2006).

Given the attributes highlighted so far in this chapter, it is quite plain to see that adipose tissue has a well-defined role in energy regulation, glucose homeostasis, lipid metabolism, sexual development and appetite control (Cousin *et al.* 1999). In recent years adipose tissue has been found to exhibit more characteristics playing important roles beyond its classical functions. In the spotlight is its potential impact on the immune system which has yet to be clearly elucidated. Adipose tissue is an important secretory source of adipokines, a diverse range of protein factors and signals (Trayhurn *et al.*, 2006). Adipokines are highly diverse in terms of protein structure and physiological function and it has been found that many are linked to the immune system. They include the classical proinflammatory cytokines (e.g. TNF- $\alpha$ , IL-6, IL-1 $\beta$ ), chemokines (macrophage chemoattractant protein-1, IL-8, macrophage migration inhibitory factor) and inflammation-related moieties (e.g. leptin, ZAG and adiponectin; Trayhurn *et al.*, 2006).

Just as its site-specific differences give rise to differential roles in lipid and glucose metabolism, this same heterogeneity has also been exhibited in inflammatory signalling. In particular, visceral adipose tissue mass correlates with the development of insulin

resistance. This has a lot to do with the greater metabolic activity in omental adipose tissue. The universally accepted opinion is that greater fatty acid contribution by metabolically active fat depots contributes to inflammation (Song *et al.*, 2006, Nyugen *et al.*, 2005, Tripathy *et al.* 2003). Adipose tissue has since been recognised as a major contributor to inflammatory status in physiology, as links between increased adiposity and inflammatory diseases continue to be identified. This provides a new impetus to study adipokine secretion in adipose tissue.

### **1.1.3 Adipose tissue alteration in obesity**

Obesity is defined as the increase in adiposity by the expansion of adipose tissue (Salans *et al.*, 1971). It usually results from a long-term positive energy balance and occurs when energy intake exceeds energy expenditure. An increase in adiposity is broadly characterised by adipocyte hypertrophy and hyperplasia. The increases in adipocyte number and size have important implications in defining the composition of its secretome, its metabolic activity and ultimately adipose tissue behaviour. For example, adipocyte hypertrophy is associated with a rise in fatty acid release, as well as the adipokine leptin, cytokines IL-6, TNF- $\alpha$  as well as growth factor TGF- $\beta$ . Other changes include the rarefaction of neural networks and vasculature in adipose tissue (Coppack, 2005). Perhaps the most defining histological change in obesity is the infiltration of adipose depots by mononuclear cells (Wellen and Hotamisligil, 2003; Weisberg *et al.*, 2003). In particular, macrophage infiltration of adipose tissue has been shown to have important implications in the development of disease states associated with obesity. It has been recognised to be the linchpin between obesity, inflammation and insulin resistance.

#### *1.1.3.1 Macrophage infiltration in obesity*

SVF cells have been known to be major contributors of inflammatory mediators such as TNF- $\alpha$  and IL-6 in adipose tissue (Zeyda *et al.* 2007). Not until recently were macrophages found to be the main contributors of inflammation in the SVF. Macrophages are found to associate in high numbers especially in omental tissue, contributing to a unifying hypothesis that explains the higher production of inflammatory

cytokines in visceral omental adipose tissue that leads to its observed predictability of comorbidities in obesity, including insulin resistance.

Macrophage localization in the adaptive immune response is meant to be a beneficial and essential process in physiology. Its classical role is to prevent or destroy pathogens and the toxic molecules produced. A novel role for macrophages is the preservation of metabolic homeostasis. Macrophage infiltration is dynamically altered in response to lipid flux in lean or obese individuals, indicating the macrophage's possible role in suppressing lipolytic signals (Kosteli *et al.*, 2010). In obesity, the type and intensity of macrophage infiltration has important implications in the manifestation of obesity comorbidities. Not only is macrophage infiltration increased, so is the tendency for a phenotypic switch of macrophages from the M2 to the M1 state (Fujisaka *et al.*, 2009). The M1 state is associated with the production of classical proinflammatory signals that generates Th1 responses and cell-mediated immunity (Zeyda and Stulnig, 2007). This leads to the production of TNF- $\alpha$ , IL-6 and IL-1 that contribute to inflammation-related comorbidities. In contrast, the M2 state that results in a Th2 response in the alternative activation state is pro-fibrotic and promotes the attenuation of the NF- $\kappa$ B signalling pathways in cells (Zeyda and Stulnig, 2007). It is associated more frequently with lean individuals and is known to offer protection against inflammation.

Macrophages have also been known to take on adipocyte-like qualities, expressing aP2 and PPAR $\gamma$  (Charriere *et al.*, 2003). Functionally, both macrophages and adipocytes have been shown to exhibit similar qualities too. Adipocytes have been observed to produce

inflammatory mediators and participate in the immune response, exhibiting phagocytic and anti-microbial activities in some conditions. Preadipocytes may even differentiate into macrophages given the right conditions. Macrophages, especially in pro-atherosclerotic conditions, may accumulate lipids to form foam cells (Wellen and Hotamisligil, 2005).

Other than being secretory entities, macrophages exert an effect on the surrounding adipose tissue, causing the adipocytes to respond in a glandular fashion, secreting proinflammatory adipokines and acute phase proteins such as TNF- $\alpha$ , IL-6, serum amyloid A (SAA), CRP, haptoglobin, MCP-1 and PAI-1 into the systemic circulation (Trayhurn and Wood, 2005). CRP is an activator of the complement system and has been implicated in ischaemic necrosis. As a result the expression of many complement genes have been shown to be upregulated in obesity. SAA can mediate the crosstalk between hypertrophied adipocytes and macrophages and PAI-1 directly accelerates the development of atherosclerosis (Poitou *et al.*, 2009; Loskutoff and Samad, 1998). MCP-1 has been known to increase the recruitment and activation of proinflammatory monocytes and macrophages (Kanda *et al.*, 2006).

#### **1.1.4 Adipokines in inflammation**

The subclinical inflammatory state associated with obesity is characterised by chronic low-level systemic inflammation in the circulation and in tissues. It is the central pathological state by which adipocyte regulatory processes contribute to the development of adipose-related comorbidities. The subclinical inflammatory state is characterised by



oxidative stress and the elevation of proinflammatory cytokines, such as TNF- $\alpha$ , IL-6, PAI-1 and MCP-1 (Fain, 2006). One school of thought attributes this to the increase in FFA turnover shown *in vitro* and *in vivo* to activate the canonical NF- $\kappa$ B pathway (Boden, 2011). Activation of NF- $\kappa$ B and the expression of MCP-1 in particular lead to a typical proinflammatory response meant as a protective response for the removal of injurious stimuli and cell-mediated immunity. Overstimulation of these inflammatory pathways, however, leads to a loss of healthy function in adipose tissue. The chronic low-grade inflammation associated with obesity has only been recognised fairly recently because adipose tissue inflammation seems to lack the classical cardinal signs of inflammation - *dolor, rubor, calor, tumor* and *functio laesa* (Rather, 1971). Adipose tissue is now a known source of TNF- $\alpha$  and IL-6, both mediators of the acute phase response (Xu *et al.*, 2003; Fantuzzi, 2005; Trayhurn and Wood, 2005). Increased levels of these mediators show molecular participation in the development of metabolic dysfunctions, by increasing adipocyte lipolysis and downregulating pro-insulinic responses in cells. The initiation of stress-dependent pathways by the influx of excess fatty acids and proteins leads to chronic conditions in ER stress and the activation of the unfolded-protein-response (UPR) cascade (Hotamisligil, 2010). ER stress reaches a point where it can no longer be relieved, UPR causes cell death and these ultimately link to the major inflammatory pathways and stress signaling networks such as *JNK-AP-1* and I $\kappa$ B-NF- $\kappa$ B pathways which also cause the production of reactive oxygen species. These events are highly related to the infiltration of T-cells preceding macrophages and may also be crucial to the activation and increased recruitment of macrophages.

### **1.1.5 Dysregulation of adipokines in obesity**

As it is already evident, the high level of coordination and overlapping biology that connects inflammatory and metabolic pathways, together with the now apparent co-localization of the two types of cells, suggests the imperative to shed light on the protein signals involved in crosstalk between adipocytes and macrophages. The next few sections endeavour to highlight some significant mediators of inflammation produced by adipose tissue.

#### *1.1.5.1 Adiponectin*

Adiponectin is a protein encoded by the *ADIPOQ* gene (Maeda *et al.*, 1996). It is produced almost exclusively by adipocytes. In contrast to the expression of other proinflammatory adipokines like TNF- $\alpha$  and IL-6, adiponectin expression is reduced in obese, insulin-resistant rodent models (Hu *et al.*, 1996). Thus increasing adiponectin levels has been postulated to play a beneficial role in suppressing obesity-linked diseases by positively modulating glucose metabolism, increasing insulin sensitivity and glucose uptake in cells (Fu *et al.* 2005). Adiponectin production is known to be upregulated with PPAR $\gamma$  activation and known to be inhibited by proinflammatory factors TNF- $\alpha$  and IL-6 (Berg *et al.*, 2005; Ouchi *et al.* 2003). Adiponectin-deficient mice were also shown to have higher levels of TNF- $\alpha$  mRNA in adipose tissue and TNF- $\alpha$  in the blood and administration of recombinant adiponectin showed a restoration of inflammatory parameters (Maeda *et al.*, 2002). Adiponectin also exerts other anti-inflammatory effects by acting on macrophages and monocytes to inhibit TNF- $\alpha$  and IL-6, as well as increase IL-10 and IL-1 receptor antagonist expression. It also shows ability to reduce the

induction of the endothelial adhesion molecules ICAM-1 and VCAM-1. Therefore, it seems that adiponectin have a protective ability against inflammation via suppression of pro-inflammatory cytokine production and may be a candidate gene in reversing metabolic dysfunction.

#### *1.1.5.2 IL-1 $\beta$*

Interleukin-1 beta (IL-1 $\beta$ ) is a cytokine protein that in humans is encoded by the *IL1B* gene. It is involved in acute-phase inflammatory response and like IL-6 it has been shown to modulate leptin secretion by adipose tissue in inflammation (Faggioni *et al.*, 1998). It has been found recently to modulate glucose metabolism in adipocytes, decreasing GLUT-1 and GLUT-4 translocation via the downregulation of IRS-1. IL-1 $\beta$  is therefore capable of impairing insulin signaling and action, acting in concert with other cytokines in the development of insulin resistance in adipocytes. IL-1 $\beta$  has been shown to upregulate the transcription of various inflammation-related genes in adipocytes (Permana *et al.*, 2006; Gao and Bing, 2011).

#### *1.1.5.3 IL-6*

Interleukin-6 (IL-6) is a protein that in humans is encoded by the *IL6* gene. IL-6 is closely related to TNF- $\alpha$  in its inflammatory effects and its serum levels have been reported to be elevated in obesity. It is produced mainly by the stromal-vascular fraction of adipose tissue. Although the production of IL-6 has been traditionally associated with cells of the immune system, recent studies showed that IL-6 from adipose tissue accounts for approximately 30% of circulating levels (Pedersen *et al.*, 2003). IL-6 levels correlate

positively with obesity and insulin resistance; high IL-6 levels are predictive of type 2 diabetes mellitus and has been shown to modulate insulin action *in vivo* and *in vitro* (Bastard *et al.*, 2002). It has been suggested that the apparent inhibition of insulin receptor signal transduction by IL-6 may be in part due to the increase in suppressor of cytokine signalling-3, increased FFA release from adipose tissue and reduced adiponectin secretion (Rotter *et al.*, 2003). Long-term exposure of human adipocytes to IL-6 has been also shown to induce a decrease in insulin-mediated glucose transport, reducing the expression of IRS-1, GLUT-4 and PPAR $\gamma$  (Rotter *et al.* 2003). An increase in IL-6 levels is also known to be responsible for the increase in hypertriglyceridaemia *in vivo* by inhibiting LPL and stimulating lipolysis (Nonogaki *et al.*, 1995; Trujillo *et al.*, 2004).

#### *1.1.5.4 Leptin*

Leptin is another key adipokine upregulated in obesity (Kettaneh *et al.*, 2007). Leptin is essentially thought to play a role in appetite control as a satiety signal in the central nervous system. Leptin has been known to be primarily proinflammatory, associating with platelet aggregation and arterial thrombosis. As such it has been known to be a good predictor of cardiovascular risk and metabolic syndrome. Recent studies also show that leptin inhibits the expression of IL-1 receptor antagonist (IL-1Ra), which exerts a protective effect on islets from glucose-mediated IL-1 secretion by beta cells. Leptin levels are also associated with the inhibition of insulin resistance through the SOC3 gene activation and suppression of proinsulin expression through MAPK activation (Seufert, 2004). While it is an essential hormone for the regulation of appetite and growth of adipocyte cells, an overproduction of leptin in obesity has been implicated in the cause of

oxidative stress in endothelial cells. This is explained by the accumulation of ROS and activation of JAK/STAT pathways by enhanced JNK activity and AP-1 DNA binding. Enhancement of NF- $\kappa$ B signalling by leptin also leads to the expression of MCP-1 in endothelial cells, increasing the recruitment of monocytes and macrophages to adipose tissue.

#### *1.1.5.5 Monocyte chemoattractant protein-1 (MCP-1)*

MCP-1 (CCL2) is a member of the CC chemokine family. Encoded by the CCL2 gene, the main function of MCP-1 is to initiate the diapedesis of monocytes, memory T cells, and dendritic cells to sites of injury and inflammation. The main producers of MCP-1 in adipose tissue are preadipocytes, adipocytes and resident mononuclear cells. Its expression is upregulated with obesity, making MCP-1 is a key candidate gene for the modulation of macrophage infiltration in obese adipose tissue. This has been supported by studies where MCP-1 and its receptor (CCR2) knockdown studies in animals presented a significant reduction of macrophages, decreased inflammatory mediators and greater insulin sensitivity (Kanda *et al.*, 2006; Weisberg *et al.*, 2006).

#### *1.1.5.6 TNF- $\alpha$*

TNF- $\alpha$  is a cytokine involved in systemic inflammation and the acute phase reaction. Expression of TNF- $\alpha$  in adipose tissue is elevated in a variety of experimental obesity models (Hotamisligil *et al.*, 1993; Hofmann *et al.*, 1994; Hamann *et al.*, 1995). Recent data have suggested a key role for TNF- $\alpha$  in the inflammatory pathogenesis of insulin resistance in obesity and non-insulin dependent diabetes mellitus by blocking the action

of insulin by inhibiting insulin receptor tyrosine kinase activity. TNF- $\alpha$  has been shown to induce SOCS-3 (suppressor of cytokine signalling-3), an intracellular signalling molecule that impairs leptin and also IRS-1 and IRS-2, PI3-K and insulin-stimulated glucose uptake. It also activates NF- $\kappa$ B, which forms the basis for its proatherogenic qualities. As majority of the TNF- $\alpha$  is produced by infiltrated macrophages, the increase in macrophage infiltration in obesity explicates the upregulation of serum TNF- $\alpha$  levels observed in obesity-linked inflammatory comorbidities.

#### *1.1.5.7 Zinc- $\alpha$ 2-glycoprotein (ZAG)*

Zinc- $\alpha$ 2-glycoprotein, a soluble protein of approximately 41 kDa, is also another known adipokine. Although the exact role of this novel adipokine has yet to be elucidated, ZAG appears to be increased in cancer cachexia (Bing *et al.*, 2004) and decreased in obesity. Zinc-alpha2-glycoprotein (ZAG) has been also found to play a role in adipose tissue lipolysis and has been proposed to be a candidate gene in body weight regulation (Gong *et al.*, 2009). Recent work by the department demonstrated that ZAG was able to increase adiponectin release by human adipocytes at physiologically relevant levels (Mracek *et al.*, 2010). The finding suggests a possible paracrine action of ZAG to stimulate adiponectin secretion in adipocytes, which is an anti-inflammatory adipokine known to exert beneficial effects on insulin sensitivity and inflammation.

### **1.1.6 The adipocyte as a model system**

It is understood that adipocytes and macrophages play essential roles in the formation of an inflammatory state by inter-potentiating each others' effects, often leading to excess

inflammation in obesity. Therefore it is essential that the web of interaction must be dissected to understand their individual roles so as to facilitate research into disease amelioration. Adipocyte response has been identified to be the focal point of this thesis as 1) They have physically important secretory functions 2) They are proactive in their nature, responding well to stimuli 3) The current belief that adipocytes cause the principle release of the initial errant signal (i.e. excessive production of leptin) in hypertrophy. Errant signalling of leptin is postulated to exert paracrine effects on the endothelial cells, including the accumulation of ROS, activation of JAK/STAT pathways and enhancement of NF- $\kappa$ B signalling, leading to enhanced recruitment of mononuclear cells which eventually ignites a proinflammatory cycle (Fantuzzi, 2005).

Adipocytes also have a unique secretory genotype with quiescent genes that once activated by a suitable environment, allows them to take on macrophage-like qualities. This is evidenced by the observed cellular plasticity of adipocyte precursors when injected into the peritoneal cavity; preadipocytes morphed into cells exhibiting high phagocyte activity and expressed five markers specific to macrophages: F4/80, Mac-1, CD80, CD86, and CD45 (Charrière *et al.*, 2003). As a result, adipocytes have been shown to exhibit macrophage-like qualities in obesity, producing increased levels of proinflammatory cytokines TNF- $\alpha$ , IL-6 and MMPs (matrix metalloproteinases). TNF- $\alpha$  and IL-6 have been shown to induce SOCS-3, an intracellular signalling molecule that impairs leptin and also IRS-1 (Insulin receptor substrate-1), IRS-2 (Insulin receptor substrate 2), PI3-K and insulin-stimulated glucose uptake (Cawthorn and Sethi, 2008).

It has also been suggested that adipocyte hypertrophy leads to increased macrophage recruitment to adipose tissue (Xu *et al.*, 2003). This increased presence of macrophages observed in the late stages of obesity has garnered great interest of late as macrophage infiltration may potentially establish the link between inflammation and obesity. A local paracrine inflammatory loop is induced by FFAs produced by hypertrophied adipocytes and macrophage-produced factors, particularly TNF- $\alpha$  (Suganami *et al.*, 2005). Studies have shown that FFAs produced by hypertrophied adipocytes bind toll-like receptor-4 (TLR-4) leading to the activation of NF- $\kappa$ B resulting in the increased production of TNF- $\alpha$  and subsequent proinflammatory cytokines such as IL-6, MCP-1, intracellular adhesion molecule-1 (ICAM-1) and iNOS (Suganami *et al.*, 2007; Yeop Han *et al.*, 2010). The release of these factors into the SVF and resultant release into the circulation may, as such, explain the chronic systemic inflammation associated with obesity.

An appropriate adipocyte model in an inflammatory environment would therefore be essential in understanding the crosstalk that occurs in obesity. The additional advantage of this model is the opportunity to study restorative agents. Agents such as adiponectin and siRNAs (Diez and Iglesias, 2003; Aouadi *et al.*, 2009) have been identified and studied in rodent models to mitigate the adverse effects of excessive inflammation associated with obesity. A potential agent that we aim to investigate in this study is vitamin D. The next chapter illustrates its emergence as an immune system modulator.



## 1.2 The Vitamin D System

Vitamin D deficiency has been extensively linked to an increased risk of developing insulin resistance and metabolic syndrome (Isaia *et al.*, 2001; Chiu *et al.*, 2004; Martini *et al.*, 2006). Hypovitaminosis D is re-emerging as a global health problem, coinciding with the doubling of official numbers of diabetic patients over the last three decades and the exponential increase in obese persons globally. The first official medical treatise on vitamin D deficiency came with the discovery of childhood rickets. Published by Francis Glisson in the 1650s, the disease was more commonly associated with the rich rather than poorer communities in society. Sniadecki was the first to recognise in 1822 that the development of rickets was due to a lack of sunlight exposure. By the mid-1800s cod liver oil was established as an effective remedy for rickets and it was later found that vitamin D was the agent in cod liver oil that gave it its anti-rachitic properties.

Today vitamin D has been shown to produce potential nonskeletal benefits in a variety of clinical outcomes, including mortality, diabetes mellitus, cardiovascular disease, cancer, multiple sclerosis, asthma, sepsis, depression and pain. History suggests that the re-emergence of vitamin D deficiency could be due to rising affluence, leading to increased sedentary lifestyles, lack of outdoor activity, ease of access to a convenience foods diet and obesity. Obesity, in particular, has been shown to be a single, independent risk factor for vitamin D deficiency (Snijder *et al.*, 2005). Decreased circulating levels of 25-hydroxyvitamin D<sub>3</sub>, a predictor of vitamin D status, have also been found to be a correlating predictor of obesity. It has been proposed that increased adiposity results in

the enhanced storage of vitamin D in adipocytes, leading to decreased circulating levels of vitamin D. The hormone leptin, whose circulating levels increase proportionately to adiposity, has also been shown to lower renal CYP27B1 gene expression, suggesting a decreased bioavailability of vitamin D in obesity (Matsunuma and Horiuchi, 2007). As such, clinicians have suggested that an increased supplementation of vitamin D is required for persons with a higher body fat percentage. Adiposity is an important determinant of assayed 25-hydroxyvitamin D levels and has been implicated as a cause for the prevailing association of low vitamin D status with obesity-linked disease outcomes, including metabolic syndrome and congestive heart failure. Multiple lines of evidence also now suggest that vitamin D also plays a role in glucose homeostasis in cells; among its modes of action are increasing transcription of the insulin receptor gene, activating PPAR- $\delta$  and enhancing insulin-mediated glucose transport *in vitro* (Maestro *et al.*, 2000, 2002; Dunlop *et al.*, 2005).

### **1.2.1 Calcitriol, VDR and the function of VDR in signalling and transcription**

Calcitriol is the active form of vitamin D<sub>3</sub> utilised by the body. Otherwise known as 1,25-dihydroxycholecalciferol or 1,25-dihydroxyvitamin D<sub>3</sub>, calcitriol is a seco-steroid in which the B-ring of the cyclopentanoperhydrophenanthrene structure is cleaved (Walters, 1992). It is formed through the conversion of 25-hydroxyvitamin D<sub>3</sub>, an inactive hormonal precursor of calcitriol, by the enzyme CYP27B1 or 1 $\alpha$ -hydroxylase which is found primarily in the kidney. Vitamin D<sub>3</sub> and its metabolites are primarily found in association with vitamin D-binding globulin, a 50-kDa protein found in the blood. The level of 25-hydroxyvitamin D in the body is determined by the intake of dietary vitamin

D or synthesis in the skin. Pre-vitamin D can be synthesised from 7-dehydrocholesterol by ultraviolet B radiation during exposure to the sun.  $1\alpha$ -hydroxylase activity is controlled by ionic and endocrine factors such as PTH and plasma calcium, and is inhibited by calcitriol through a negative feedback loop mechanism (Jones *et al.*, 1998). Interestingly, significant extrarenal sources  $1\alpha$ -hydroxylase suggest a possibility of higher local tissue concentrations of calcitriol and a possible autocrine/paracrine role of 1,25-dihydroxyvitamin D<sub>3</sub> (Jones *et al.*, 1998; Zehnder *et al.*, 2001).

The seco-steroid is the natural ligand for the vitamin D receptor (VDR), a ligand-activated nuclear transcription factor and a member of the steroid-thyroid-retinoid receptor gene superfamily (Mangelsdorf *et al.*, 1995). Receptors of the steroid-thyroid-retinoid receptor gene superfamily have a highly conserved DNA-binding domain (DBD) and a more variable Ligand-binding domain (LBD). The human VDR consists of 427 amino acids and has a molecular mass of about 48 kDa. Its main components consist of the A/B region, the DBD, the LBD and a transactivation AF-2 region (Issa *et al.*, 1998).

The A/B region of the VDR consists of a truncated domain lacking the usual AF-1 transactivation function of nuclear hormone receptors, suggesting that this domain has little or no function in the VDR. Studies have also shown that the removal of the region does not seem to affect DNA binding, ligand binding or its transactivation properties (Issa *et al.*, 1998).

The VDR DBD is located between amino acids 24 and 90. It contains nine highly conserved cysteine residues that enable the DBD to fold into two loops of 12-13 amino

acids each (Malloy *et al.*, 1999). Each loop contains 4 cysteine residues that enables the binding of a zinc atom, yielding a two “zinc-finger” structure. In the amino-terminal zinc finger loop, an  $\alpha$ -helical P-box makes contact with specific nucleotide bases in the major groove of the DNA-binding site. At the carboxyl-terminal zinc finger module, two  $\alpha$ -helices form the D and T-boxes. The D-box appears to participate in DNA binding, serving as a dimerization interface for interaction with a partner protein. The T-box has been shown to provide key interactions with partner proteins, making minor groove contacts with nucleotides located between two DNA half-sites, enhancing the interaction of the VDR with the DNA-binding elements and thus the heterodimerization with the Retinoid X receptor (RXR).

The D region that follows the DBD, also termed a hinge region, displays a site for serine phosphorylation which suggests additional functional roles of the hinge region - although this has not been clearly defined (Issa *et al.*, 1998). The hinge region has been known to facilitate nuclear transfer of the receptor. The LBD of VDR is multifunctional and serves three main purposes: binding of the calcitriol ligand, hetero- or homodimerization and recruitment of regulatory factors required for transcriptional activation (Issa *et al.*, 1998). The structural arrangement of the VDR LBD is complex and stretches over two-thirds of the protein. The VDR LBD is made up of 12  $\alpha$ -helices (H1 to H12) and 1  $\beta$ -sheet. Its three-dimensional structure suggests that conserved residues in a 34-amino acid cluster form a hydrophobic core by holding together a series of  $\alpha$ -helices and loops while another series of  $\alpha$ -helices and loops form a three-dimensional pocket as an occupation site for the ligand. The  $\alpha$ -helices H11 and H12 are thought to function together as a

'retractable lid' that serves to trap and hold the ligand in position. The 1 $\alpha$ -hydroxyl group forms a hydrogen bond with Ser237 and Arg274 found lining the LBD and the 3-OH moiety forms a hydrogen bond with Ser278 and Tyr143. The 25-hydroxyl group forms hydrogen bonds with His305 and His397.

Upon binding of the ligand, VDR undergoes a conformational change that facilitates its dimerization with RXR, as well as its binding to DNA and coactivators. The AF-2 domain, encompassing the H12 helix and the E1 region (between amino acids 232 and 272) are essential for transactivation (Malloy *et al.*, 1999). Once the nuclear VDR heterodimerises with the RXR it binds to vitamin D response elements (VDREs) in the promoter region of target genes. The binding of the heterodimer to the VDRE results in a concomitant recruitment of co-activator proteins that form multi-protein complexes that together with basal transcriptional machinery and histone modifiers, stimulate transcription of genes with VDREs. In addition, many heterogeneous target genes for the VDR have been identified, reflecting the vast continuum of gene expression regulatory activity modulated by calcitriol (Carlberg, 2003). Calcitriol has also been known to associate with vitamin D membrane-associated rapid response steroid hormone binding protein (1,25-MARRS) which can stimulate rapid changes in the plasma membrane, possibly playing a role in Ca<sup>2+</sup> signalling and homeostasis within the cell (Khanal and Namere, 2007).

### **1.2.2 Immunomodulating effects of vitamin D or VDR activation**

Until much recently, calcitriol has been increasingly recognised as a potent immunomodulating agent. Besides its topical use in the treatment in psoriasis, calcitriol has been shown in experimental studies to inhibit the production of IL-2, IL-6, IFN- $\gamma$  and GM-CSF in peripheral blood mononuclear cells (Inoue *et al.*, 1998). Calcitriol has also been shown to inhibit the development of immune diseases and particularly effective in inflammatory bowel disease. Microarray studies of the colons of calcitriol-treated mice showed an inhibition of TNF- $\alpha$ , LPS-induced TNF- $\alpha$  factor and TNF- $\alpha$  receptor. Vitamin D supplementation also resulted in lower TNF- $\alpha$  concentrations in patients with congestive heart failure (Schleithoff *et al.*, 2006). It has been known to exert specific effects on monocytes, T-cells and antigen-presenting cells such as macrophages, dendritic cells, lowering IL-1 through 6 and IFN- $\gamma$  (Lin and White, 2004; Haussler *et al.*, 1998). There is a considerable amount of evidence that shows vitamin D has a significant effect on the enhancement of immune system function as well as the inhibition of autoimmunity development.

The effects of calcitriol, however, have not been studied extensively in adipocytes. Studies done on 3T3-L1 adipocytes by Sun and Zemel (2008) revealed that calcitriol up-regulated macrophage colony-stimulating factor, macrophage inflammatory protein, IL-6 as well as MCP-1 expression. However on examination of presented data it seemed that anti-inflammatory cytokine expression had also increased. Anti-inflammatory cytokine production was neither highlighted in the paper, nor was it discussed. This is particularly important as it could suggest the adipocyte's immunoregulatory role – possibly playing a

role in attenuating macrophage and monocyte activity in the course of their localization. IL-4 and IL-13 are known to inhibit proinflammatory cytokine production, attenuate monocyte/macrophage function and promote Th2 helper cell proliferation. It was also not established whether the source of the cytokine production in the co-culture study was the macrophages or adipocytes. The calcitriol-mediated upregulation of IL-10 could also present potential benefits. Hong *et al.* (2009) demonstrated that IL-10 increased insulin sensitivity, protected from obesity-induced macrophage infiltration and protects against the deleterious effects of proinflammatory cytokines on insulin signalling. IL-6 seems to exhibit an equivocal effect, exhibiting both proinflammatory and anti-inflammatory effects. In particular, IL-6 inhibits TNF- $\alpha$  and IL-1 production by macrophages (Opal and DePalo, 2000). Calcitriol also exerted an anti-inflammatory effect on 3T3-L1 adipocytes, reducing IL-6 without reducing IL-10 when supplemented together with vitamin E (Lira *et al.*, 2011).

### **1.2.3 Vitamin D and obesity**

Studies suggest that plasma concentrations of vitamin D are lowered in obesity (Parikh, 2004; Hultin 2010). Hyppönen (2007) described vitamin D levels as being lower in obese persons compared to lean individuals in a major cohort study. Although it was postulated to be due to the tendency of obese persons to spend time indoors and a decreased inclination to sun exposure, the global incidence of vitamin D deficiency suggests that the amount of UV exposure may only represent one causal link. In addition to epidemiological links of insulin resistance to vitamin D deficiency, vitamin D was also recently associated with metabolic syndrome in morbid obesity, showing a positive

correlation with serum triglyceride concentration (Botella-Carretero *et al.*, 2007). With vitamin D and adiposity both showing converging links to the same comorbidities, there now lies considerable impetus to determine the exact effects of vitamin D on adipose tissue biology.



### **1.3 Aims of the study**

Based on recent studies it is understood that macrophage infiltration in adipose tissue has a complex and manifold effect in physiology, especially in its upregulation in obesity and the pathogenesis of its comorbidities. Crosstalk of macrophages with adipocytes has been hypothesised to induce the observed increase in macrophage infiltration and inflammatory response in obese WAT. Macrophage-derived cytokines have been observed to exert an array of physiological effects on various tissues and organs via the components of the immune system, many of which have known links to metabolic diseases. A better understanding of adipocyte response in an inflammatory environment may help to develop better treatment strategies for obesity and its consequent comorbidities.

Given the limited amount of research conducted on the effects of calcitriol on macrophage and adipocyte crosstalk, the initial aim of this study is to investigate the effects of macrophage-derived factors on the inflammatory responses of human primary adipocytes. After which, a proposed role for calcitriol in the reversal of inflammatory responses in adipocytes is investigated.

The working hypothesis is that calcitriol treatment ameliorates inflammation through modulating the expression and secretion of inflammatory mediators by adipocytes. Therefore, the specific aims of this study are to:

1. Establish an *in vitro* inflammatory environment for adipose cells by exposure of adipocytes to macrophage-conditioned medium.
2. Determine gene expression and protein release of inflammatory mediators by adipocytes stimulated with macrophage-derived factors.
3. Study the signalling pathways that are involved in macrophage-induced inflammatory response in adipocytes.
4. Examine the effects of vitamin D supplementation on crosstalk between adipocytes and macrophages.

## **Chapter 2**

### **Materials and methods**

## 2.1 Reagents and equipment

Table 2.1 Chemical reagents

Reagents	Supplier
Pure ethanol	Sigma
1- $\alpha$ , 25-Dihydroxyvitamin D <sub>3</sub>	Enzo Life Sciences
$\beta$ -Mercaptoethanol	SERVA
(3-(4,5-Dimethylthiazol-2-yl)-2,5-diphenyltetrazolium bromide (MTT)	Sigma
3-isobutyl-1-methylxanthine (IBMX)	Sigma
Acrylamide/Bisacrylamide	Bio-rad
Ammonium persulphate	Bio-rad
Anti- $\alpha$ -Tubulin mouse mAb	Sigma
Bicinchoninic acid	Sigma
Biotin	Sigma
Bisacrylamide	Bio-Rad
Bovine Serum Albumin	Sigma
Bromophenol blue	Sigma
Chloroform	Fisher Scientific
Coomassie Brilliant Blue dye	Fisher Scientific
Copper sulphate	Sigma
Dexamethasone	Sigma
Dulbecco's Modified Eagle's Medium/Ham's Nutrient Mixture F12	Sigma
Fetal Calf Serum	Sigma
Glycerol	Sigma
Glycine	Sigma
Hydrochloric acid	Fisher Scientific
Insulin	Sigma
Isopropanol	Sigma
Human I $\kappa$ B $\alpha$ Mouse mAb	New England Biolabs

L-Thyroxine	Sigma
Methanol	Fisher Scientific
PageRuler prestained protein ladder	Fermentas
Penicillin/Streptomycin mix	Sigma
Penicillin/Streptomycin/Fungizone mix	Sigma
Phorbol-12-myristate-13-acetate	Sigma
Phosphate-buffered saline tablets	Sigma
Phospho p38 MAPK Rabbit mAb	New England Biolabs
Phospho-NF- $\kappa$ B p65 Rabbit mAb	New England Biolabs
Phospho-p44/42 MAPK Rabbit mAb	New England Biolabs
Ponceau S	Sigma
Protease inhibitor cocktail	Sigma
Phosphatase inhibitor cocktail	Sigma
RNase AWAY	Molecular BioProducts, Inc.
Rosiglitazone	Enzo Life Sciences
Roswell Park Memorial Institute medium (RPMI-1640)	Sigma
Skimmed milk powder	Lidl
Sodium dodecyl sulphate	Sigma
Sodium Chloride	Sigma
SYBR Green I dye	Eurogentec
SYBR Green primers	Sigma
Taqman primers	Eurogentec
Taqman probes	Eurogentec
Tetramethylethylenediamine (TEMED)	Sigma
TNF- $\alpha$	Sigma
Total Akt Rabbit antibody	New England Biolabs
Tricine	Sigma
Trizma BASE	Sigma
TRIzol <sup>®</sup> reagent	Sigma
Trypsin-EDTA solution	Sigma

Water, molecular biology reagent (DEPC-treated, ultra-pure water)	Sigma
---	-------

**Table 2.2 Commercial kits**

<b>Kits</b>	<b>Supplier</b>
Cytotoxicity Detection Kit	Roche
Free glycerol determination kit	Sigma
Human adiponectin DuoSet® ELISA development system	R & D Systems
Human IL-1β DuoSet® ELISA development system	R & D Systems
Human IL-6 DuoSet® ELISA development system	R & D Systems
Human MCP-1 DuoSet® ELISA development system	R & D Systems
Human Zinc-alpha-2-glycoprotein ELISA	BioVendor
iScript cDNA synthesis kit	Bio-rad
qPCR Core kit	Eurogentec
SuperSignal® West Pico ECL kit	Thermo Scientific

**Table 2.3 Equipment**

<b>Equipment</b>	<b>Supplier</b>
12/24 well tissue culture plates	Techno Plastic Products
96-well real time PCR plates	Starlab
Benchmark™ Plus Microplate Spectrophotometer	Bio-Rad
Bio-Rad Mini-PROTEAN™ Tetra Electrophoresis System	Bio-Rad
Biophotometer	Eppendorf
Bottle top 0.2 µm filters	Techno Plastic Products
ChemiDoc™ XRS+ System	Bio-Rad
Disposable serological pipette tips	Starlab
Hybridizer hybridization oven	UVP
LABNET Multigene Gradient thermal cycler	Labnet International
Mx3005P QPCR system	Stratagene (Agilent)
Nikon Diaphot inverted microscope/D50 camera	Nikon

Nunc MaxiSorp® flat-bottom 96 well plate	Thermo Scientific
Hybond ECL nitrocellulose membrane	Amersham
Real-time PCR Sealing Film	Elkay
Refrigerated microcentrifuge	Eppendorf
Syringe 0.2 µm filters	Techno Plastic Products
UVette plastic disposable cuvettes	Eppendorf

**Table 2.4 Software**

<b>Software</b>	<b>Supplier</b>
Camera Control Pro	Nikon
Graphpad Prism Software	GraphPad Software, Inc.
Image Lab™ image acquisition and analysis software	Bio-Rad
Microplate Manager 5.2	Bio-Rad
MxPro QPCR software	Stratagene
SPSS (PASW) v18.0.0	IBM

**Table 2.5 Suppliers' addresses and URLs**

<b>Company</b>	<b>Address and URLs</b>
<b>Amersham</b>	Amersham Pl, Little Chalfont, Buckinghamshire, United Kingdom, Tel: [44] 0870 606 1921. <a href="http://www.amershambiosciences.com">http://www.amershambiosciences.com</a>
<b>Bio-Rad</b>	Bio-Rad Laboratories Ltd, Bio-Rad House. Maxted Road, Hemel Hempstead, Hertfordshire HP2 7DX, United Kingdom. <a href="http://www.bio-rad.com">http://www.bio-rad.com</a>
<b>BioVendor</b>	BioVender GmbH, Im Neuenheimer Feld 583, D-69120 Heidelberg, Germany. <a href="http://www.biovendor.com">http://www.biovendor.com</a>
<b>Elkay</b>	Elkay Laboratory Products (UK) Limited, Unit E, Lutyens Industrial Centre, Bilton Road, Basingstoke, Hampshire RG24 8LJ, United Kingdom. <a href="http://www.elkay-uk.co.uk">http://www.elkay-uk.co.uk</a>
<b>Enzo Life Sciences</b>	Enzo Life Sciences (UK) LTD, Palatine House , Matford Court, Exeter EX2 8NL, United Kingdom. <a href="http://www.enzolifesciences.com">http://www.enzolifesciences.com</a>
<b>Eppendorf</b>	Eppendorf UK Limited, Endurance House, Vision Park, Chivers Way, Histon, Cambridge CB24 9ZR, United Kingdom. <a href="http://www.eppendorf.co.uk">http://www.eppendorf.co.uk</a>
<b>Eurogentec</b>	Eurogentec Ltd. Old Headmasters House, Unit 1, Building 1, Forest Business Centre, Fawley Road, Fawley, Southampton, Hampshire SO45 1FJ, United Kingdom. <a href="http://www.eurogentec.com">http://www.eurogentec.com</a>
<b>Fermentas</b>	European Head Office Germany. Fermentas GmbH, Opelstrasse 9, 68789 St. Leon-Rot, Germany. <a href="http://www.fermentas.de">http://www.fermentas.de</a>
<b>Fisher Scientific</b>	Fisher Scientific UK Ltd. Bishop Meadow Road, Loughborough, Leicestershire, LE11 5RG, United Kingdom. <a href="http://www.fisher.co.uk">http://www.fisher.co.uk</a>
<b>GraphPad Software, Inc.</b>	GraphPad Software, Inc. 2236 Avenida de la Playa, La Jolla, CA 92037, USA. <a href="http://www.graphpad.com">http://www.graphpad.com</a>
<b>IBM SPSS</b>	2 New Square, Bedfont Lakes, Feltham, Middlesex TW14 8HB, United Kingdom. <a href="http://www-01.ibm.com/software/uk/analytics/spss/">http://www-01.ibm.com/software/uk/analytics/spss/</a>
<b>Labnet International</b>	Labnet International. PO Box 841, Woodbridge, NJ 07095, USA. <a href="http://www.labnet.com">http://www.labnet.com</a>
<b>Molecular BioProducts, Inc.</b>	Molecular BioProducts, Inc. B399389 Waples Street, San Diego, CA 92121-3903. <a href="http://www.mbpinc.com">http://www.mbpinc.com</a>



<b>New England Biolabs</b>	New England Biolabs (UK) Ltd. 75/77 Knowl Piece, Wilbury Way, Hitchin, Herts. SG4 0TY, United Kingdom. <a href="http://www.neb.com">http://www.neb.com</a>
<b>Nikon</b>	Nikon UK Limited. 380 Richmond Road, Kingston upon Thames, Surrey KT2 5PR, United Kingdom. <a href="http://www.europe-nikon.com">http://www.europe-nikon.com</a>
<b>R &amp; D Systems</b>	R&D Systems Europe Ltd. 19 Barton Lane, Abingdon Science Park, Abingdon, OX14 3NB, United Kingdom. <a href="http://www.rndsystems.com">http://www.rndsystems.com</a>
<b>Roche</b>	Roche Diagnostics Limited. Charles Avenue, Burgess Hill, West Sussex RH15 9RY. United Kingdom. <a href="http://www.rocheuk.com">http://www.rocheuk.com</a>
<b>SERVA</b>	SERVA Electrophoresis GmbH. Carl-Benz-Str. 7 P.O.B. 10 52 60, 69115 Heidelberg, Germany. <a href="http://www.serva.de">http://www.serva.de</a>
<b>Sigma</b>	Sigma-Aldrich Company Ltd. Fancy Road, Poole, Dorset BH12 4QH, United Kingdom. <a href="http://www.sigmaaldrich.com/united-kingdom.html">http://www.sigmaaldrich.com/united-kingdom.html</a>
<b>Starlab</b>	STARLAB (UK), Ltd. Unit 4 Tanners Drive, Blakelands, Milton Keynes MK14 5NA, United Kingdom. <a href="http://www.starlab.de">http://www.starlab.de</a>
<b>Stratagene (Agilent)</b>	Agilent Technologies, Inc. Life Sciences and Chemical Analysis, Group 5301, Stevens Creek Boulevard, Santa Clara, CA 95051-7201, USA
<b>Techno Plastic Products</b>	TPP Techno Plastic Products AG, Zollstrasse 155, CH-8219, Trasadingen, Switzerland
<b>Thermo Scientific</b>	Thermo Fisher Scientific Inc. Unit 9 Altey Way North Nelson Industrial Estate Cramlington, Northumberland, NE23 1WA. <a href="http://www.thermoscientific.com">http://www.thermoscientific.com</a>
<b>UVP</b>	Ultra-Violet Products Ltd, Unit 1, Trinity Hall Farm Estate, Nuffield Road, Cambridge CB4 1TG, United Kingdom. <a href="http://www.uvp.com">http://www.uvp.com</a>

## **2.2 Cell culture**

For THP-1 and human primary adipocyte cell culture, all precautions were taken to prevent any contamination of the cells. All glassware was autoclaved and sterile plastic ware was used. The UV-C lamp in the laminar flow cabinet or tissue culture hood was switched on to sterilise the shell for 20 minutes and wiped with 1% Vircon solution followed by 70% ethanol prior to use. The laminar flow cabinet was allowed to run for 15 minutes prior to use. All bottles and universals were opened within a sterile tissue culture hood. Media components were pipetted using single-use serological pipette tips (Starlab, Milton Keynes, UK) and filtered through a 0.22 µm filter membrane (Techno Plastic Products, Trasadingen, Switzerland). Prepared media were kept at 4°C for a maximum of 2 weeks if required later for experiments and pre-warmed at 37°C in a HB-1000 hybridization oven (UVP, Cambridge, UK) before usage.

### **2.2.1 THP-1 monocytes culture and preparation of macrophage-conditioned medium**

#### *2.2.1.1 Human THP-1 cell culture medium*

Reagents and equipment

1 x Roswell Park Memorial Institute 1640 medium

10% foetal calf serum

100 U/ ml penicillin and 100 µg/ ml streptomycin mix

75cm<sup>2</sup> cell culture flasks

Pipette and sterile pipette tips

50ml centrifuge tubes

100 nM phorbol 12-myristate 13-acetate (PMA)

#### 2.2.1.2 *Human monocytes*

The human THP-1 acute monocytic leukaemia cell line was kindly provided by Professor Helen R Griffiths (Aston University, UK). Vials of cells were stored in liquid nitrogen until the day of subculture.

#### 2.2.1.3 *Cell generation and maintenance*

A frozen vial of aliquoted human THP-1 monocytes ( $1 \times 10^6$  cells/ml) was removed from liquid nitrogen storage and defrosted in a water bath at 37°C. Cells were cultured in 24-well plates at 37°C. 1 ml of pre-warmed human THP-1 cell culture medium was added to the aliquot to help defrosting and gentle pipetting was performed to aid with the thawing. The thawed aliquot was then added to a 75 cm<sup>2</sup> flask with 25ml of THP-1 cell culture medium and incubated at 37°C for 24 hours in a humidified atmosphere of 5% CO<sub>2</sub> / 95% air. The cells were extracted and spun down at 249 x g for 5 minutes, the supernatant was removed and the cells were reconstituted with 5 ml of fresh cell culture media. The reconstituted cells were dispensed into a 75 cm<sup>2</sup> cell culture flask and 25 ml of culture media was added to the flask. Cells were passaged every 3 – 4 days when cell density reached  $10^6$  /ml.

#### *2.2.1.4 Differentiation of THP-1 cells and preparation of macrophage-conditioned medium*

For the preparation of macrophage-conditioned (MC) medium, THP-1 monocytes were differentiated by the addition of 100 nM PMA (Sigma) for 48 h and then replaced with serum-free RPMI-1640 medium (without PMA) for 24 h to a cell density of  $10^6$  /ml. The MC medium was then collected and stored at  $-80^{\circ}\text{C}$  until required.

### **2.2.2 Culture and differentiation of human preadipocytes**

#### *2.2.2.1 Reagents*

##### *Human preadipocyte subculture medium*

1 x Promocell preadipocyte growth medium

1 x Promocell preadipocyte supplement mix

100 U/ml penicillin, 100  $\mu\text{g/ml}$  streptomycin and 0.25  $\mu\text{g/ml}$  amphotericin B mix

##### *Human preadipocyte differentiation medium*

1 x Dulbecco's Modified Eagle's Medium-Ham's F-12 (1:1, vol/vol)

Biotin 32  $\mu\text{M}$

Insulin 100 nM

Dexamethasone 1  $\mu\text{M}$

3-isobutyl-1-methylxanthine 200  $\mu\text{M}$

L-Thyroxine 11 nM

Rosiglitazone 8  $\mu\text{M}$

### *Human primary adipocyte maintenance medium*

1 x Dulbecco's Modified Eagle's Medium-Ham's F-12 (1:1, vol/vol)

3 % foetal calf serum

100 nM insulin

32  $\mu$ M biotin

1  $\mu$ M dexamethasone

100 U/ml penicillin, 100  $\mu$ g/ml streptomycin and 0.25  $\mu$ g/ml amphotericin B mix

### *Cell culture reagents*

Trypsin-EDTA solution (0.05% / 0.02%)

Autoclaved phosphate-buffered saline

#### *2.2.2.2 Human preadipocyte storage*

Human white preadipocytes used in the experiments were derived from subcutaneous adipose tissue of a female Caucasian subject (BMI 21; age 44 years) and were obtained from PromoCell (Heidelberg, Germany). Aliquots were stored in liquid nitrogen until required.

#### *2.2.2.3 Resuspending preadipocytes from cryopreservation*

Preadipocytes were resuspended and cultured according to the protocol provided by Promocell (Heidelberg, Germany). Preadipocyte aliquots were removed from liquid nitrogen and immediately submerged in 37°C water bath for 90 seconds. 20 ml of preadipocyte growth medium was added to a 150 cm<sup>2</sup> cell culture flask. Cells were

resuspended in 5 ml of growth medium and the contents pipetted into the flask. Flasks were incubated at 37°C in a humidified atmosphere of 5% CO<sub>2</sub> / 95% air for 24 hours. Cells were then removed from incubation and checked for viability under a phase contrast Diaphot inverted microscope (Nikon, Surrey, UK). The cell culture was then decanted into a 50 ml centrifuge tube and centrifuged at 249 x g for 5 minutes. Cells were resuspended and incubated for 3 to 4 days to 70% confluency to ensure cells do not undergo growth arrest at 100% confluence.

#### *2.2.2.4 Preadipocyte subculture*

Preadipocytes were observed under the phase contrast microscope to ensure approximately 70% confluency. The spent medium was aseptically removed and cell monolayer was washed twice with phosphate-buffered saline (PBS) by streaming the saline from the non-coated side of the flask and swirling the flask. The PBS was aspirated after each washing step. 3 ml of trypsin solution was added to the flask and left at room temperature for 5 minutes to dislodge adhered cells. The cells were observed under the microscope for roundness of cells and >90% detachment. When cells were sufficiently detached, 4 ml of preadipocyte growth medium was added to the flask and swirled to neutralise the trypsin solution. An aliquot of the flask contents was obtained for cell count and the remaining was decanted into a 15 ml centrifuge tube. Cells were counted using a haemocytometer to obtain approximate total number of cells. The total number of cells was divided accordingly to calculate the cell suspension volume required to obtain a cell plating density of 40,000 cells per millilitre/well. The cells were spun at 249 x g for 5 minutes. The supernatant was then aspirated from the tube and resuspended first in 5ml

of preadipocyte growth medium to ensure homogeneity, then added to the rest of the resuspension volume. The flask was swirled to ensure further homogeneity. 1 ml of cell suspension was dispensed into each well. The cells were incubated for 3 to 4 days to confluence.

#### *2.2.2.5 Preadipocyte differentiation*

At confluence, cells were induced to differentiate at day 0 by incubation for 3 days in human preadipocyte differentiation medium. After induction, cells were further maintained in maintenance medium containing 3 % FCS, 100 nM insulin, 32  $\mu$ M biotin and 1  $\mu$ M dexamethasone until full differentiation into adipocytes which was verified by the phase contrast microscopy of lipid droplets accumulated intracellularly using a Diaphot inverted microscope (Nikon, Surrey, UK).

## **2.3 Cell Culture Treatment**

### **2.3.1 Macrophage-induced inflammation in adipocytes**

To examine the effect of a moderate inflammatory environment on human primary adipocytes, 25% MC medium was prepared by mixing MC medium and maintenance medium in the ratio 1:3. A control medium containing 25% RPMI-1640 medium was also prepared concurrently by mixing RPMI medium with maintenance medium in the ratio 1:3. Each mixture was subsequently filtered through a 0.22  $\mu$ m filter prior to use for the treatment of cells. The maintenance medium in wells of confluent cells were aspirated and replenished every three days. Fresh maintenance medium was replenished on day 11.

The maintenance medium was aspirated on day 13 and incubated in 25% MC medium. Control cells were incubated in 25% RPMI medium. The medium, cell lysates and TRIzol® extracts (section 2.5 and 2.7) were collected after 24 or 48 hours.

### **2.3.2 Effects of vitamin D on macrophage-induced inflammatory response in adipocytes**

To study adipocytes' behaviour to calcitriol treatment, 1 mg/ml calcitriol stock solution (Enzo, USA) was diluted in DMSO (0.22 µm filtered) and added to maintenance medium to produce medium of varying calcitriol concentrations ( $10^{-8}$ M and  $10^{-11}$ M) for dose-response study. Groups of cells were then treated with calcitriol-supplemented medium at each concentration on day 11 post-confluence. A separate group of cells was replenished with maintenance medium on day 11 as a control. Wells were incubated for 48 hours prior to inflammatory stimulation. Calcitriol was added to 25% RPMI and 25% MC medium to produce medium with varying calcitriol concentrations ( $10^{-8}$ M and  $10^{-11}$ M). The maintenance medium was aspirated from the wells on day 13 and treated with corresponding calcitriol concentrations in 25% RPMI or 25% MC. Cells used for the study of inflammatory stimulus on adipocytes were used as a control for this study. The cells were incubated for 24 or 48 hours at 37°C in a humidified atmosphere of 5% CO<sub>2</sub> and 95% air.

### **2.3.3 Effect of vitamin D on TNF- $\alpha$ induced inflammatory response in adipocytes**

To study the effect of TNF- $\alpha$  on adipocytes, cells were treated with maintenance medium with varying calcitriol concentrations ( $10^{-8}$ M and  $10^{-11}$ M) or maintenance medium



without calcitriol supplementation on day 11 post-confluence for 48 hours. Cells were then treated on day 13 with 5ng/ml human recombinant TNF- $\alpha$  (Sigma, Poole, UK) in 25% RPMI medium either supplemented with calcitriol at varying concentrations or without supplementation. Cell and medium collection was performed on day 15.

## **2.4 Cell and media collection**

For cell and media collection from cell cultures, all precautions were taken to prevent any contamination of the cells and medium. All glassware was autoclaved and sterile plastic ware was used. The UV-C lamp in the laminar flow cabinet or tissue culture hood was switched on to sterilise the shell for 20 minutes and wiped with 1% Vircon solution followed by 70% ethanol prior to use. The laminar flow cabinet was allowed to run for 15 minutes prior to use. All collection work was performed within a sterile tissue culture hood. Cell extracts and media were aspirated using single-use serological pipette tips (Starlab, Milton Keynes, UK) into RNase-free 2 ml centrifuge tubes.

### **2.4.1 Cell culture medium collection**

#### *2.4.1.1 Principles*

The cell culture medium is an excellent source of cell-secreted proteins and hence it was used to analyze the environment change caused by cells in a given treatment.

#### *2.4.1.2 Method*

##### *Reagents and equipment*

Pipette and sterile pipette tips

Sterile centrifuge tubes

Cell medium was aspirated and centrifuged at 249 x g for 10 minutes. The supernatant was aspirated and transferred to a sterile centrifuge tube and stored at -80°C.

## **2.4.2 TRIzol® collection for total RNA analysis**

### *2.4.2.1 Principles*

Total adipocyte RNA was obtained by guanidinium thiocyanate–phenol–chloroform extraction (Chomczynski and Sacchi, 2006). Guanidinium thiocyanate in the TRIzol® solution used is a strong inhibitor of ribonucleases and phenol is utilised for partitioning of aqueous supernatant for RNA isolation.

### *2.4.2.2 Method*

#### *Reagents and equipment*

Cell cultures in plates

TRIzol® solution

Pipette and sterile pipette tips

Rocking platform

RNase-free centrifuge tubes

RNA isolation was performed according to the Trizol Reagent Protocol (Invitrogen, Paisley, UK). After the cell medium was aspirated, 500 µl of TRIzol® reagent was added in each well and rocked on a rocking platform for 5 minutes to remove cells from the bottom of the well. The mixture of TRIzol® and cells was repeatedly pipette up and

down to mechanically dislodge cells. The mixture from each well was then collected into RNase-free tubes and stored at -80°C to prevent RNA degradation.

### **2.4.3 Cell lysate collection**

#### *2.4.3.1 Principles*

Cell lysis is a cell disruption method used to release biological molecules from inside a cell. A detergent is used to disrupt cells in this method. Detergent-based lysis is used in conjunction with mechanical disruption of cell membranes to achieve a more homogenous extract. The sodium dodecyl sulphate detergent used in this study works by disrupting the lipid barrier surrounding cells by disrupting lipid-lipid, lipid-protein and protein-protein interactions within the cell. Cell lysates were used solely for protein assessment by western blotting. In cell signal transduction events, phosphorylation and dephosphorylation of proteins define a multitude of cellular processes such as cell division, cell proliferation and cell death. Target proteins are phosphorylated by protein kinases which work by transferring a phosphate group to a specific protein, usually at serine or tyrosine residues. Phosphorylation of a protein tends to change the conformation of the protein, altering its ability to interact or bind its complementary ligands. The phosphorylated state of these proteins can be diminished if the phosphate group is removed by the action of endogenous or exogenous phosphatases. It is therefore highly critical that phosphatase inhibitors be used in the lysis to preserve the phosphorylated state of the proteins. Endogenous proteases released during the disruption of cells may

also degrade proteins. Thus, a broad spectrum protease inhibitor cocktail is used for protection of proteins when performing the lysing step.

#### *2.4.3.2 Reagents and equipment*

Cell lysis buffer consisting of:

50mM Tris-HCl, pH 6.7

10% Glycerol

4% SDS

2%  $\beta$ -mercaptoethanol

Protease inhibitor cocktail (1:100)

Phosphatase inhibitor cocktail (1:100)

Autoclaved phosphate-buffered saline

Pipette and sterile pipette tips

RNase-free centrifuge tubes

#### *2.4.3.3 Method*

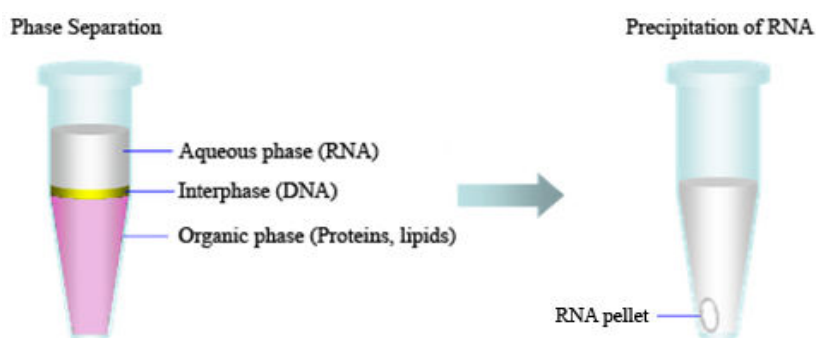
After the cell medium in each well had been aspirated, the cell monolayer was washed with three times with 1 ml of autoclaved PBS. Subsequently 50  $\mu$ l of cell lysis buffer was added to each well and pipetted up and down repeatedly to ensure maximum recovery of cells. Extracts were aspirated and transferred to RNase-free 2 ml centrifuge tubes.

## **2.5 Total RNA isolation**

### **2.5.1 Principles**

TRIzol® was used to perform guanidinium thiocyanate–phenol–chloroform extraction for the isolation of RNA (Chomczynski and Sacchi, 2006). TRIzol® contains guanidinium isothiocyanate, which is a strong chaotropic agent that disrupts cells, solubilises their components, denatures endogenous RNases and separates rRNA from ribosomes. Guanidinium thiocyanate demolishes the three-dimensional structure of proteins, converting them to a randomly coiled state, including RNases which as a result will not be able to act on RNA. This allows the RNA to come in the free form. The solution also contains phenol in an acidic environment which is required for the partitioning of RNA into aqueous supernatant for separation (Figure 2.1). Phenol also solubilises the proteins. Chloroform used in the technique works to solubilise lipids. A low pH is critical for the isolation of RNA as a higher pH will cause DNA to partition into the aqueous phase. The other cell proteins and DNA should be confined to the interphase and lower organic phase. Total RNA is then recovered by precipitation of the aqueous phase with isopropanol and washed of impurities with 75% ethanol. The RNA is then dissolved in DEPC-treated water and frozen if not used immediately.

**Figure 2.1 Isolation of RNA from TRIzol® extracts**



During phase separation the phenol-chloroform mixture separates the cell homogenate into three phases: a clear aqueous phase with the RNA, a white interphase containing DNA and a pink organic phase containing cell proteins and lipids. After the precipitation step with isopropanol, a white pellet is generated at the bottom of the tube. This is subsequently washed with 75% ethanol and solubilised with DEPC-treated water.

### 2.5.3 Method

#### *Reagents and equipment*

RNase AWAY®

TRIzol® extracts (Section 2.4.2)

Chloroform

75% ethanol

Isopropanol

Refrigeration centrifuge

23-gauge needle and syringe

Sterile pipette tips and pipette

Sterile filter pipette tips

RNase AWAY® was sprayed on gloves and all glass and plastic ware to eliminate RNase and DNA contamination from labware. TRIzol® extracts were homogenised by passing the cells through a 23 gauge needle four times, ensuring that the needle was changed between wells. TRIzol® extracts were thawed in a box of ice and 100 µl of chloroform was added into each tube of extract. The tubes were then shaken vigorously for 15 seconds and left to stand for 10 minutes at room temperature. It was then centrifuged at 20,800 x g for 15 minutes at 4°C to create three phases: an upper colourless aqueous phase containing RNA, a white interphase containing DNA and a lower red phenol phase containing protein. The top layer was carefully aspirated into a fresh RNase-free tube, ensuring that the interphase DNA was not aspirated as well. 250 µl of isopropanol was added to each tube of aqueous extract, vortexed and allowed to stand at room temperature

for 10 minutes. The extracts were then centrifuged at 20,800 x g for 15 minutes at 4°C. The supernatant was subsequently discarded with care not to dislodge the pellet from the base of the tube, which was then vortexed in 100 µl of ethanol. The samples were then centrifuged at 15,300 x g for 10 minutes at 4°C. The supernatant was removed and pellets were left to air dry for 5 minutes. The pellet was dissolved in 12 µl of ultra-pure water (Sigma) and stored at -80°C if not used immediately.

#### **2.5.4 RNA quantification**

The concentration and the purity of the RNA was determined by measuring the absorbance at 260/280 nm using a spectrophotometer (Biophotometer Eppendorf, Cambridge, UK) according to the current protocol for RNA extraction (Chomczynski and Sacchi, 2006). RNA extracts were thawed and kept on ice throughout the quantitation. 1 µl of RNA was diluted with 69 µl of ultra-pure water and the absorbance was measured at 260 nm and 280 nm with ultra-pure water used as a blank. The RNA concentration (µg/µl) was automatically calculated by the spectrophotometer.

The maximum absorbance of nucleic acids is at 260 nm and since RNA has an extinction coefficient of 44.19 at that wavelength, the concentration of RNA using the Beer-Lambert (Beer, 1852) law is as follows:

$$\text{Concentration of RNA } (\mu\text{g}/\mu\text{l}) = A_{260} \times 44.19 \times \text{Dilution Factor} / 1000$$

The ratio between  $A_{260}$  and  $A_{280}$  was used as a measure of RNA purity, where a value of 2 indicates a pure sample, whereas a value of 1.6 and below is indicative of



contamination, which is usually due to protein. RNA extracts were diluted to a concentration of 0.1 µg/ µl using the formula as follows:

$$\text{Concentration of RNA extract} \times 1 \mu\text{l} = 0.1 \mu\text{g}/\mu\text{l} \times \text{total volume of dilution}$$

## **2.6 Reverse-transcription polymerase chain reaction**

### **2.6.1 First-strand cDNA synthesis**

#### *2.6.1.1 Principles*

This procedure was used to generate single-stranded DNA strands complementary to the mRNA sequences in the total RNA of samples (Krug and Berger, 1987). The iScript first strand cDNA Synthesis Kit (Bio-Rad, Hertfordshire, UK) was used and features oligo(dT) and random hexamer primers in a unique ratio in the reaction mix. This procedure was used to generate first-strand DNA complementary to the mRNA sequences in total RNA samples. An RNA-dependent DNA polymerase is derived from the retrovirus Molone Murine Leukaemia Virus (MMLV) is used as the reverse transcriptase enzyme. The poly(A) tail found at the 3' end of the mRNA acts as a starting point for the reverse transcriptase to which a short complementary synthetic oligonucleotide (oligo dT primer) is hybridised to form a polyT-polyA hybrid. Random hexamers were incorporated to enable priming throughout the length of RNA for uniform representation of all RNA sequences, ensures transcription of 5' ends of long mRNAs and also allows for reverse transcription of RNAs without poly(A) tails. All four deoxynucleotide triphosphates, Mg<sup>2+</sup> cofactors and a neutral pH maintained by the kit

buffer provide the necessary conditions and resources for cDNA synthesis on the mRNA template (Figure 2.2).

#### *2.6.1.2 Method*

cDNA was synthesised using 0.5 µg of RNA and the iScript first strand cDNA Synthesis Kit (Bio-Rad, Hertfordshire, UK). The kit consisted of:

5X cDNA synthesis kit buffer

iScript enzyme mixture

Nuclease-free water

0.1µg/µl RNA sample

The procedure was performed using sterile RNase and DNase-free tubes and filter tips. A master mix was prepared using 2 µl of reaction mix, 0.5 µl of reverse transcriptase and 2.5 µl of nuclease-free water per RNA template. 5 µl of master mix and 5 µl of RNA template were added to each PCR tube, vortexed and pulse-spun to gather the contents to the bottom of the tube. The samples were then placed in a thermal cycler programmed to run the following protocol:

5 min at 25°C

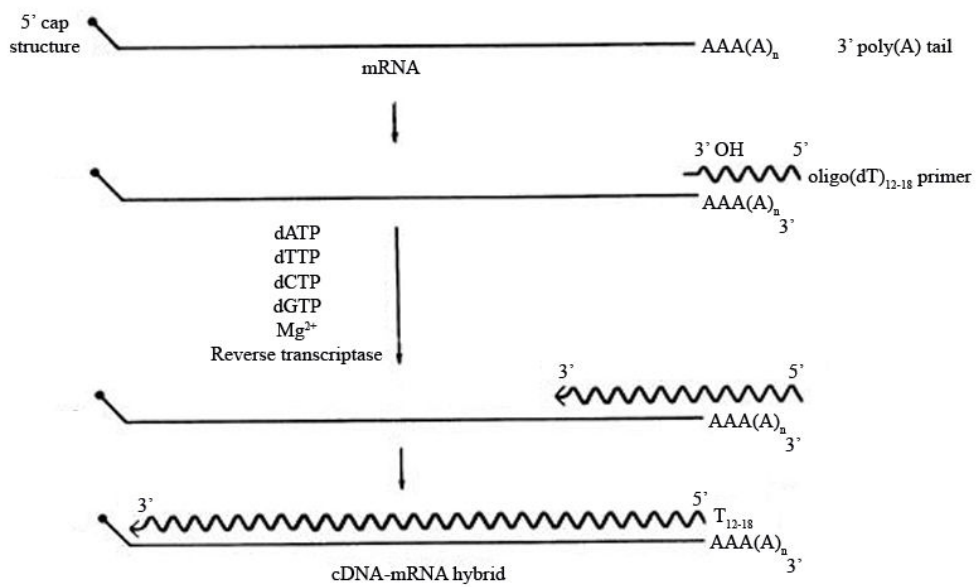
30 min at 42°C

5 min at 85°C

Hold at 4°C

Once the reaction is complete, 30 µl of ultra-pure water was added to each PCR tube and used immediately or stored in -20°C to prevent degradation.

**Figure 2.2 First-strand cDNA synthesis**



cDNA synthesis using an oligo-d(T) primer and reverse transcriptase.

## **2.7 Real-time polymerase chain reaction (RT-qPCR)**

Real-time PCR is the ‘gold-standard’ for quantitating steady-state mRNA levels. It is based on the classic principles of PCR and quantifies a targeted DNA molecule during the exponential phase based on amplification of DNA. The exponential phase is deemed to occur very efficiently early in the reaction process, allowing reliable quantitation of the starting DNA. Two types of PCR detection chemistries were used in this study – the TaqMan® and SYBR® Green systems.

### **2.7.1 Taqman system principles**

The TaqMan® chemistry, also known as ‘fluorogenic 5' nuclease chemistry’, measures specific PCR product accumulation using a set of primers and a dual-labeled fluorogenic oligonucleotide probe (Holland *et al.*, 1991). The probe is composed of a short oligonucleotide sequence of 20 to 30 bases long labelled with two different fluorescent dyes. The reporter dye is located at the 5' terminus and a quenching dye (usually TAMRA) is located at the 3' terminus. A probe homologous to an internal target sequence amplicon anneals to PCR product. When the probe is intact, energy transfer occurs between the two fluorophores and emission from the reporter is quenched by the quencher by a process called FRET (Förster or fluorescence resonance energy transfer). During the extension phase Taq polymerase cleaves the probe, releasing the reporter from the oligonucleotide quencher. This ends the activity of FRET and the reporter dye starts to emit fluorescence (518nm for FAM) which increases during each cycle proportional to the rate of probe cleavage. In the real-time Mx3005P QPCR system, the laser light source

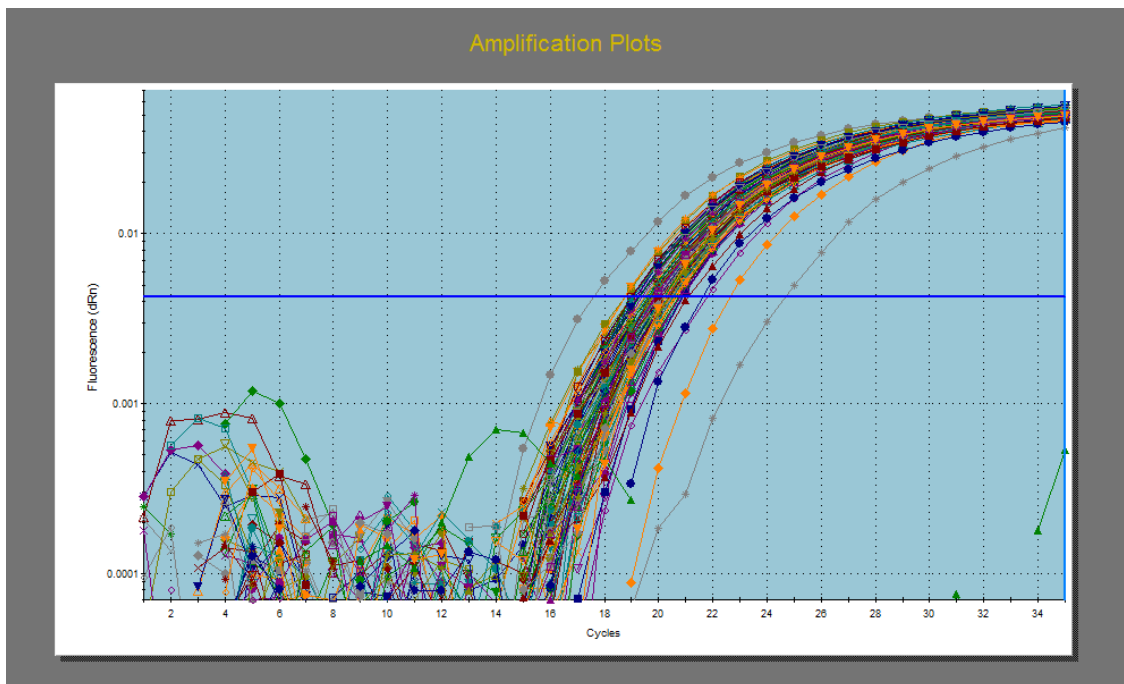
excites each well and a CCD camera measures the fluorescence spectrum and intensity from each well. A specific requirement for fluorogenic probes is that there should not be a G at the 5' end of the probe sequence; a 'G' adjacent to the reporter dye is able to quench reporter fluorescence even after cleavage. The MxPro qPCR software measures the fluorescent activity of reporter dyes and a software algorithm is used to calculate and normalise the increase of reporter emission intensity over the extension phase (dRn) to a passive reference dye (ROX). Normalization is essential to correct for differences in reaction mix volumes between wells. The amplification plot is examined at a point early in the log phase of product accumulation. This is done by assigning a fluorescence threshold and a cycle threshold ( $C_t$ ) value is determined when the fluorescence from a sample crosses the threshold.

### **2.7.2 SYBR Green principles**

SYBR Green I is an asymmetrical cyanine dye used as a nucleic acid stain in molecular biology (Zipper *et al.*, 2004). SYBR Green I stains DNA and RNA, although it binds preferentially to double-stranded DNA and stains single-strand DNA and RNA with lower performance. The resulting DNA-dye-complex absorbs blue light ( $\lambda_{\max} = 488 \text{ nm}$ ) and emits green light ( $\lambda_{\max} = 522 \text{ nm}$ ). SYBR®-Green based detection uses the SYBR Green I dye which functions to detect PCR product as it accumulates during PCR cycles. When the dye is added to a sample, it immediately intercalates between the base pairs of all double-stranded DNA present in the sample (Ponchel *et al.*, 2003). During the PCR reaction, AmpliTaq Gold® DNA Polymerase amplifies the target sequence, creating new double-stranded DNA or amplicons. The SYBR Green I dye then binds to each new

amplicon as the reaction progresses and more amplicons are generated, resulting in an increase in fluorescence intensity proportionate to the amount of PCR product produced. The MxPro qPCR software measures the fluorescent activity of the dye and a software algorithm is used to calculate and normalise the increase of fluorescent emission intensity over the extension phase (dRn) to a passive reference dye (ROX). Again, normalization is essential to correct for differences in reaction mix volumes between wells. The amplification plot is examined at a point early in the log phase of product accumulation. This is done by assigning a fluorescence threshold and a cycle threshold ( $C_t$ ) value is determined when the fluorescence from a sample crosses the threshold. The SYBR Green chemistry follows a slightly different protocol from the TaqMan chemistry. Real time SYBR Green PCR amplification cycling steps features a 95°C denaturation step for 10 minutes followed by 40 cycles consisting of a 95°C denaturation step for 15 seconds and an annealing-cum-extension step 60°C for 1 minute) and an additional dissociation cycle (95°C for 1 min, 55°C for 30 s and 95°C for 30 s). The dissociation step shows the number of PCR products and is used to gauge the specificity of the amplification. This is important as the SYBR Green dye is capable of binding to any double-stranded amplicon, by binding with non-specific double-stranded DNA sequences and generating false-positive signals. False-positive signals can be minimised or prevented by using a master mix and primer combination that only generates a single gene-specific amplicon without producing secondary non-specific products.

**Figure 2.3 Amplification plot**



The figure shows a screenshot of an amplification plot with default settings as viewed from the MxPro software. The baseline is adjusted ideally above the background fluorescence as exemplified here, within the exponential phase of the PCR.

## 2.7.3 Preparation of 96 well plates for real-time PCR

### 2.7.3.1 Taqman assay reagents

qPCR core kit consisting of:

10 x reaction buffer

50mM magnesium chloride

5mM dNTP mix

5 U/ ml Hot Goldstar enzyme

Forward and reverse primers

Taqman probe

Ultra-pure water

### 2.7.3.2 Taqman assay method

Working solutions of primers and probes were reconstituted to produce a 100  $\mu$ M stock.

Each 12.5  $\mu$ l reaction contained the following:

<b><i>Component</i></b>	<b><i>Amount (<math>\mu</math>l) per well</i></b>
<b>10x buffer</b>	1.25
<b>MgCl<sub>2</sub></b>	1.25
<b>dNTP</b>	0.5
<b>Forward Primer</b>	0.038
<b>Reverse Primer</b>	0.038
<b>Probe</b>	0.063
<b>Hot Goldstar Enzyme</b>	0.0625
<b>Ultra-pure water</b>	8.3
<b>Total master mix volume per well</b>	11.5



A master mix sans cDNA was made up with a 2-well excess to allow for pipetting errors. 1 µl of the synthesised cDNA (equivalent to 10 ng of cDNA) was loaded into each well of a 96 well plate for RNA detection. Real-time amplification was performed in a final volume of 12.5 µl made up of cDNA, optimised concentrations of primers, Taqman probe (FAM-TAMRA) and a master mix made from a qPCR core kit (Eurogentech, Seraing, Belgium). Real time PCR amplification was performed in duplicates in a Strategene Mx3005P instrument. A non-template control well was added to each plate. The plate was spun at 500 x g for 1 minute to gather the contents to the bottom of the wells. The plate was inserted into the heat block of the Mx3005P qPCR instrument with an optical pad placed on top and aligned with the well positions. PCR cycling conditions were as follows: 95°C denaturation step for 10 minutes followed by 40 cycles (95°C denaturation step for 15 seconds and annealing-cum-extension step at 60°C for 1 minute). Data was collected automatically in real-time by the MxPro software and analysed at the end of the run.

#### 2.7.3.3 *SYBR Green assay reagents*

qPCR core kit consisting of:

10 x reaction buffer

50mM magnesium chloride

5mM dNTP mix

5 U/ ml Hot Goldstar enzyme

Forward and reverse primers

Ultra-pure water

#### 2.7.3.4 SYBR Green assay method

Working solutions of primers were reconstituted to produce a 100  $\mu$ M stock. Each 12.5  $\mu$ l reaction contained the following:

<b><i>Component</i></b>	<b><i>Amount (ul) per well</i></b>
<b>10x buffer</b>	1.25
<b>MgCl<sub>2</sub></b>	0.875
<b>dNTP</b>	0.5
<b>Forward Primer</b>	0.038
<b>Reverse Primer</b>	0.038
<b>SYBR Green dye</b>	0.375
<b>Hot Goldstar Enzyme</b>	0.062
<b>Ultra-pure water</b>	8.362
<b>Total master mix volume per well</b>	11.5

Real-time amplification of VDR and GLUT-4 RNA was performed by preparing a master mix sans cDNA was made up with a 2-well excess to allow for pipetting errors. 1 $\mu$ l of the synthesised cDNA (equivalent to 10 ng of cDNA) was loaded into each well of a 96 well plate for RNA detection. Real-time amplification was performed in a final volume of 12.5  $\mu$ l made up of cDNA and master mix. Real time PCR amplification was performed in duplicates in a Strategene Mx3005P instrument. A non-template control well was added to each plate. The plate was spun at 500 x g for 1 minute to gather the contents to the bottom of the wells. The plate was inserted into the heat block of the Mx3005P qPCR instrument with an optical pad placed on top and aligned with the well positions.

Real time PCR amplification was performed in duplicates and PCR cycling conditions were as follows: 95°C denaturation step for 10 minutes followed by 40 cycles consisting of a 95°C denaturation step for 15 seconds and an annealing-cum-extension step 60°C for 1 minute) and 1 dissociation cycle (95°C for 1 min, 55°C for 30 s and 95°C for 30 s). The dissociation step shows the number of PCR products and is used to gauge the specificity of the amplification. This is important as the SYBR Green dye is capable of binding to any double-stranded amplicon, which lowers its specificity.

#### **2.7.4 Analysis of real-time PCR data**

Amplification plots were converted to log scale using the MxPro software and the threshold was manually adjusted following these following parameters:

1. Linear phase of amplification

The threshold should be placed within the exponential phase of amplification across all the amplification plots. The linear region is depicted in the log plots and should not be placed too close to the plateau phase or the initial linear phase of amplification where it is too low and extends into the background fluorescence.

2. Precision maximization

The threshold should be set at a point where the most precise points of amplification can be measured. The precision of replicates tend to increase as the reaction progresses along the exponential phase. This is usually achieved by adjusting the threshold within the exponential range above the background noise.

3. Sensitivity maximization

The threshold should be set upon the point where it best reflects the orders of magnitudes across the assay.

The  $C_t$  values for each gene was exported to Microsoft Excel and gene expression was analysed by relative quantification by using the  $2^{-\Delta\Delta C_t}$  method (Livak and Schmittgen, 2001).  $\beta$ -actin was used as a reference gene. All samples were normalised to the  $\beta$ -actin  $C_t$  values and the results expressed as fold changes of  $C_t$  value relative to controls.

### **2.7.5 Primer and probe sequences**

The sequences of primers and probes for human  $\beta$ -actin, ZAG, Adiponectin, IL-1 $\beta$ , IL-6, MCP-1 and VDR are described in Table 2.1. The primers for human  $\beta$ -actin, ZAG, adiponectin and IL-6 are as described in Bao *et al.* (2005). The primer for MCP-1 is as described in Wang *et al.*, (2005). IL-1 $\beta$  and VDR primers were designed using Primer Premier 5 software (Biosoft International, California, USA) and synthesised commercially (Sigma, Poole, Dorset, UK).

**Table 2.6 Primer and probe sequences of human target genes**

<i>Transcript</i>	<i>Primer sequence</i>
Human $\beta$ -actin	
Forward	5'-GGATGCAGAAGGAGATCACTG-3'
Reverse	5'-CGATCCACACGGAGTACTTG-3'
Probe	5'-FAM-CCCTGGCACCCAGCACAATG-TAMRA
Human ZAG	
Forward	5'-ACGACAGTAACGGGTCTCACGTA-3'
Reverse	5'-TCCTTTCCATCATAGTAATATTTCCAGAA-3'
Probe	5'-FAM-CAGGGAAGGTTTGGTTGTGAGATCGAGAATAAC-TAMRA
Human Adiponectin	
Forward	5'-CCCAAAGAGGAGAGAGGAAGCT-3'
Reverse	5'-GCCAGAGCAATGAGATGCAA-3'
Probe	5'-FAM-TTCCCAGATGCCCCAGCAAGTGTAAC-TAMRA
Human IL-6	
Forward	5'-GGTACATCCTCGACGGCATCT-3'
Reverse	5'-GTGCCTCTTTGCTGCTTTCAC-3'
Probe	5'-FAM-TGTTACTCTTGTTACATGTCTCCTTTCTCAGGGCT-TAMRA
Human MCP-1	
Forward	5'-CATAGCAGCCACCTTCATTCC-3'
Reverse	5'-TCTGCACTGAGATCTTCTATTGG-3'
Probe	5'-FAM-CAGCCAGATGCAATCAATGCCCC-TAMRA
Human IL-1 $\beta$	
Forward	5'-TGGCCCTAACAGATGAAGTGC-3'
Reverse	5'-GTAGTGGTGGTCGGAGATTCG-3'
Probe	5'-FAM-ACCTGGACCTCTGCCCTCTGGATGG-TAMRA
Human VDR (SYBR green)	
Forward	5'-AAGCGGAAGGAGGAGGAG-3'
Reverse	5'-TGGCAGAAGTCGGAGTAGG-3'

## **2.8 Enzyme-linked immunosorbent assay (ELISA)**

### **2.8.1 ELISA principles**

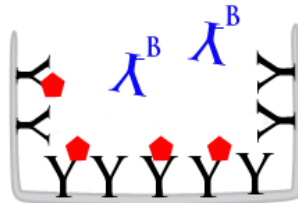
Enzyme-linked immunosorbent assay (ELISA) is a biochemical technique used to detect the release of proteins by human primary adipocytes (Engvall and Perlmann, 1971). A molecule of protein is detected by antibodies that have been made against it. The ELISA kits used in this study are suited for the measurement of natural or recombinant target proteins produced by human cells and are designed for the analysis of cell culture supernates. The technique involves the capture of target proteins from cell culture supernates to the wells of a microtiter plate coated with a monoclonal antibody against the target protein. The coated wells are first blocked of non-specific binding sites before incubating with cell culture supernates. The wells are then washed with a washing buffer and a secondary biotinylated detection antibody (anti-human target protein antibody) is added and incubated to bind with the antigens. Unbound antibodies are washed away and a streptavidin-horseradish peroxidase conjugate is added, which binds to the biotin on the detection antibody. The unbound conjugates are washed away and a substrate solution consisting of equal volumes of hydrogen peroxide and tetramethylbenzidine (TMB) is added and the wells are incubated at room temperature. The horseradish peroxidase (HRP) enzyme catalyzes the electron transfer from TMB to the peroxide, oxidising TMB and a blue colour develops. Colour development is stopped by adding an acid, turning the solution colours to yellow. The absorbance is subsequently measured at 450nm with a wavelength correction set to 570nm. Adiponectin, IL-1 $\beta$ , IL-6 and MCP-1 in cell culture

medium were measured using this method in DuoSet ELISA Development kits purchased from R&D (Abingdon, UK).

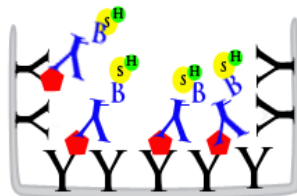
**Figure 2.4 Schematic diagram of ELISA**



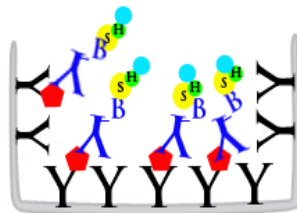
Plates are coated with antibodies specific for protein of interest. Unbound antibodies are washed away, then blocked to prevent non-specific binding. Samples are added to bind to immobilized antibodies in wells.



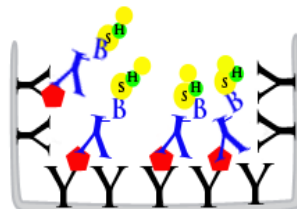
Biotin-labeled detection antibodies specific for protein of interest is added, which binds to a second epitope on the antibody-bound protein.








Streptavidin-HRP is added and binds to the biotin-labeled detection antibody.



TMB substrate in the presence of peroxide as an oxidising agent, is oxidised by HRP to produce a blue colour.



The reaction is halted by added an acidic stop solution, which converts the TMB solution to a yellow colour.

-  TMB
-  Capture antibody
-  Detection antibody-biotin conjugate
-  Horseradish peroxidase-Streptavidin conjugate
-  Protein of interest

Diagrammatic representation of an enzyme-linked immunosorbent assay.



Human ZAG was measured in cell culture medium using an ELISA kit purchased from BioVendor (Heidelberg, Germany). The ELISA technique used was slightly different from the other kits used in the study. Wells pre-coated with polyclonal anti-human ZAG were incubated with samples and standards and the wells were subsequently washed of unbound material. Instead of using a biotinylated detection antibody, polyclonal anti-human ZAG antibodies conjugated with HRP were added to the wells, incubated and washed. The bound HRP conjugates are then allowed to react with the TMB substrate solution to produce a blue colour and the reaction was subsequently stopped with acid solution. The resulting yellow product is measured at 450nm with a reference wavelength of 630nm. Unknown concentrations were determined using a standard curve constructed by plotting absorbance values against known concentrations of standards in the Microplate Manager version 5.2 software provided by Bio-Rad.

## **2.8.2 Method**

### *2.8.2.1 MCP-1, IL-6, Adiponectin, IL-1 $\beta$ ELISA using R&D Systems development kits*

#### *Reagents and equipment*

Phosphate-buffered saline (PBS)

Reagent diluents (1% BSA in PBS)

Capture antibody (Diluted to working concentration with PBS)

Detection antibody (diluted to working concentration with reagent diluent)

Recombinant human standard (Diluted in various 2-fold serial dilutions for 7 point standard curve, excluding blank)

Streptavidin-HRP

Wash buffer (0.05% Tween-20 in PBS)

Substrate solution mixture (1:1 in volume of hydrogen peroxide and tetramethylbenzidine)

Stop solution (2M Sulphuric acid)

96-well MaxiSorp® flat-bottom microplate

Benchmark™ Plus Microplate Spectrophotometer

Multi-channel pipette

The capture antibody is diluted with PBS to produce a working solution (Table 2.2). A 96-well MaxiSorp® flat-bottom microplate was coated with 100 µl of antibody working solution and sealed to incubate overnight. The wells were washed with wash buffer the following day using a multi-channel pipette and plates were blocked with 300 µl of reagent diluent for an hour. The wells were washed with wash buffer again and 100 µl of sample and diluted standards were added to each well in duplicates. The wells were covered with an adhesive strip and left to incubate at room temperature for 2 hours. The wells were washed with wash buffer again and 100 µl of detection antibody working solution (Table 2.2) was added to each well. The wells were incubated for 2 hours and washed again with wash buffer. 100 µl of Streptavidin-HRP was then added to each well and incubated for 20 minutes at room temperature, taking care not to expose the plate to direct light. The wells were washed with wash buffer. 100 µl of substrate solution was then added to each well and incubated for another 20 minutes or till the colour was

developed satisfactorily. When a satisfactory development end-point had been reached, 50  $\mu$ l of Stop Solution was added to each well and the wells were gently tapped to ensure thorough mixing. The optical density was determined by reading the plate in the microplate spectrophotometer at 450nm with a reference wavelength of 570nm to correct for optical imperfections on the plate. The concentrations of proteins were determined using the standard curve generated, ensuring any dilution factors used were entered into the calculation. Samples treated with macrophage-conditioned medium were diluted 1 in 6 for IL-6 determination and 1 in 10 for MCP-1 determination based on pilot studies. Adiponectin and IL-1 $\beta$  was analysed neat. Data was collected and plotted using the Microplate Manager v5.2 software. A standard curve was generated and points were plotted to achieve a best-fit correlation coefficient of >0.96. The ideal correlation coefficient is 1, although an R-value of more than >0.96 was accepted for generated standard curves. The equation of the best-fit curve or line was used to calculate the concentration of proteins.

**Table 2.7 Antibody and standard concentrations used for ELISA**

<b>Protein measured</b>	<b>Capture antibody working solution concentration</b>	<b>Detection antibody working solution concentration</b>	<b>Concentration of S1 (first point)</b>
<b>Human adiponectin</b>	2.0 µg/ ml	2.0 µg/ ml	4000 pg/ ml
<b>Human IL-1β</b>	4.0 µg/ ml	200 ng/ ml	250 pg/ ml
<b>Human IL-6</b>	2.0 µg/ ml	50 ng/ ml	600 pg/ ml
<b>Human MCP-1</b>	1.0 µg/ ml	100 ng/ ml	1000 pg/ ml

2.8.2.2 *ZAG ELISA using BioVendor kits*

*Reagents and equipment*

Antibody coated microtitre strips

Conjugate solution

Substrate solution

Stop solution

Dilution buffer concentrate 2x (diluted in double distilled water to prepare 1x working solution)

Recombinant human ZAG master standard

Streptavidin-HRP

Wash solution concentrate 10x (diluted ten-fold in distilled water to prepare 1x working solution)

Double distilled water

Sterile centrifuge tubes

Orbital microplate shaker

Benchmark<sup>TM</sup> Plus Microplate Spectrophotometer

Multi-channel pipette

100 µl of diluted standard and dilution buffer (as blank) and samples were pipette into assigned wells. The plate was incubated at room temperature for 1 hour on the orbital microplate shaker. Wells were washed thrice with wash solution using a multi-channel pipette. 100 µl of conjugate solution was added into each well and the plate was incubated for 1 hour at room temperature on the orbital microplate shaker. The wells were washed thrice again and tapped strongly against a paper towel to remove excess wash solution. 100 µl of substrate solution was added into each well, ensuring the plate was not exposed to direct sunlight. The plate was incubated for 10 minutes and checked for its colour. More time was given for it to develop if the development was unsatisfactory (possibly due to colder room temperatures). The colour development was stopped by adding 100 µl of stop solution. The OD for each well was read at 450nm with a reference wavelength of 630nm to correct for plate imperfections. Concentrations of proteins were determined from a standard curve generated using the Microplate Manager v5.2 software. A standard curve was generated and points were plotted to achieve a best-fit correlation coefficient of >0.96. The ideal correlation coefficient is 1, although an R-value of more than >0.96 was accepted for generated standard curves. The equation of the best-fit curve or line was used to calculate the concentration of proteins.

## 2.9 Protein detection using western blotting

### 2.9.1 Western blotting principles

The western blotting technique (Towbin *et al.*, 1979) was used to detect protein expression within human primary adipocytes. Cell lysates were collected with lysis buffer added with protease and phosphatase inhibitor cocktails. *A priori*, a protease inhibitor cocktail serves to prevent resident and exogenous proteases from breaking down proteins in the lysate. Similarly, a phosphatase-inhibitor cocktail was added to the lysis buffer to prevent phosphatases from breaking down phosphorylated proteins (i.e. phosphorylated p38 MAPK signalling proteins). Cell lysates were first quantified by the bicinchoninic acid (BCA) method. The concentration value of proteins measured by the BCA method was obtained and used to calculate the amount of lysate that should be added to each well. Lysates were then stained with a loading buffer containing SDS and  $\beta$ -Mercaptoethanol. SDS gives the protein a negative charge and  $\beta$ -Mercaptoethanol prevented the reformation of disulphide bonds. Diluted lysates were then added to each well of a sodium dodecyl sulphate polyacrylamide gel electrophoresis (SDS-PAGE) gel (Shapiro *et al.*, 1967). After the proteins were sufficiently separated electrophoretically, they were transferred from the gel to a nitrocellulose membrane and probed using antibodies binding-specifically to a protein of interest. Western blotting relies on the ability of the primary antibody to detect the protein of interest from the total amount of protein in each individual lysate. To achieve this, the nitrocellulose membrane is blocked with a solution of bovine serum albumin or skimmed milk before the addition of a

primary antibody. A secondary antibody-HRP conjugate specific to the primary antibody used is then added to bind to the nitrocellulose membrane. The HRP conjugated to the secondary antibody converts a luminol substrate to a chemiluminescent substance and the signal intensity is then detected with the CCD camera of the ChemiDoc™ XRS+ molecular imager. Western blotting was used in this study as a semi-quantitative method to assess the relative expression of proteins between treatment groups.

## **2.9.2 Protein quantification by the Bicinchoninic acid method**

### *2.9.2.1 Reagents and equipment*

Bicinchoninic acid solution

Copper (II) sulphate solution

1 mg/ ml bovine serum albumin protein standard

Double distilled water

96-well microplate

Orbital microplate shaker

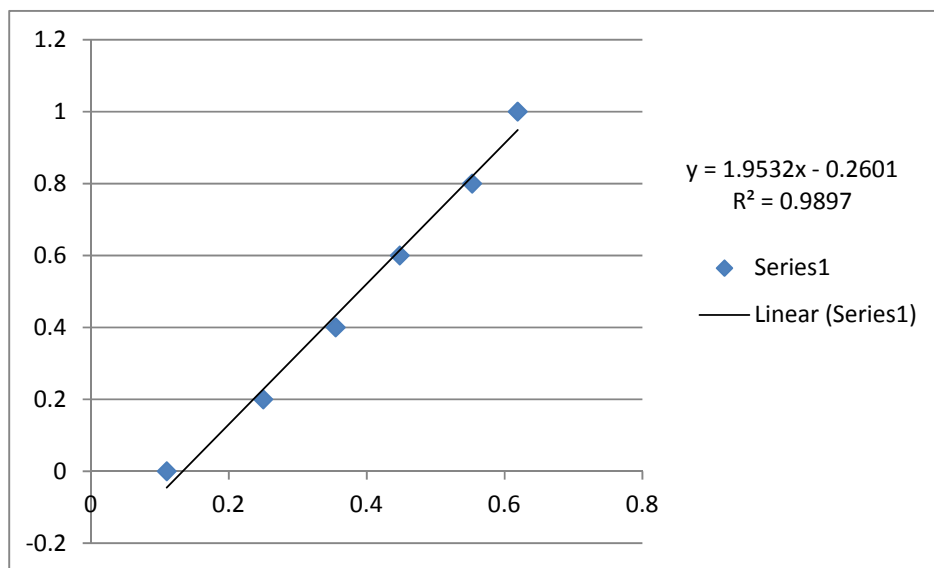
Benchmark™ Plus Microplate Spectrophotometer

Total cellular protein was measured using the bicinchoninic acid method (Smith *et al.*, 1985). Total cellular protein samples were prepared by lysing cells in lysis buffer (50mM Tris-HCl, pH 6.7, 10% Glycerol, 4% SDS, 2% 2-mercaptoethanol) with freshly added protease inhibitor cocktail and phosphatase inhibitor cocktail (both from Sigma, Poole, Dorset, UK). A standard curve was plotted by serial diluting a bovine serum albumin

(BSA) standard with double distilled water with final concentrations of 0.2, 0.4, 0.6, 0.8, 1.0 mg/ ml. Cell lysates were 0.5x diluted in wells by pipetting 5  $\mu$ l of double distilled water to 5  $\mu$ l of cell lysate. A 50:1 bicinchoninic acid to copper sulphate solution was prepared and 200  $\mu$ l of this mixture was added to each well of a diluted sample or standard. The plates were shaken on an oscillator for 1 minute and then incubated in an hybridization oven for 30 minutes. The plate was then read in a spectrophotometer at 570nm. The concentrations of proteins were determined using the standard curve generated (Figure 2.5) and multiplying it by a dilution factor of 2. Data was collected and plotted using the Microplate Manager v5.2 software. A standard curve was generated and points were plotted to achieve a best-fit correlation coefficient of  $>0.99$ . The ideal correlation coefficient is 1, although an R-value of more than  $>0.99$  was accepted for generated standard curves. The equation of the best-fit curve or line was used to calculate the concentration of proteins of lysates.



**Figure 2.5 Standard curve generation for Bicinchoninic acid method**



A sample standard curve was generated using a diluted BSA standard. Standard curve was used to determine protein concentrations of samples.

## **2.9.4 Sodium dodecyl sulphate polyacrylamide gel electrophoresis (SDS-PAGE)**

### *2.9.4.1 Reagents and equipment*

PageRuler protein marker (Fermentas)

#### *Loading buffer*

1 ml 0.5M Tris-HCL, pH 6.8

1.6 ml 10% SDS

0.4 ml  $\beta$ -Mercaptoethanol

1 ml Glycerol

0.01g Bromophenol blue

#### *3 x Gel Buffer*

18.16g Trizma base

10 ml 5M hydrochloric acid

0.75 ml 20% SDS

Double-distilled water (made up to 50 ml total volume)

#### *Separating gel*

2 ml 48% acrylamide/ 1.5% bisacrylamide mix

3.64 ml double distilled water

3.3 ml 3 x gel buffer

1 ml glycerol

50 µl ammonium persulphate

6 µl tetramethylethylenediamine (TEMED)

*Stacking gel*

0.4 ml 48% acrylamide/ 1.5% bisacrylamide mix

3.36 ml double distilled water

1.2 ml 3 x gel buffer

40 µl ammonium persulphate

4 µl TEMED

*Cathode buffer*

12.11g Trizma base (100 mM)

17.92g Tricine (100 mM)

5 ml 20% SDS (0.1%)

Double distilled water (made up to 1000 ml total volume)

*Anode buffer*

24.22 Trizma base

6 ml 1M hydrochloric acid

Double distilled water (made up to 2000 ml total volume)

*Gel electrophoresis equipment*

Bio-Rad Mini-PROTEAN™ Tetra System

2.0 mm notched glass plates

2.0 mm plain glass plates

1.0mm comb, 10 or 15 wells

Casting base with silicone seals

Components were mixed together in a sterile 2 ml centrifuge tube to make the loading buffer. Any unused loading buffer was stored at -20°C for not more than 3 months. All gel electrophoresis components were cleaned with ethanol, dried and assembled according to the manufacturer's instructions. The glass plates were assembled and locked into position onto the casting base. Distilled water was first poured between the glass plates to ensure there were no leaks. The water was removed using filter paper. The separating gel was prepared and pipetted quickly and carefully between the glass plates, preventing the formation of bubbles and leaving a third of the space for the stacking gel. 0.1% SDS was added to the top of the gel to prevent the gel from drying out while it sets. Once the gel had set, the SDS was tipped out and the excess was removed with filter paper. The stacking gel was prepared and pipetted to fill the remaining third of space between the glass plates. The comb was promptly inserted and the stacking gel was allowed to set for 30 minutes. Samples were diluted 10x with loading buffer and placed in a heating block at 80°C to denature proteins for 5 minutes. The combs were removed and gels were taken off the casting base and assembled into the gel tank. The tank was then filled with cathode buffer between the glass plates to the brim to completely submerge the gel. 40µg of each sample was added to each lane and a PageRuler™ protein marker was added to occupy one lane. Anode buffer was added to the exterior compartment to the designated mark. The electrodes were connected and run at 45V for

an hour for distinct separation of cells and then 85V till the bromophenol blue dye runs out of the gel.

## **2.9.5 Electroblotting**

### *2.9.5.1 Reagents and equipment*

#### *Transfer buffer*

3.03g Tris-base (25mM)

14.4g Glycine (192mM)

200 ml methanol (20%)

Double distilled water (made up to 1000ml volume)

#### *Electroblotting equipment*

Fibre pads

Thick blotting paper

Hybond ECL nitrocellulose membrane

Compression Cassettes

Bio-Rad Mini-PROTEAN™ Tetra cell running tank

Internal electroblotting adapter

*0.1% TTBS*

0.1% Tween-20

20 mM Tris-base

500 mM sodium chloride

Double distilled water

Filter paper and nitrocellulose membrane was soaked in distilled water and then transfer buffer. The cassettes were opened and the sandwich was assembled by laying components in the following order from the bottom: foam pad – blotting paper – transfer membrane – gel – blotting paper – foam pad. Care was taken to ensure there were no bubbles between the transfer membrane and gel. The cassettes were closed and locked and inserted into the adapter. The setup was run at 100V for 70 minutes. The membrane was washed in a 0.1% TTBS and stained in Ponceau S solution. The membrane was briefly rinsed and the gel was scanned using an HP precision imaging scanner.

## **2.9.6 Immunological detection of proteins**

### *2.9.6.1 Reagents and equipment*

5% BSA in 0.1% TTBS (Blocking solution)

0.1% TTBS

Primary antibodies

Secondary antibodies

Luminol enhancer and stable peroxide buffer (Supersignal® West Pico ECL kit)

The membrane was washed of Ponceau S stain and blocked with 5% BSA for 30 minutes at room temperature. Primary antibodies were added to the BSA incubation solution to a 1:1000, 1:2000 or 1:20,000 ratio depending on the instructions furnished on the insert.

The membrane was incubated on a shaking platform overnight at 4°C. Monoclonal

antibodies were preferred over polyclonal antibodies to reduce the background associated with non-specific binding. The membranes were washed were 10 minutes 4 times with fresh 0.1% TTBS each time on a shaking platform. The membrane was submerged in 5% BSA and secondary antibodies conjugated with HRP were added to a ratio according to the insert provided and incubated for 1 hour at room temperature on a shaking platform. The membrane was subsequently washed for 4 times again in 0.1% TTBS for 10 minutes each time. To reduce the signal induced by Tween-20, the membrane was rinsed in TBS before moving on to the enhanced chemiluminescence (ECL) step. The luminol enhancer and stable hydroxide peroxide solution was added in a 1:1 ratio, incubated for 1 minute and the excess solution mixture was dripped off. The membrane was enclosed in clear plastic folder, carefully ensuring bubbles were not introduced into the folder. The development was scanned in the ChemiDoc™ XRS+ System and the cumulative signals were read over a period of 40 minutes. The antibody concentrations and conditions reflected in Table 2.8 were used for each probe.

**Table 2.8 Antibody dilutions and conditions used for western blots**

<b>Antibodies</b>	<b>Provider</b>	<b>Dilutions</b>	<b>Incubating solution</b>
<b>GAPDH (Housekeeping protein)</b>	Abcam	1:2000	5% BSA in TBS and 0.1% Tween-20
<b>Human I<math>\kappa</math>B<math>\alpha</math></b>	New England Biolabs	1:1000	5% BSA in TBS and 0.1% Tween-20
<b>Insulin-receptor 1<math>\beta</math></b>	Sigma	1:1000	5% skimmed milk in TBS and 0.1% Tween-20
<b>Phosphorylated NF-<math>\kappa</math>B p65</b>	Sigma	1:1000	5% BSA in TBS and 0.1% Tween-20
<b>Phosphorylated p38 MAPK</b>	New England Biolabs	1:1000	5% BSA in TBS and 0.1% Tween-20

### **2.9.7 Relative quantitation of proteins**

The optical density of band images produced by the molecular imager was determined by densitometry using the Image Lab software provided along with the Chemidoc XRS+ molecular imager. The volume values were exported to Excel and the relative densities were measured against the optical density for GAPDH as a housekeeping reference protein.



## **2.10 Cytotoxicity tests**

### **2.10.1 LDH Assay**

#### *2.10.1.1 Principles*

The cell-free culture medium is incubated with substrate mixture using a colourimetric cytotoxicity detection kit (Roche Diagnostics GmbH, Mannheim, Germany). LDH activity is determined using a coupled enzymatic reaction where the tetrazolium salt is reduced to formazan. The water-soluble formazan dye is measured at 492nm with a reference wavelength of 620nm. The formazan dye intensity increases with the amount of LDH enzyme activity associated with an increase in the number of dead cells.

#### *2.10.1.2 Method*

##### *Reagents and equipment*

Catalyst (Diaphorase/NAD + mixture)

Dye solution (INT and sodium lactate)

Benchmark™ Plus Microplate Spectrophotometer

96-well microplate

Orbital microplate shaker

The release of lactate dehydrogenase (LDH) into the cell culture medium after treatment with 25% THP-1 MC medium or 25% RPMI, with or without calcitriol, was performed using a colourimetric cytotoxicity detection kit (Roche Diagnostics GmbH, Mannheim,

Germany). LDH concentration was measured with a spectrophotometer at 492nm with a reference wavelength of 620 nm at room temperature.

## **2.11 Transmigration assay**

### **2.11.1 Principles**

The Chemicon QCM™ 5µm 96-well Migration Assay is used for this technique based on the Boyden chamber (Boyden, 1962). Migratory cells on the bottom of the insert membrane dissociate from the membrane when incubated with Cell Detachment Buffer. These cells are subsequently lysed and detected by the MTT assay method. The MTT assay is a colorimetric assay that measures the reduction of yellow 3-(4,5-dimethylthiazol-2-yl)-2,5-diphenyltetrazolium bromide (MTT) by mitochondrial succinate dehydrogenase. The MTT solution enters the cell mitochondria where it is reduced to a dark purple formazan product. The cells are then solubilised with a lysis buffer with an organic solvent and the released solubilised formazan product is measured spectrophotometrically. This assay works with the principle that reduction of MTT was only occur in metabolically active cells with mitochondrial activity and the intensity of formazan product can only be measured with live cells. Most migration assays utilise an 8µm pore size, as this is appropriate for most cell types, e.g. epithelial and fibroblast cells. However the Chemicon QCM™ 5µm 96-well Migration Assay features a 5µm pore size, which was chosen for its suitability for studying monocyte/macrophage migration.

### 2.11.2 Method

#### *Reagents and equipment*

QCM™ Chemotaxis 5µm 96-Well Cell Migration Assay kit consisting of a feeder tray and cell suspension chamber inserts

RPMI-1640 medium

Cell culture medium samples

THP-1 cell monocyte suspension

5 mg/ ml MTT solution

*Lysis buffer consisting of:*

20% SDS

50% dimethylformamide

2% glacial acetic acid to adjust solution to pH 4.7

Orbital microplate shaker

Benchmark™ Plus Microplate Spectrophotometer

Pipette and sterile pipette tips

Human THP-1 monocytes were prepared at a density of  $2 \times 10^6$  cells/ml in 11 ml of RPMI 1640 medium. THP-1 cells were counted to obtain a total of  $22 \times 10^6$  cells for a 96-well analysis. Cells were centrifuged for 5 minutes and washed once with RPMI1640 medium. Cells were then resuspended to its former density in RPMI-1640 medium. 150 µl of human primary adipocyte culture medium from the cell culture treatments were added into the wells of the feeder tray of a QCM™ Chemotaxis 5µm 96-Well Cell

Migration Assay kit (Fisher Scientific, Loughborough, UK). 100  $\mu$ l of THP-1 monocyte suspension was added into the cell suspension chamber. The plate was covered and incubated for 4 hours at 37°C in a humidified atmosphere of 5% CO<sub>2</sub> and 95% air. A cell density curve plate containing a series of human THP-1 cell concentrations was also prepared concurrent to the test plate. 25  $\mu$ l of MTT solution (5 mg/ml in PBS, 0.22  $\mu$ m filtered) was added to the wells of the feeder tray and standard curve plate and incubated for 4 hours. 50  $\mu$ l MTT lysis buffer was added to each well and the wells were incubated overnight. The wells were read spectrophotometrically at 570 nm in a plate reader. Cell numbers from each OD reading were calculated based on the cell density standard curve.

## **2.12 Statistical analysis**

All results are presented as means  $\pm$  standard deviation (SD) and group size varied between experiments. Differences between two groups were analysed by Student's unpaired t-test, while differences among more than two groups were assessed by one-way ANOVA coupled with Bonferroni's *t*-test. Differences were considered as statistically significant when  $P < 0.05$ . All P-values were two-sided. Statistical tests were performed using Graphpad Prism version 5.03 (Graphpad software Inc., California, USA) and SPSS (PASW), release version 19.0 (IBM SPSS, Feltham, UK)

## **Chapter 3**

# **Macrophage-induced inflammatory response in human primary adipocytes**

### 3.1 Introduction

Several researchers have found that the increased macrophage infiltration in adipose tissue in obesity provides a central link between inflammation and metabolic disease (Weisberg *et al.*, 2003; Cancello *et al.*, 2005, Curat *et al.*, 2006). It is believed that macrophage infiltration of adipose tissue contributes to low-grade inflammation, causing a chronic elevation of inflammatory cytokines in the systemic circulation which is commonly associated with metabolic disease.

Macrophage-secreted factors have been shown to exert profound effects on the behaviour of adipose tissue. Some effects include the decrease of adiponectin production in preadipocytes (Constant *et al.*, 2006), stimulating leptin expression in mice adipose tissue (Hirasaka *et al.*, 2007) and the expression of many inflammation-related genes in human adipocytes (O'Hara *et al.*, 2009). Recent studies by our group showed the decrease in production of zinc- $\alpha$ 2-glycoprotein (ZAG) by human primary adipocytes incubated with macrophage-conditioned medium (Gao *et al.*, 2010). Gao and Bing (2011) also showed an upregulation of matrix metalloproteinases MMP1 and MMP3 which are involved in adipose tissue remodelling and inflammatory responses in obesity. It was postulated in Fain (2006) that many of these effects caused by inflammatory mediators produced by macrophages and cells of the SVF.

There is, however, a lack of studies that seek to define the mechanisms of inflammation resulting from specifically human primary adipocyte and macrophage crosstalk. This is

particularly important as current evidence suggests that this crosstalk can modulate adipocyte responses (Suganami *et al.*, 2005). The evidence also suggests that adipokines produced by adipocytes present the initial errant signal that could possibly spark off the 'inflammatory chain reaction'. The vast expanse of the adipose organ throughout the human body would also mean that any change, even if small in magnitude, is capable to producing important paracrine and endocrine outcomes - especially in the long-term.

*In vitro* studies on human primary adipocytes, therefore, are essential to find the exact effect by which macrophages increase inflammation in fat tissue. Such a model allows better resolution of a cause-effect relationship as one is able to eliminate more confounding variables compared to an *in vivo* model. This study features the novel use of human adipocytes and monocytes with the purpose of enhancing the clinical relevancy of the findings. The use of a 25% THP-1 monocyte conditioned medium also creates a physiological model for macrophage infiltration within adipose tissue. Macrophage-conditioned medium is obtained from PMA-differentiated THP-1 monocytic cells maintained in RPMI-1640 medium for 24 hours to collect cytokines and chemokines secreted by THP-1 macrophages. This may include TNF- $\alpha$ , IL-6, MCP-1, RANTES, IL-8 (Gao *et al.*, 2010) and IL-1 $\beta$  (Xu *et al.*, 2003; Wen *et al.*, 2011). The harvested THP-1 conditioned medium, diluted to 25% with cell maintenance medium, is used for the studies of crosstalk between macrophages and human primary adipocytes. To study the specific effect of TNF- $\alpha$ , a proinflammatory cytokine produced by macrophages, cells are incubated with TNF- $\alpha$  to identify its specific effect on human primary adipocytes.

## **3.2 Changes in proinflammatory mediator production by human primary adipocytes stimulated by macrophage-secreted factors**

### **3.2.1 Gene expression and secretion of MCP-1, IL-6 and IL-1 $\beta$ by adipocytes stimulated with macrophage-conditioned medium or TNF- $\alpha$**

Human primary adipocytes (at day 13 post-differentiation) were incubated with 25% MC medium or 25% RPMI medium for 24 hours to assess the effects on macrophage-derived factors on adipocyte production of MCP-1, IL-6 and IL-1 $\beta$ . A separate group of adipocytes were also incubated with or without 5 ng/ ml of TNF- $\alpha$  for 24 hours to determine if the augmentation of inflammatory molecule production is induced by TNF- $\alpha$  production. The results show that gene expression of MCP-1, IL-6 and IL-1 $\beta$  in adipocytes is increased by factors produced by macrophages. The increase is also observed in adipocytes incubated with 5 ng/ ml TNF- $\alpha$ , suggesting that TNF- $\alpha$  is a key participant in the proinflammatory response of adipocytes.

#### *3.2.1.1 MC medium increases MCP-1 gene expression in adipocytes with 25% MC medium stimulation*

MCP-1 gene expression was increased 22-fold when incubated with 25% MC medium when compared to MCP-1 gene expression in control adipocytes (Figure 3.1A).



#### *3.2.1.2 TNF- $\alpha$ stimulates MCP-1 gene expression in adipocytes*

MCP-1 gene expression were increased 55-fold when incubated with 5 ng/ ml TNF- $\alpha$  ( $P < 0.001$ ; Figure 3.1A).

#### *3.2.1.3 MC medium increases IL-6 gene expression in adipocytes*

It is observed that IL-6 gene expression in adipocytes incubated with 25% MC medium was increased 467-fold compared to controls ( $P < 0.001$ ; Figure 3.1B).

#### *3.2.1.4 TNF- $\alpha$ stimulates IL-6 gene expression in adipocytes*

IL-6 gene expression in cells treated with 5 ng/ ml TNF- $\alpha$  increased 51-fold ( $P < 0.001$ ; Figure 3.1B) compared to controls.

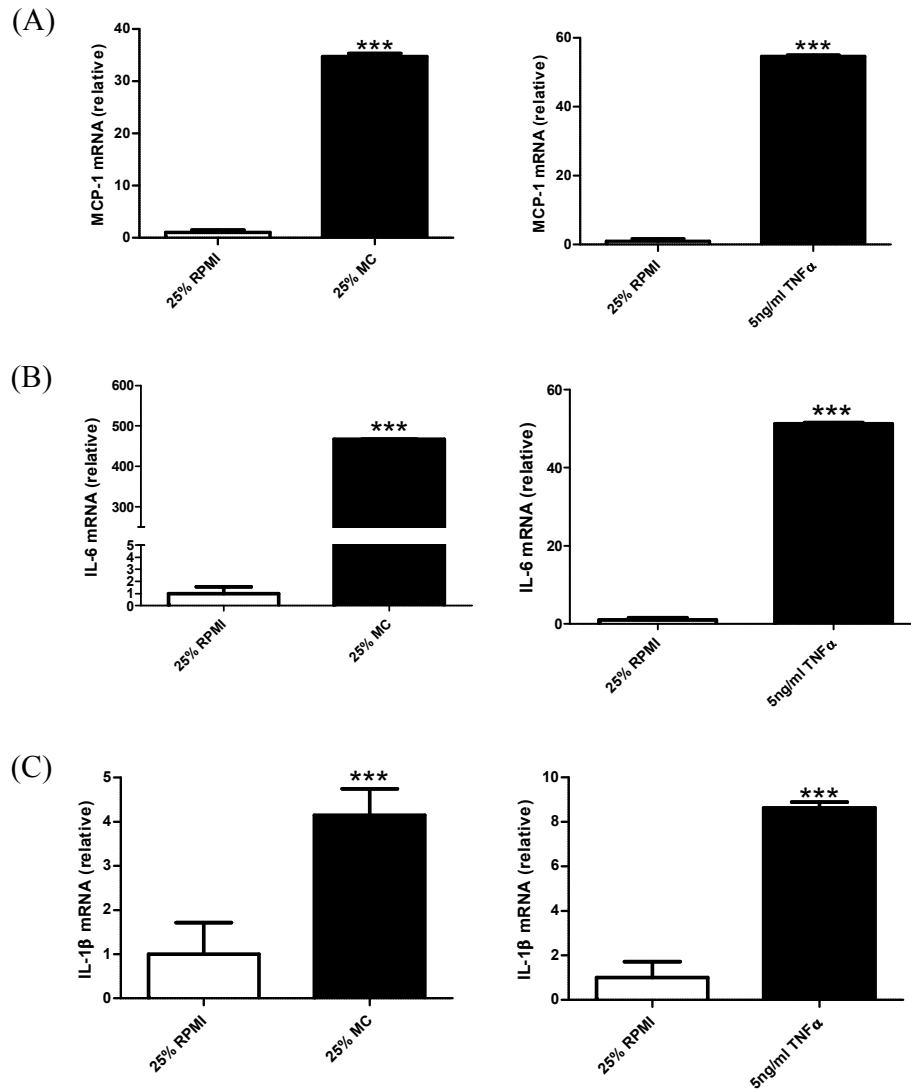
#### *3.2.1.5 MC medium increases IL-1 $\beta$ gene expression in adipocytes*

IL-1 $\beta$  gene expression was increased 4.2-fold in cells treated with 25% MC medium compared to controls ( $P < 0.001$ ; Figure 3.1C).

#### *3.2.1.6 TNF- $\alpha$ stimulates IL-1 $\beta$ gene expression in adipocytes*

IL-1 $\beta$  gene expression increased 8.6-fold in cells treated with 5 ng/ ml TNF- $\alpha$  medium compared to control cells ( $P < 0.001$ ; Figure 3.1C).

**Figure 3.1 Gene expression of MCP-1, IL-6 and IL-1 $\beta$  in adipocytes stimulated with 25% MC medium or TNF- $\alpha$**



Gene expression of MCP-1 (A), IL-6 (B) and IL-1 $\beta$  (C) in human primary adipocytes (day 13 post differentiation) stimulated with 25% MC medium or 5ng/ ml TNF- $\alpha$ . Cell culture maintenance medium was replaced with 25% MC medium in maintenance medium (25% MC) on day 13 post-differentiation. For the TNF- $\alpha$  study, medium was replaced with TNF- $\alpha$  in 25% RPMI (25% RPMI + 5ng/ ml TNF $\alpha$ ). Medium for a group of cells was replaced with 25% RPMI-1640 in maintenance medium (25% RPMI) as a control. Cells were harvested after 24 hours. Gene expression in adipocytes incubated with 25% MC medium, measured by real-time PCR and normalised to  $\beta$ -actin, are expressed relative to control. Results are given as means  $\pm$  SD for groups of 6. \*\*\*P < 0.001 vs control (unpaired Student's *t*-test).

### **3.2.2 Protein secretion of MCP-1 and IL-6 by adipocytes stimulated with macrophage-conditioned medium or TNF- $\alpha$**

Protein release of MCP-1, IL-6 and IL-1 $\beta$  by adipocytes was measured as concentrations in cell culture medium by ELISA. IL-1 $\beta$  levels could not be established from ELISA analysis as the levels produced by adipocytes in 1 ml of medium were lower than the detection limit of the method.

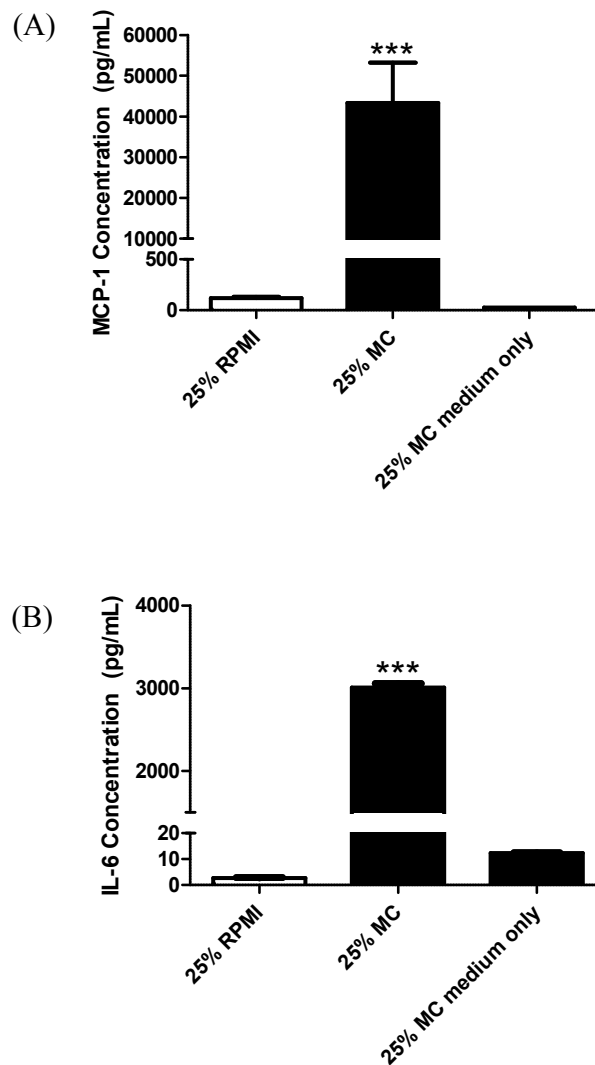
#### *3.2.2.1 MCP-1 production was increased by MC medium*

MCP-1 release by adipocytes treated with 25% MC medium was increased 40-fold compared to the basal MCP-1 production by control adipocytes ( $P < 0.001$ ; Figure 3.2A) after correcting for macrophage-secreted MCP-1 in 25% MC medium ( $52.9 \pm 0.8$  pg/ ml)

#### *3.2.2.2 IL-6 production was increased by MC medium*

IL-6 release by adipocytes treated with 25% MC medium was increased 1124-fold ( $P < 0.001$ ; Figure 3.2) after correcting for basal levels of IL-6 in 25% MC medium ( $12.26 \pm 0.06$  pg/ ml).

**Figure 3.2 MCP-1 and IL-6 release by adipocytes stimulated with 25% MC medium**



MCP-1 and IL-6 protein levels in cell culture medium of adipocytes were measured by ELISA. Basal levels of MCP-1 and IL-6 in 25% MC medium were determined by ELISA with a mean of  $52.9 \pm 0.8$  pg/ml and  $12.26 \pm 0.06$  pg/ml respectively. Results are given as means  $\pm$  SD for groups of 3-4 for IL-6, groups of 6 for MCP-1. \*\*\* $P < 0.001$  vs control (25% RPMI; Unpaired student's *t*-test).

### **3.3 Effects of macrophage-secreted factors on adipokine production by human primary adipocytes**

#### **3.3.1 Gene expression of adiponectin and ZAG**

##### *3.3.1.1 MC medium decreases adiponectin gene expression*

Groups of cells treated as described in section 3.2.1 were also measured for adipokine mRNA level. There was an 8-fold decrease in the gene expression level of adiponectin in adipocytes stimulated by 25% MC medium, compared to its basal levels in unstimulated adipocytes ( $P < 0.001$ ; Figure 3.3A).

##### *3.3.1.2 TNF- $\alpha$ decreases adiponectin gene expression*

Cells treated with 5 ng/ ml of TNF- $\alpha$  showed a 2.7-fold decrease in adiponectin gene expression compared to basal expression levels in unstimulated adipocytes ( $P < 0.001$ ; Figure 3.3A).

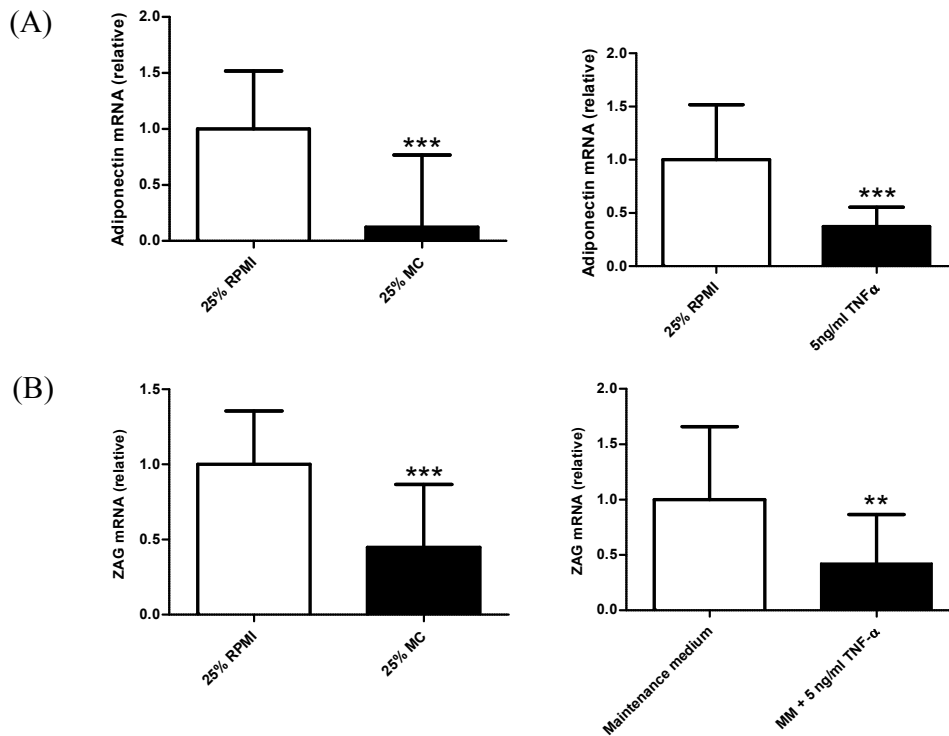
##### *3.3.1.3 MC medium decreases ZAG gene expression*

There was a 2.2-fold decrease in ZAG gene expression of adipocytes incubated with 25% MC medium ( $P < 0.001$ ; Figure 3.3B) compared to basal expression levels in unstimulated adipocytes. The result for 25% MC treated cells is also in agreement with a previous ZAG study conducted in the department (Gao, 2010) where ZAG gene expression decreased similarly in adipocytes treated with neat (100%) MC medium.

#### *3.3.1.4 TNF- $\alpha$ decreases ZAG gene expression*

ZAG gene expression significantly decreased 2-fold in adipocytes stimulated with 5ng/ml TNF- $\alpha$  when compared to basal levels in unstimulated adipocytes (P = 0.033; Figure 3.3B).

**Figure 3.3 Relative expression of adiponectin and ZAG mRNA in adipocytes stimulated with 25% MC or TNF- $\alpha$**



Cell culture maintenance medium was replaced with 25% macrophage-conditioned medium in maintenance medium (25% MC) on day 13 post-differentiation. Cells were harvested after 24 hours. A separate group of cells were treated with 5ng/ ml TNF- $\alpha$  in 25% RPMI. Cells incubated in 25% RPMI or maintenance medium (MM) were used as a control. mRNA expression in adipocytes treated with 25% MC medium treated cells or TNF- $\alpha$ , measured by real-time PCR and normalised to  $\beta$ -actin, are expressed relative to controls. Results are given as means  $\pm$  SD for groups of 6. \*\*P < 0.01, \*\*\*P < 0.001 vs control (Unpaired student's *t*-test).

### **3.3.3 Adiponectin and ZAG production by adipocytes stimulated with 25% MC medium or TNF- $\alpha$**

#### *3.3.3.1 25% MC medium stimulation suppresses adiponectin release*

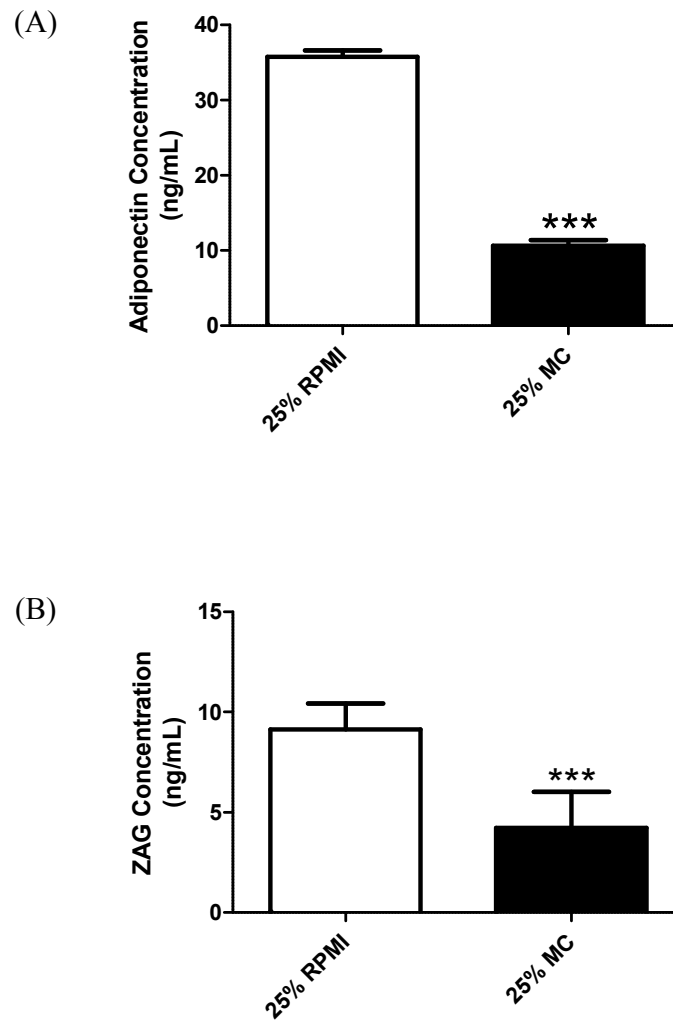
Treatment with 25% MC medium for 48 hours induced a statistically significant 3.4-fold reduction of adiponectin production by human primary adipocytes in comparison to basal adiponectin release by unstimulated adipocytes ( $P < 0.001$ ; Figure 3.4A).

#### *3.3.3.2 25% MC medium stimulation suppresses ZAG release*

25% MC medium induced a 2.2-fold decrease in ZAG production by human primary adipocytes over a 48 hour period ( $P < 0.001$ ; Figure 3.4B).



**Figure 3.4 Adiponectin and ZAG production by human primary adipocytes**



Cell culture maintenance medium was replaced with 25% RPMI-1640 in maintenance medium (25% RPMI) as a control or 25% macrophage-conditioned medium in maintenance medium (25% MC) on day 13 post-differentiation. Medium was collected after 48 hours. Adiponectin (A) and ZAG (B) concentrations in the culture medium of adipocytes were measured by real-time PCR. Results are given as means  $\pm$  SD for groups of 3-4 for adiponectin, groups of 6 for ZAG. \*\*\* $P < 0.001$  vs control (Unpaired student's *t*-test).

### **3.4 Activation of NF- $\kappa$ B and MAPK signalling pathways in adipocytes by macrophage-conditioned medium**

I $\kappa$ B $\alpha$  is a member of a family of intracellular proteins that inhibits NF- $\kappa$ B – a protein complex associated with proinflammatory gene transcription. I $\kappa$ B $\alpha$  masks nuclear localization signals of NF- $\kappa$ B proteins and keeps them sequestered in an inactive state in the cytoplasm. A decrease in anti-inflammatory gene expression is also known to be due to NF- $\kappa$ B's inhibitory effect on PPAR- $\gamma$ -mediated transcriptional activity (Suzawa, 2003). Phosphorylation of serine residues in NF- $\kappa$ B p65 is required to elicit a conformational change to allow efficient recruitment of transcriptional cofactors (e.g. CBP) for activation of NF- $\kappa$ B pathways (Zhong *et al.*, 1998). p38 MAPK is the subunit in the mitogen-activated kinase (MAPK) pathway and its activation is required for transcription of TNF- $\alpha$ , IL-1 $\beta$  and the transactivation of NF- $\kappa$ B p65 subunits in TNF- $\alpha$  mediated IL-6 gene expression (Guan *et al.*, 1998; Vanden Berghe *et al.*, 1998).

#### **3.4.1 Protein abundance of I $\kappa$ B $\alpha$ is decreased and phosphorylated NF- $\kappa$ B p65 increased in adipocytes treated with 25% MC medium**

Prior to this section, it has been observed that 25% MC medium increased the expression of proinflammatory molecules (MCP-1, IL-6 and IL-1 $\beta$ ) and decreased the expression of anti-inflammatory molecules adiponectin and ZAG. In line with results from the gene expression profile, MC medium had a stimulatory effect on the NF- $\kappa$ B signalling

pathway. The protein abundance of I $\kappa$ B $\alpha$  was decreased and phosphorylated NF- $\kappa$ B p65 increased, consistent with the activation of NF- $\kappa$ B.

#### *3.4.1.1 MC medium decreases I $\kappa$ B $\alpha$ protein abundance*

MC medium stimulated adipocytes had a 3.4-fold decrease in I $\kappa$ B $\alpha$  levels compared to basal levels in control adipocytes (Figure 3.5; P = 0.0032).

#### *3.4.1.2 MC medium increases phosphorylated NF- $\kappa$ B p65 protein abundance*

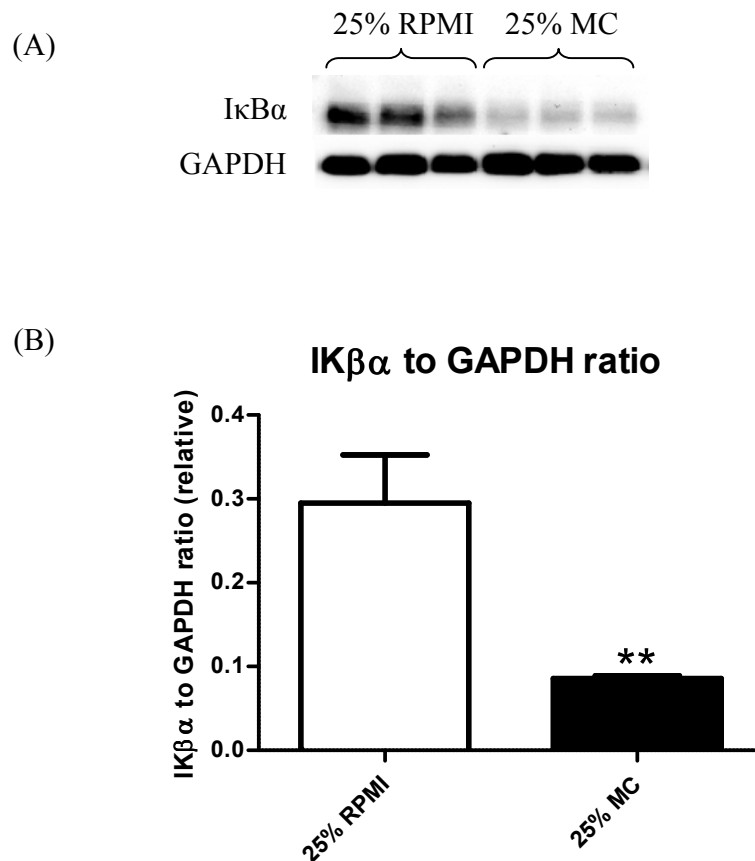
A significant increase (1.7-fold) in phosphorylated NF- $\kappa$ B p65 protein abundance in stimulated adipocytes was also observed (Figure 3.6; P = 0.0301), in comparison to basal levels in control adipocytes.

### **3.4.2 MC medium increases protein abundance of phosphorylated p38 MAPK in adipocytes**

#### *3.4.2.1 Phosphorylated p38 MAPK levels increase with 25% MC medium stimulation*

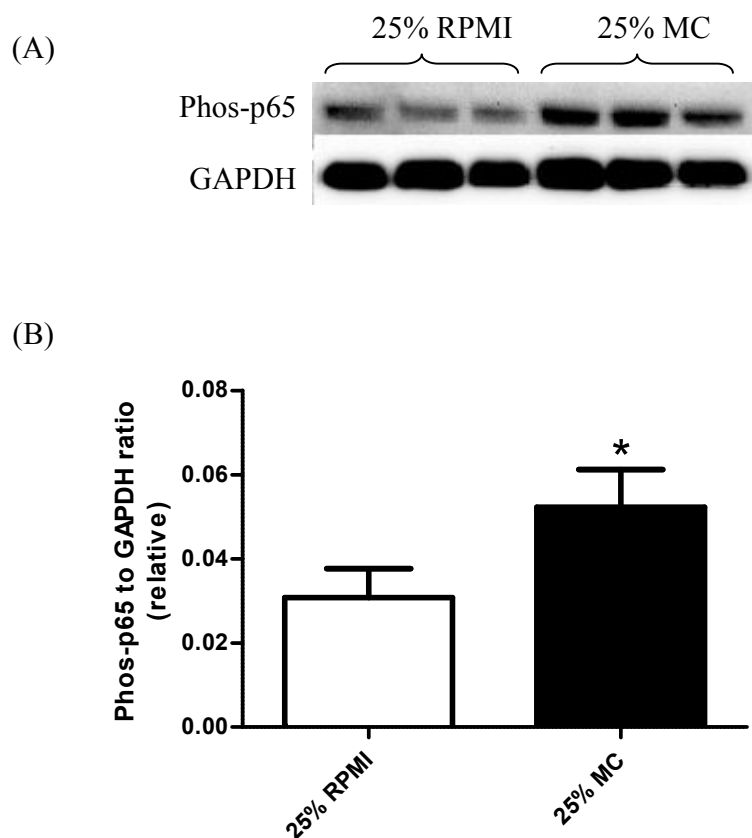
Phosphorylated p38 MAPK levels were increased 2.8-fold with 25% MC medium stimulation (Figure 3.7; P = 0.0202) when compared to basal levels in control adipocytes.

**Figure 3.5 I $\kappa$ B $\alpha$  protein expression in human primary adipocytes stimulated with 25% MC medium**



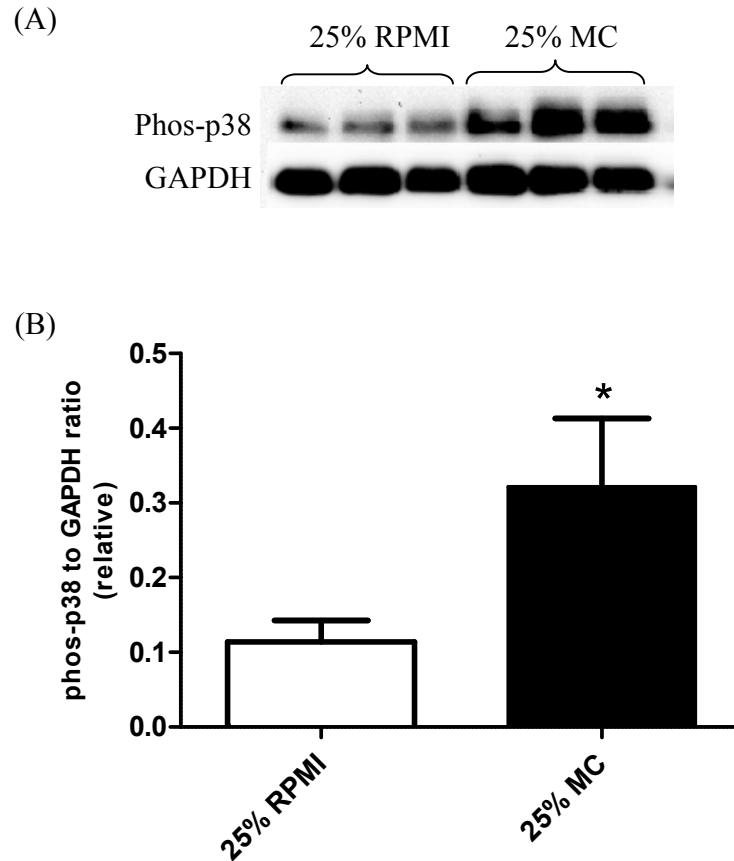
I $\kappa$ B $\alpha$  protein expression in human primary adipocytes incubated with 25% RPMI or 25% MC medium for 24 hours. (A) Protein expression in cell lysates were analysed by Western blotting and GAPDH was used as loading control. (B) Densitometric analysis of signal intensity was used for semi-quantitative analysis of I $\kappa$ B $\alpha$  levels. Data are means  $\pm$  SD for groups of 3, normalised to GAPDH levels. \*\*P < 0.01 vs controls (Unpaired student's *t*-test)

**Figure 3.6 Phosphorylated NF- $\kappa$ B p65 protein expression in human primary adipocytes stimulated with 25% MC medium**



Phosphorylated NF- $\kappa$ B p65 protein expression in human primary adipocytes incubated with 25% RPMI or 25% MC medium for 24 hours. (A) Protein expression in cell lysates was analysed by Western blotting and GAPDH was used as loading controls. (B) Densitometric analysis of signal intensity was used for semi-quantitative analysis of phosphorylated NF- $\kappa$ B p65 levels. Data are means  $\pm$  SD for groups of 3, normalised to GAPDH levels. \* $P < 0.05$  vs controls (Unpaired student's  $t$ -test).

**Figure 3.7 Phosphorylated p38 MAPK protein expression in human primary adipocytes stimulated with 25% MC medium**



Phosphorylated p38 MAPK protein expression in human primary adipocytes incubated with 25% RPMI or 25% MC medium for 24 hours. (A) Protein expression in cell lysates was analysed by western blotting and GAPDH was used as loading controls. (B) Densitometric analysis of signal intensity was used for semi-quantitative analysis of phosphorylated p38 MAPK levels. Data are means  $\pm$  SD for groups of 3, presented relative to controls and normalised to GAPDH levels. \*P < 0.05 compared to controls (Unpaired student's *t*-test).

## **Chapter 4**

### **The effects of calcitriol supplementation on inflammatory response in human primary adipocytes**

## **4.1 Introduction**

Calcitriol, a specific ligand of VDR, was used to treat adipocytes before subjecting them to inflammatory stress to assess the efficacy of calcitriol supplementation on inflammation caused by macrophage-produced factors in the SVF. To understand the specific effect that macrophage-produced cytokines might have on adipocytes, cells were incubated with human recombinant TNF- $\alpha$  and concurrently treated with calcitriol to study if the cytokinic profile parallels that of the cells subjected to macrophage-produced inflammatory stimuli. A transmigration assay was also performed to study the chemotaxis of macrophages to a simulated adipose tissue environment in inflammation. The same study was applied to cells treated with calcitriol to determine if calcitriol supplementation to adipocytes could potentially reduce the effects of chemotactic factors responsible for the enhancement of the inflammatory response.

## **4.2 The effects of calcitriol on the production of proinflammatory mediators by adipocytes**

### **4.2.1 Calcitriol has no effect on basal expression of genes related to inflammation**

*4.2.1.1 Calcitriol does not affect gene expression of proinflammatory mediators in adipocytes*



One-way ANOVA analysis with post-hoc Bonferroni's t-tests showed that there were no significant differences in gene expression of MCP-1, IL-6 and IL-1 $\beta$  between calcitriol supplemented and unsupplemented cells (Figure 4.1).

#### **4.2.2 Calcitriol decreases basal production of MCP-1 and IL-6 by adipocytes**

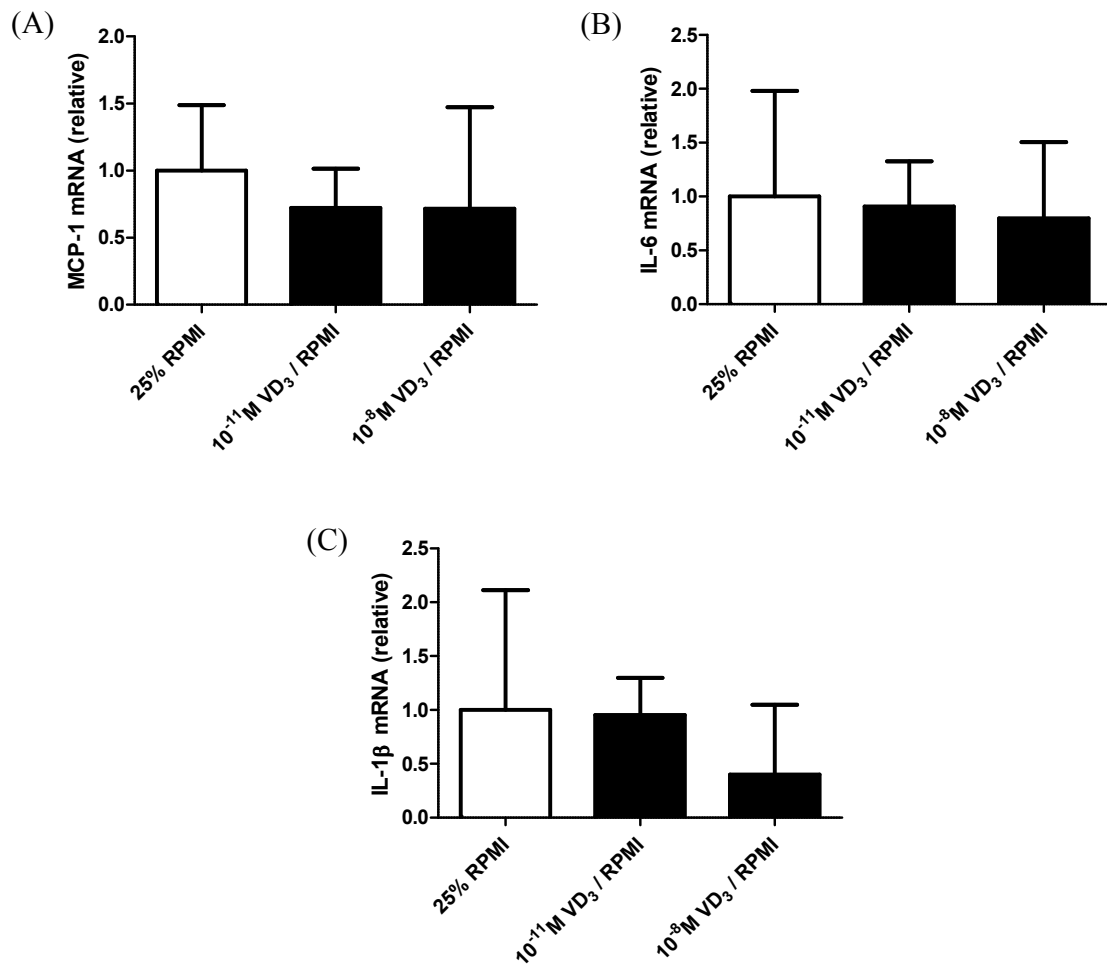
##### *4.2.2.1 Calcitriol reduces MCP-1 release by adipocytes*

Protein release data (Figure 4.2), in contrast to mRNA data, showed a highly significant 1.3-fold decrease in MCP-1 for low dose calcitriol supplementation and a 3.1-fold decrease in MCP-1 for high dose supplementation (P = 0.0054 for low dose, P < 0.001 for high dose).

##### *4.2.2.2 Calcitriol reduces IL-6 release by adipocytes*

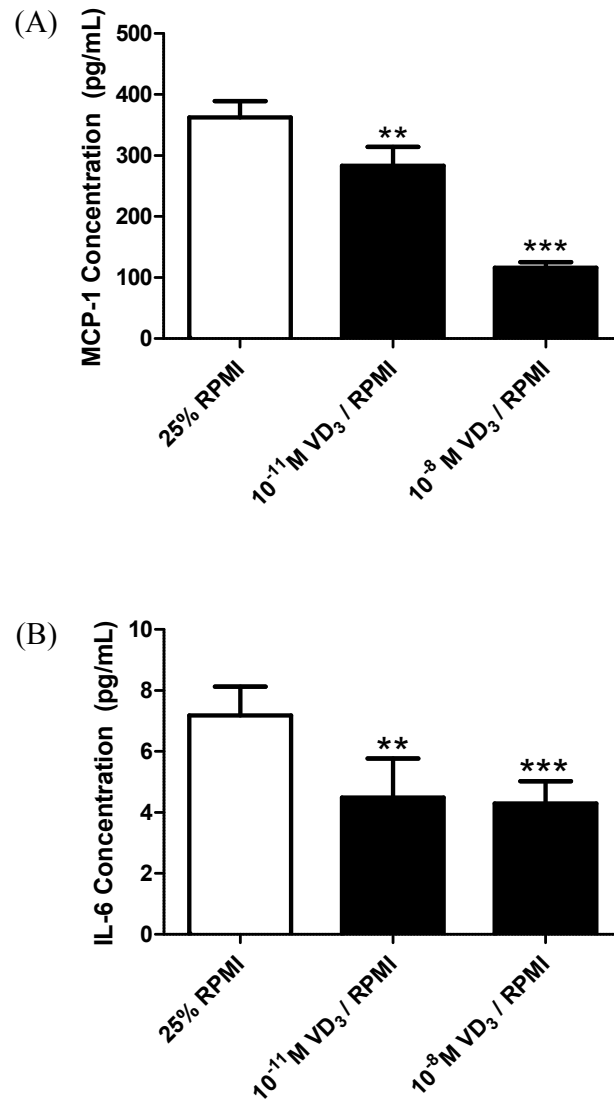
IL-6 release by adipocytes also decreased 1.6-fold for both high and low dose supplemented groups (P = 0.0021 for low dose, P < 0.001 for high dose).

**Figure 4.1 Gene expression of proinflammatory mediators in adipocytes pretreated with calcitriol**



MCP-1 (A), IL-6 (B), IL-1 $\beta$  (C) gene expression in cells supplemented with calcitriol. Cells were treated on day 11 post-differentiation with varying concentrations of calcitriol ( $VD_3$ ) in 25% RPMI-1640 medium in maintenance medium (25% RPMI). The incubation medium was replaced on day 13 with fresh 25% RPMI with the same corresponding calcitriol concentrations and harvested after 24 hours. (NT, No treatment;  $10^{-11}$  M;  $10^{-8}$  M) mRNA expression was measured by real-time PCR and normalised to  $\beta$ -actin. Results are given as means  $\pm$  SD for groups of 6.

Figure 4.2 MCP-1 and IL-6 production by adipocytes pretreated with calcitriol



MCP-1 (A) and IL-6 (B) release from adipocytes supplemented with calcitriol. Cells were treated on day 11 post-differentiation with varying concentrations of calcitriol (VD<sub>3</sub>) in maintenance medium containing 25% RPMI-1640 medium. The incubation medium was replaced on day 13 with fresh 25% RPMI with the same corresponding calcitriol concentrations. Cell medium was collected after 24 hours; MCP-1 and IL-6 concentrations were determined by ELISA. Results are given as means  $\pm$  SD for groups of 4-6. \*\*P < 0.01, \*\*\*P < 0.001 vs untreated controls (One-way ANOVA)

#### **4.2.3 Effect of calcitriol on gene expression of proinflammatory mediators in adipocytes with proinflammatory stimulation**

To study the effects of calcitriol on MC medium-induced inflammatory response in adipocytes, cells were treated with fresh maintenance medium with low dose ( $10^{-11}$ M) and high dose ( $10^{-8}$ M) calcitriol on day 11 post-differentiation for 48 hours. A group of cells incubated in only fresh maintenance medium was maintained simultaneously as a control. On day 13 post-differentiation, the cell culture medium was replaced with 25% MC medium with low and high concentrations of calcitriol ( $10^{-11}$ M,  $10^{-8}$ M). A group of cells incubated in 25% MC medium without calcitriol treatment and another group of cells maintained in 25% RPMI medium without calcitriol treatment was maintained as a control.

To study the effect of calcitriol supplementation on TNF- $\alpha$  mediated inflammatory response in adipocytes, day 11 adipocytes were pretreated with calcitriol ( $10^{-11}$ M or  $10^{-8}$ M) for 48 hours. On day 13 post-differentiation the cell culture medium was replaced with 25% RPMI with 5 ng/ ml of TNF- $\alpha$  with calcitriol at low and high dose concentrations ( $10^{-11}$ M,  $10^{-8}$ M). Similarly, a group of cells incubated in 25% RPMI with 5 ng/ ml of TNF- $\alpha$  and another group of cells maintained in only 25% RPMI medium was used as controls. For multiple-group comparisons, the data was statistically tested with One-way ANOVA with post-hoc Bonferroni comparisons.

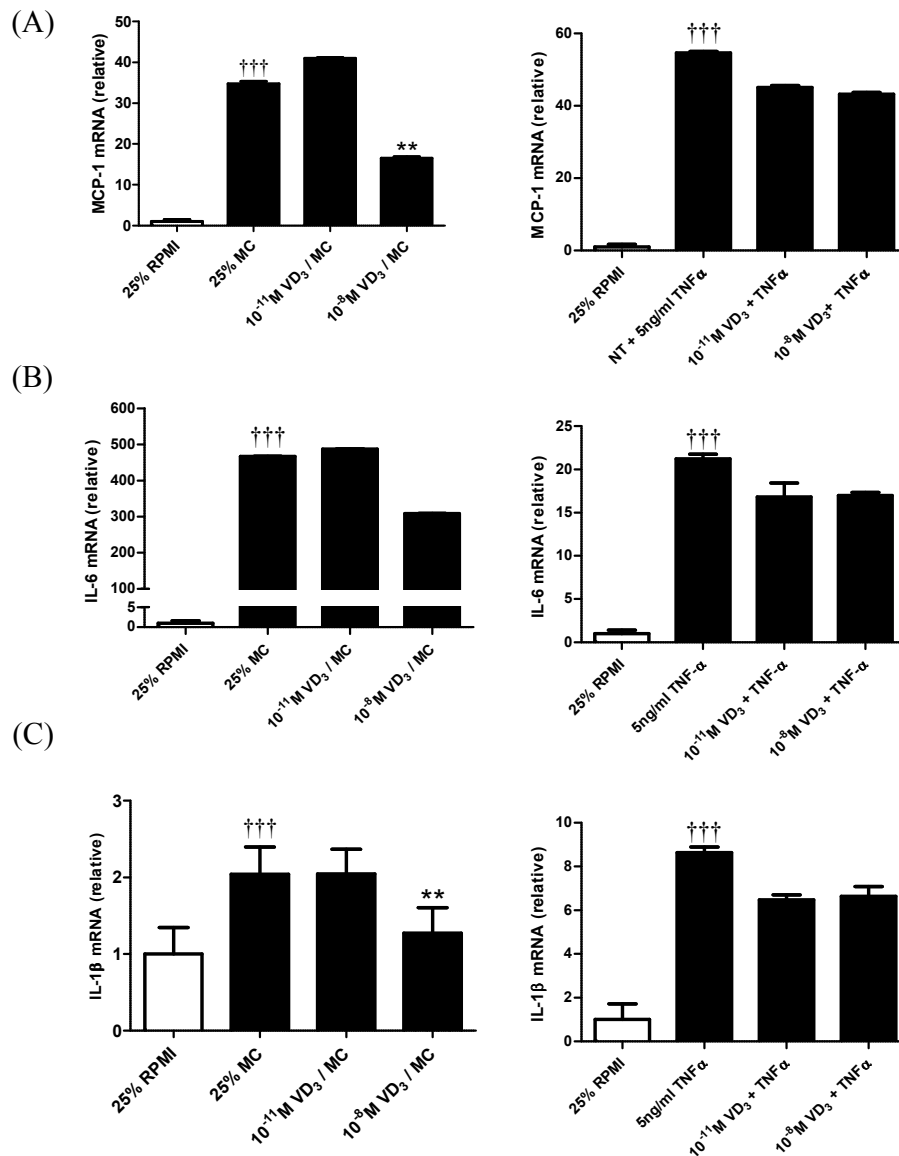
#### *4.2.3.1 Calcitriol supplementation decreases MCP-1 and IL-1 $\beta$ gene expression*

There were no observed changes in MCP-1, IL-6 and IL-1 $\beta$  gene expression of low-dose calcitriol supplemented adipocytes stimulated with 25% MC medium (Figure 4.3). The inclusion of a 25% RPMI control served to ensure that MC medium stimulation did occur. High dose calcitriol treatment ( $10^{-8}$ M) significantly decreased MCP-1 ( $P = 0.0031$ ) and IL-1 $\beta$  ( $P = 0.0063$ ) gene expression. However, the reduction in IL-6 gene expression was not considered to be statistically significant.

#### *4.2.3.2 Gene expression of MCP-1, IL-6 and IL-1 $\beta$ in adipocytes stimulated with TNF- $\alpha$*

There was no statistical significance in changes observed in MCP-1 gene expression of adipocytes with both high ( $10^{-8}$ M) and low dose ( $10^{-11}$ M) calcitriol supplemented samples compared to unsupplemented cells upon TNF- $\alpha$  stimulation (Figure 4.3A). Similarly, calcitriol supplementation had no statistically significant effect on IL-6 gene expression (Figure 4.3B) and IL-1 $\beta$  gene expression (Figure 4.3C).

**Figure 4.3 Gene expression of MCP-1, IL-6 and IL-1 $\beta$  in calcitriol-supplemented adipocytes stimulated with 25% MC medium**



MCP-1, IL-6 and IL-1 $\beta$  gene expression in calcitriol-supplemented adipocytes (10<sup>-11</sup>M or 10<sup>-8</sup>M) treated with 25% MC medium and 5 ng/ ml TNF- $\alpha$ . The cell medium was replaced on day 13 with fresh 25% MC medium with the same corresponding calcitriol concentrations and harvested after 24 hours. Results are given as means  $\pm$  SD for groups of 6 for 25% MC medium study, 3-4 for TNF- $\alpha$  study. \*P < 0.05, \*\*P < 0.01 vs untreated stimulated controls. †††P < 0.001 vs unstimulated controls (One-way ANOVA).

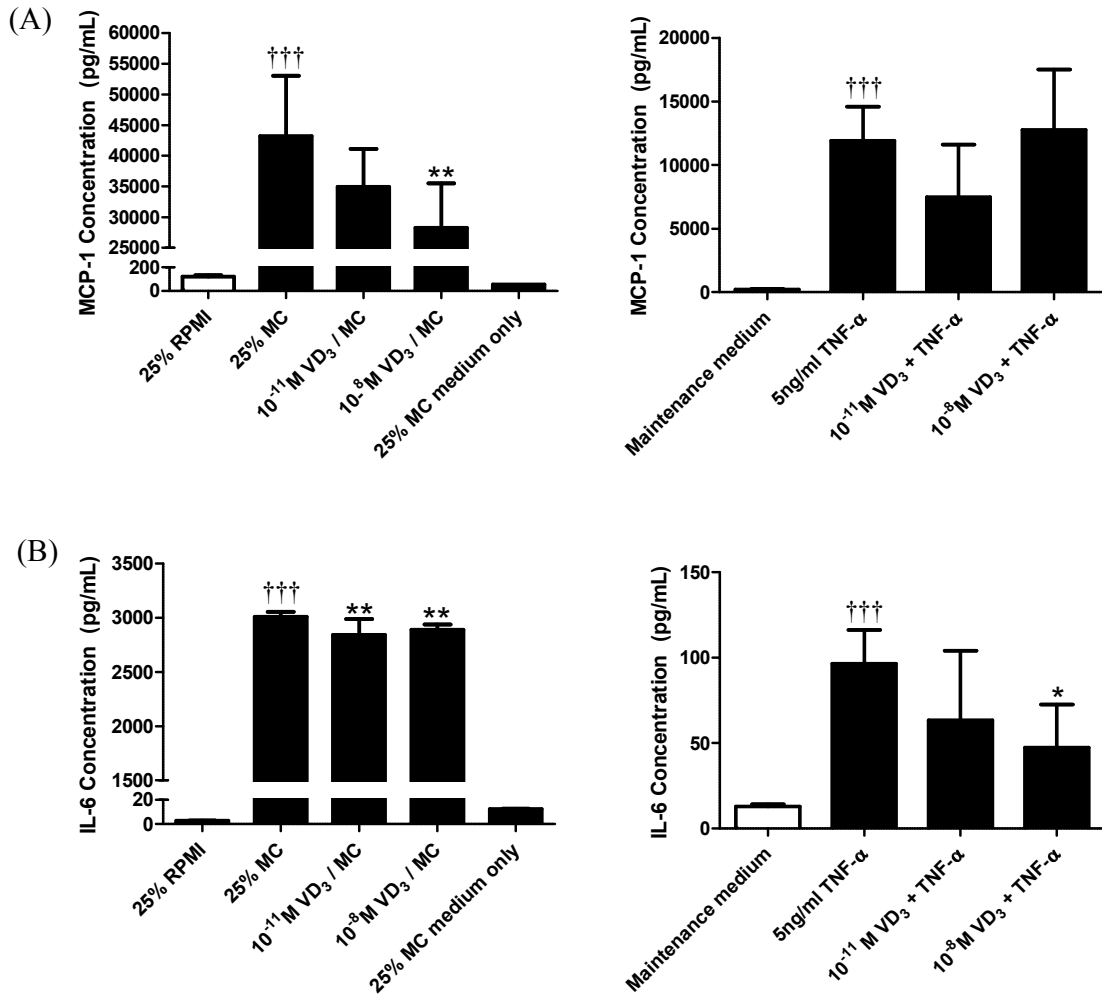
*4.2.3.3 Production of MCP-1 and IL-6 by calcitriol-supplemented adipocytes stimulated with MC medium.*

The MCP-1 and IL-6 produced by adipocytes was measured by ELISA. MCP-1 levels were decreased significantly after 24 hours of incubation with high dose calcitriol treatment ( $P = 0.007$ ; Figure 4.4A). MCP-1 levels did not decrease significantly with low dose calcitriol. There were also significant reductions in IL-6 release by adipocytes incubated with both low dose ( $P = 0.001$ ; Figure 4.4B) and high dose calcitriol ( $P = 0.009$ ).

*4.2.3.4 MCP-1 and IL-6 production by calcitriol-supplemented adipocytes stimulated with TNF- $\alpha$*

There was no significant change in MCP-1 concentration in the medium of calcitriol-supplemented adipocytes (Figure 4.4A). IL-6 concentration was significantly decreased in adipocytes with high dose calcitriol supplementation ( $P = 0.023$ ; Figure 4.4B)

**Figure 4.4 MCP-1 and IL-6 concentration in medium of calcitriol-supplemented adipocytes stimulated with 25% MC medium and TNF- $\alpha$**



MCP-1 and IL-6 measured as the concentrations in cell culture medium of adipocytes treated as described in Figure 4.3. Results are given as means  $\pm$  SD for groups of 6 for MCP-1, 3-4 for IL-6 for the MC study; groups of 6 for the TNF- $\alpha$  study. \*P < 0.05, \*\*P < 0.01 vs MC-stimulated controls. †††P < 0.001 vs unstimulated controls (One-way ANOVA).



### **4.3 The effects of calcitriol on the production of the adipokines, adiponectin and ZAG, by human adipocytes**

#### **4.3.1 Calcitriol increases basal adiponectin and ZAG transcription in adipocytes with MC medium stimulation**

Figure 4.5 shows the effects of low and high dose calcitriol supplementation on basal gene expression levels of adiponectin and ZAG in adipocytes.

##### *4.3.1.1 High dose calcitriol increases basal adiponectin gene expression*

There was a 2-fold increase in adiponectin gene expression ( $P = 0.001$ ) in adipocytes with high-dose ( $10^{-8}\text{M}$ ) calcitriol supplementation in comparison to controls (Figure 4.5A). Adiponectin levels did not change significantly with low dose ( $10^{-11}\text{M}$ ) calcitriol treatment (Figure 4.5A).

##### *4.3.1.2 Low and high dose calcitriol increases basal ZAG gene expression levels*

ZAG gene expression in adipocytes increased with both low dose ( $P = 0.039$ ) and high dose ( $P < 0.001$ ) calcitriol supplementation in comparison to controls (Figure 4.5B).

#### **4.3.2 Effects of calcitriol on basal adiponectin and ZAG production by adipocytes**

Calcitriol supplementation did not cause any significant effect on basal adiponectin release by adipocytes (Figure 4.6A). A significant decrease in ZAG release ( $P = 0.009$ ) was observed with low dose calcitriol supplementation of adipocytes but there was no effect on ZAG release of high dose supplemented adipocytes (Figure 4.6B).

### **4.3.3 Effects of calcitriol on gene expression of adiponectin and ZAG in adipocytes stimulated with MC medium**

Figure 4.7 shows the effects of low and high dose calcitriol supplementation on adiponectin and ZAG gene expression in adipocytes stimulated with 25% MC medium.

#### *4.3.3.1 Effects of calcitriol supplementation on adiponectin gene expression of adipocytes stimulated with MC medium*

Adiponectin gene expression was decreased in low dose calcitriol supplemented adipocytes stimulated with 25% MC medium in comparison to controls without calcitriol supplementation (Figure 4.7A;  $P = 0.018$ ). However, high dose calcitriol supplementation partially reversed the inhibitory effect that 25% MC medium had on adiponectin gene expression ( $P = 0.017$ ).

#### *4.3.3.2 High dose calcitriol reverses the inhibitory effect of MC medium on ZAG gene expression*

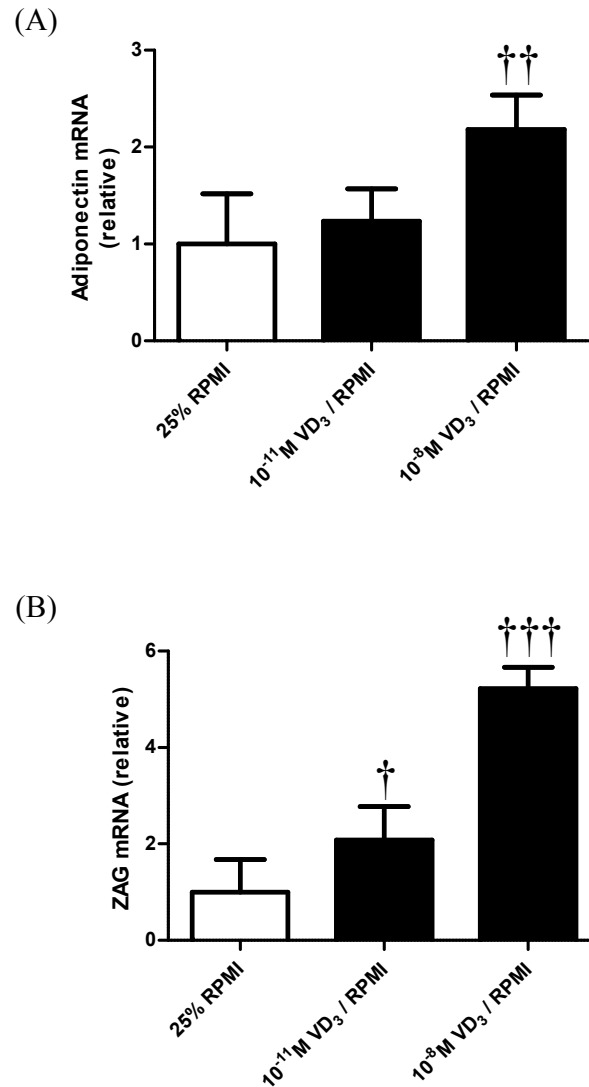
ZAG gene expression significantly increased (Figure 4.7B;  $P = 0.004$ ) with high dose supplementation whereas the increase in ZAG gene expression was not statistically significant in low dose supplemented cells.

### **4.3.4 Effects of calcitriol on adiponectin and ZAG release by adipocytes stimulated with MC medium**

Low-dose calcitriol treatment had no effect on MC medium-induced decrease in adiponectin release by adipocytes. There was a reduction in adiponectin levels with high

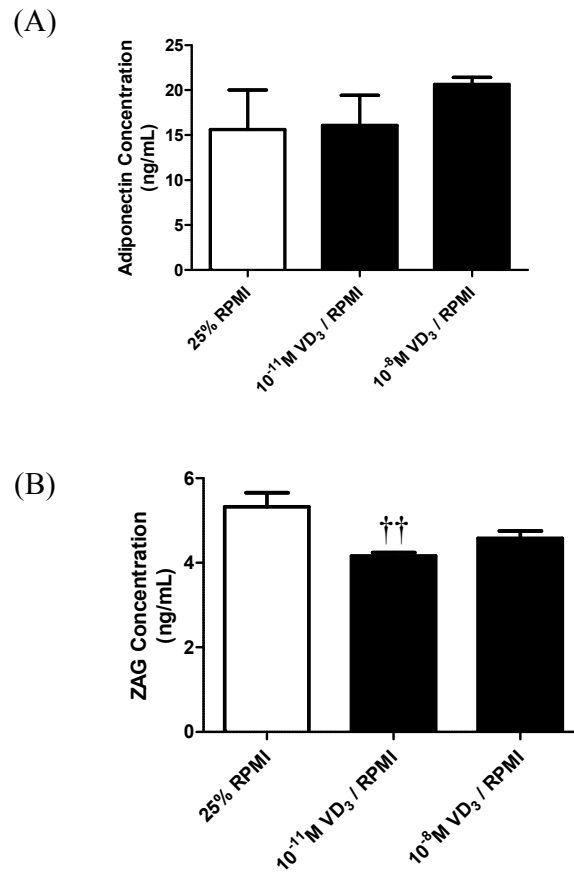
dose calcitriol supplemented adipocytes stimulated with MC medium ( $P < 0.001$ ). Calcitriol supplementation did not reverse the inhibitory effect of MC medium on ZAG production over the same time period (Figure 4.8).

**Figure 4.5 Gene expression of adiponectin and ZAG in adipocytes treated with calcitriol**



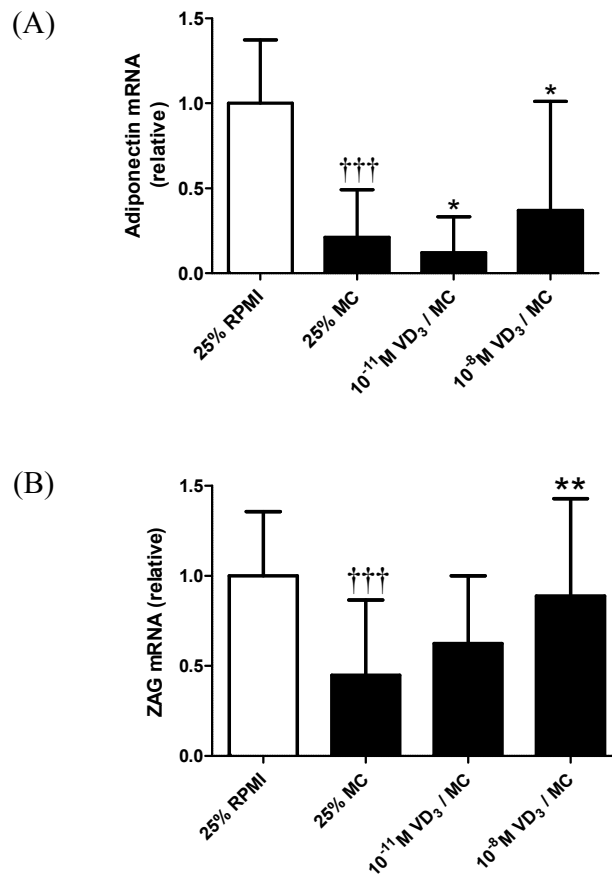
Adiponectin and ZAG gene expression in calcitriol supplemented human adipocytes. Cells were harvested after 24 hours of incubation. mRNA expression was determined by real-time PCR and normalised to  $\beta$ -actin. Results are given as means  $\pm$  SD for groups of 6.  $^\dagger P < 0.05$ ,  $^\dagger^\dagger P < 0.01$  and  $^\dagger^\dagger^\dagger P < 0.001$  compared with unsupplemented controls. (One-way ANOVA).

**Figure 4.6 Adiponectin and ZAG production by adipocytes treated with calcitriol**



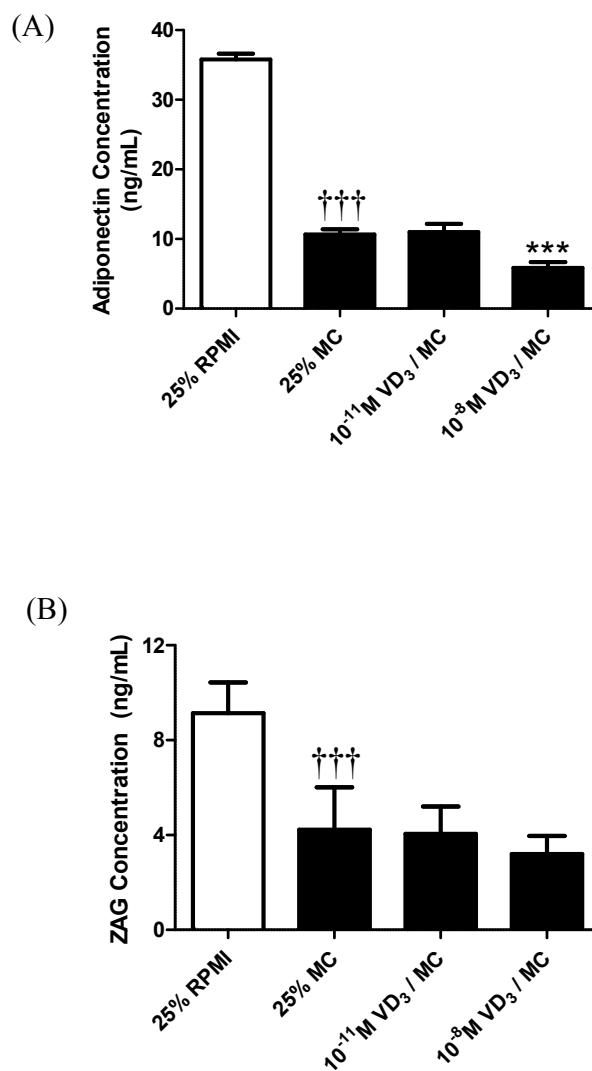
Adiponectin and ZAG concentration in cell culture medium of adipocytes incubated with calcitriol for 48 hours, measured by ELISA. Results are given as means  $\pm$  SD for groups of 4 for adiponectin and for ZAG. <sup>††</sup>P < 0.01 compared with unsupplemented controls (One-way ANOVA).

**Figure 4.7 Gene expression of adiponectin and ZAG in calcitriol supplemented adipocytes stimulated with 25% MC medium**



Adiponectin and ZAG gene expression in calcitriol-supplemented human adipocytes. Cells were harvested after 24 hours of incubation with MC medium for ZAG and leptin and 48 hours incubation with MC medium for adiponectin. mRNA expression was determined by real-time PCR and normalised to  $\beta$ -actin. Results are given as means  $\pm$  SD for groups of 6. \* $P < 0.05$ , \*\* $P < 0.01$  vs unstimulated, MC-stimulated controls. ††† $P < 0.001$  vs unstimulated controls (One-way ANOVA).

**Figure 4.8 Adiponectin and ZAG release from calcitriol-supplemented adipocytes stimulated with 25% MC medium**



Adiponectin and ZAG concentration in cell culture medium of calcitriol-supplemented adipocytes stimulated with 25% MC medium for 48 hours, measured by ELISA. Results are given as means  $\pm$  SD for groups of 4 for adiponectin and groups of 6 for ZAG. \*\*\*P < 0.001 compared with unsupplemented, stimulated controls. †††P < 0.001 compared with unstimulated controls (One-way ANOVA).

## **4.4 The effects of calcitriol on the intracellular signalling involved in inflammatory response in human adipocytes**

### **4.4.1 Calcitriol supplementation reverses the effects of MC medium on I $\kappa$ B $\alpha$ , phosphorylated NF- $\kappa$ B p65 and phosphorylated p38 MAPK in adipocytes**

As observed before in Chapter 3, I $\kappa$ B $\alpha$  protein expression in adipocytes was decreased when adipocytes were exposed to inflammatory molecules while phosphorylated NF- $\kappa$ B p65 and phosphorylated p38 MAPK expression were increased, suggesting that the activation of NF- $\kappa$ B and MAPK signalling pathways are central to the resulting inflammatory response observed in adipocytes. Both high and low dose calcitriol supplementation was observed to restore the intracellular signalling profile altered by proinflammatory stimuli from 25% MC medium or TNF- $\alpha$ .

#### *4.4.1.1 Calcitriol supplementation attenuates the decrease of I $\kappa$ B $\alpha$ induced by MC medium*

No increase in basal I $\kappa$ B $\alpha$  production was observed with low dose. However, at high dose supplementation, I $\kappa$ B $\alpha$  production was increased ( $P = 0.042$ ) in unstimulated adipocytes. In the 25% MC medium stimulated cells, high doses of calcitriol were able to significantly reverse ( $P = 0.005$ ; Figure 4.9) the decrease in I $\kappa$ B $\alpha$  protein levels. There was no significant change in I $\kappa$ B $\alpha$  levels in adipocytes supplemented with low doses of calcitriol.



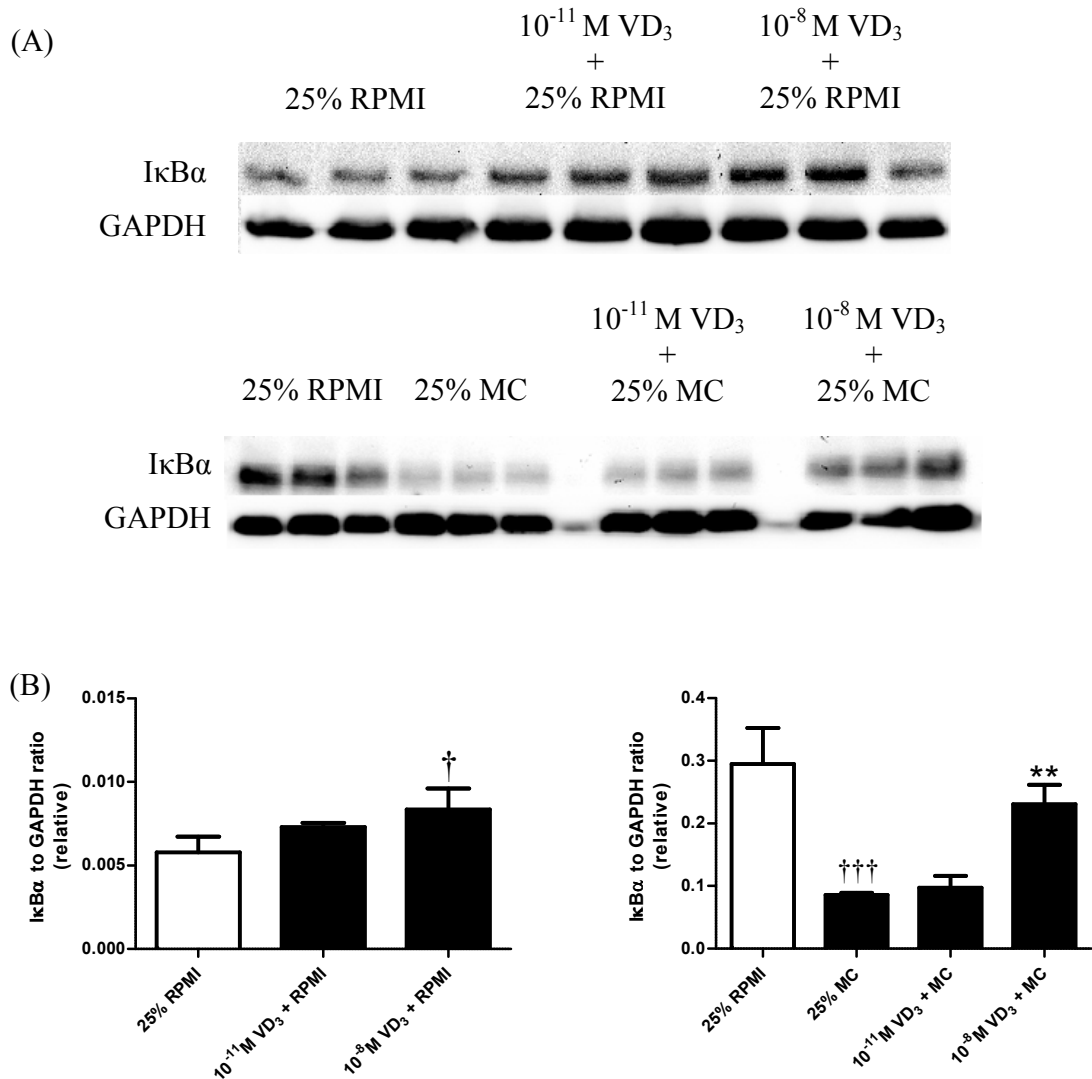
*4.4.1.2 Calcitriol supplementation attenuates the increase in phosphorylated NF- $\kappa$ B p65 protein abundance induced by MC medium*

Phosphorylated NF- $\kappa$ B p65 protein expression was decreased with low dose and high dose calcitriol supplementation (Figure 4.10) in unstimulated adipocytes although the decreases were not statistically significant. Elevated levels of phosphorylated NF- $\kappa$ B p65 in adipocytes stimulated with 25% MC medium were also observed to return to similar levels in both the low dose (P = 0.003) and high dose (P = 0.033) supplementation groups.

*4.4.1.3 Calcitriol supplementation attenuates the increase in phosphorylated p38 MAPK protein abundance induced by MC medium*

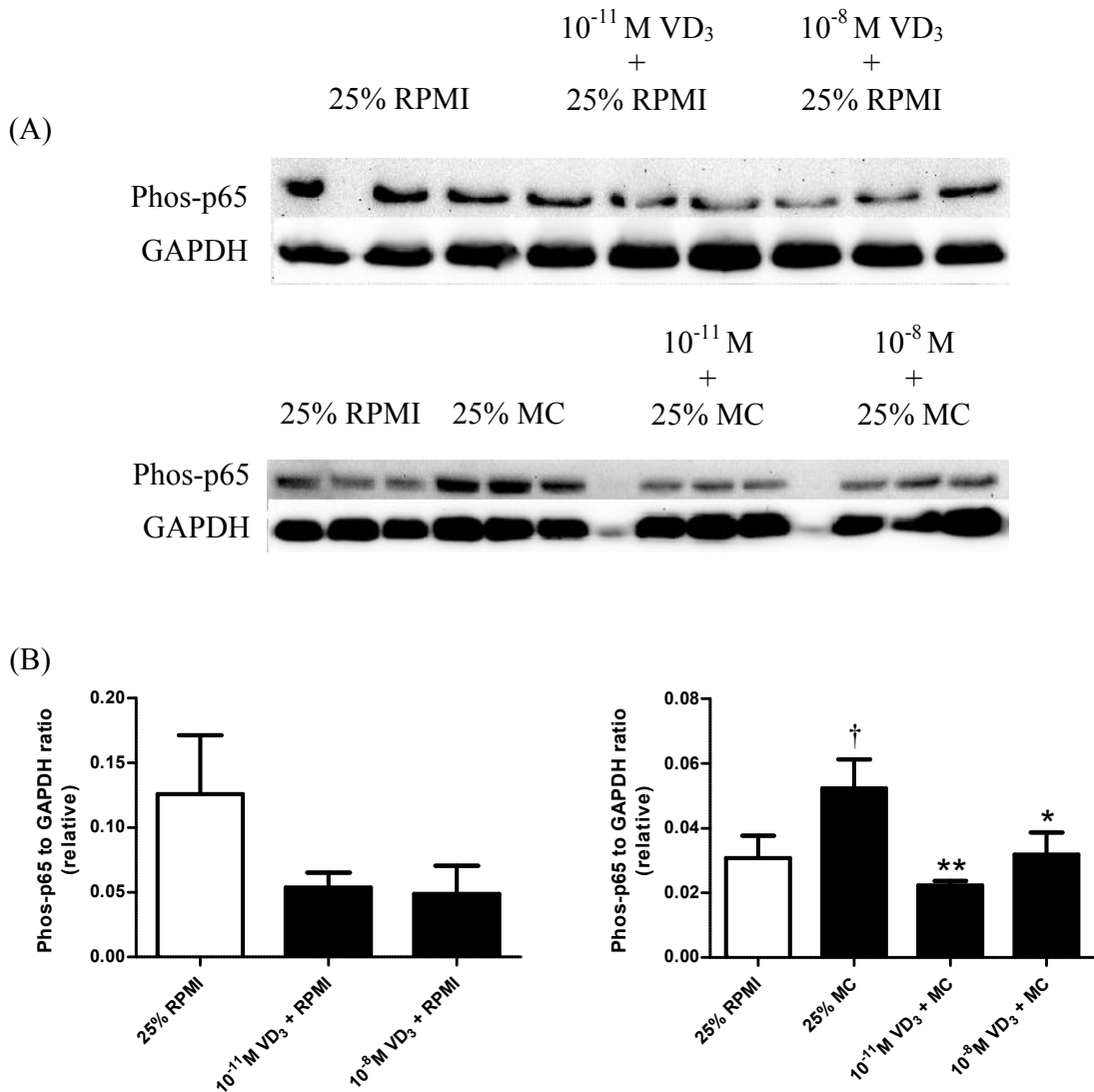
Basal levels of phosphorylated p38 MAPK decreased with high dose calcitriol supplementation (P = 0.025; Figure 4.11). In adipocytes stimulated with 25% MC medium, levels of phosphorylated p38 MAPK also decreased significantly with low dose calcitriol supplementation (P = 0.007) and high dose calcitriol supplementation (P = 0.014) when compared to unsupplemented cells stimulated with 25% MC medium (Figure 4.11).

**Figure 4.9 IκBα protein expression in human adipocytes supplemented with calcitriol**



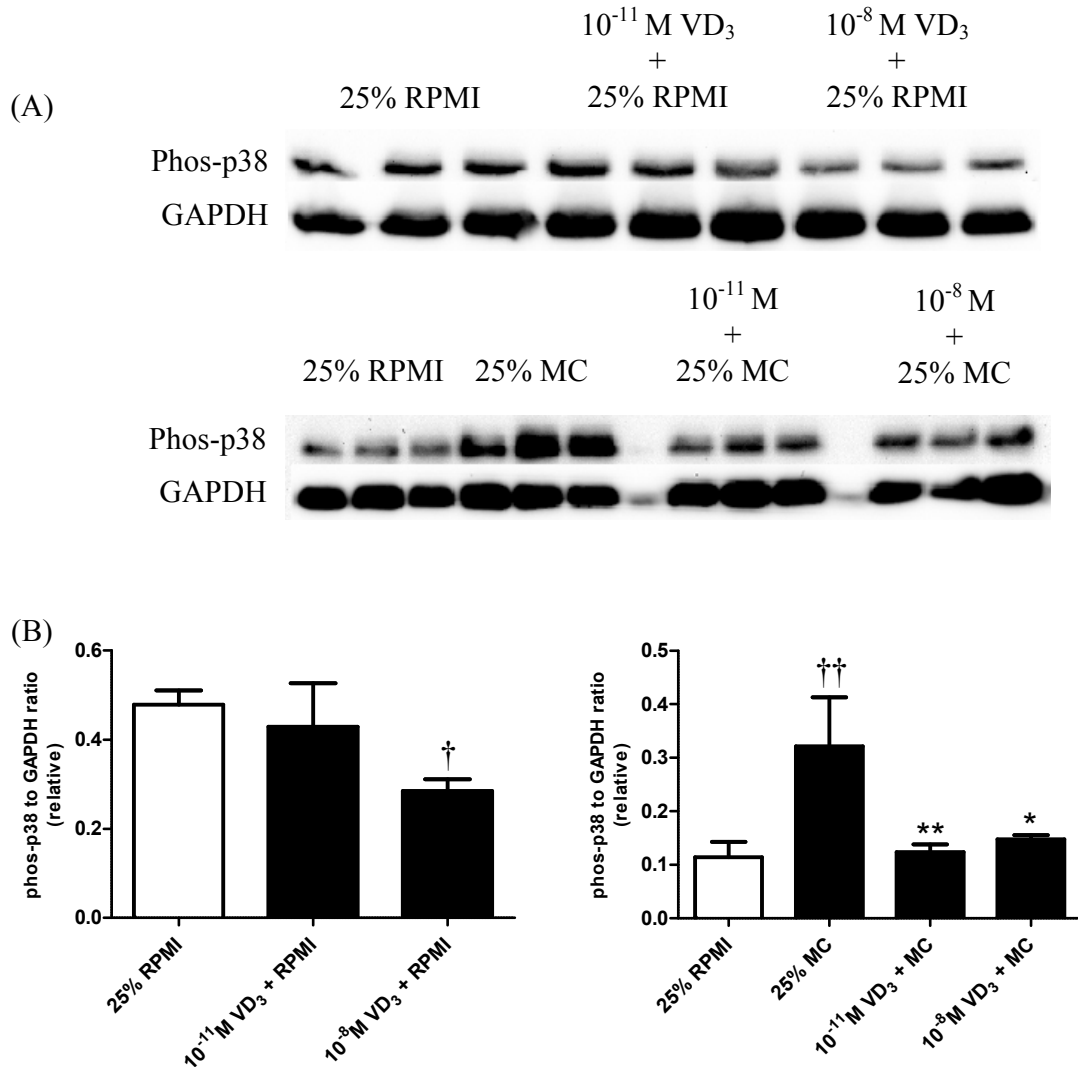
IκBα protein expression in calcitriol-treated adipocytes incubated in 25% MC medium (25% MC) and 25% RPMI as determined by western blotting. (A) Western blots of adipocyte lysates. (B) Densitometric analysis of blots was used for semi-quantitative analysis of IκBα levels. Data are means ± SD for groups of 3, normalised to GAPDH levels. \*\*P < 0.01 vs unstimulated, stimulated controls. ††P < 0.01, †††P < 0.001 vs unstimulated controls. (One-way ANOVA)

**Figure 4.10 Phosphorylated NF- $\kappa$ B p65 protein expression in human adipocytes supplemented with calcitriol**



Phosphorylated NF- $\kappa$ B p65 protein expression in human primary adipocytes incubated in 25% MC medium (25% MC) and 25% RPMI as determined by western blotting. (A) Western blots of adipocyte lysates. (B) Densitometric analysis of signal intensity was used for semi-quantitative analysis of NF- $\kappa$ B p65 levels. Data are means  $\pm$  SD for groups of 3, normalised to GAPDH levels. \*P < 0.05, \*\*P < 0.01 vs unstimulated, stimulated controls. †P < 0.05 vs unstimulated controls (One-way ANOVA).

**Figure 4.11 Phosphorylated p38 MAPK protein expression in human adipocytes supplemented with calcitriol**



Phosphorylated p38 MAPK protein expression in calcitriol-treated adipocytes incubated in 25% MC medium (25% MC) and 25% RPMI as determined by western blotting. (A) Protein expression in cell lysates was analysed by Western Blotting and GAPDH used as loading controls. (B) Densitometric analysis of signal intensity was used for semi-quantitative analysis of phosphorylated p38 MAPK levels. Data are means  $\pm$  SD for groups of 3, normalised to GAPDH levels. \*P < 0.05, \*\*P < 0.01 vs unsupplemented, stimulated controls. †P < 0.05, ††P < 0.01 vs unstimulated controls (One-way ANOVA).

## **4.6 The effects of calcitriol on monocyte migration**

### **4.6.1 Calcitriol supplementation decreases THP-1 monocyte migration**

The medium of calcitriol supplemented adipocytes (consisting of 25% RPMI) induced a highly significant decrease in THP-1 monocyte migration (Figure 4.12E) compared to controls and this effect was observed for both low dose ( $10^{-11}$ M;  $P < 0.001$ ) and high dose ( $10^{-8}$ M;  $P < 0.001$ ) calcitriol supplemented groups. Estimated cell numbers of control groups were compared to serum-supplemented and unsupplemented DMEM medium to correct the effect on cell migration mediated by foetal bovine serum and DMEM medium.

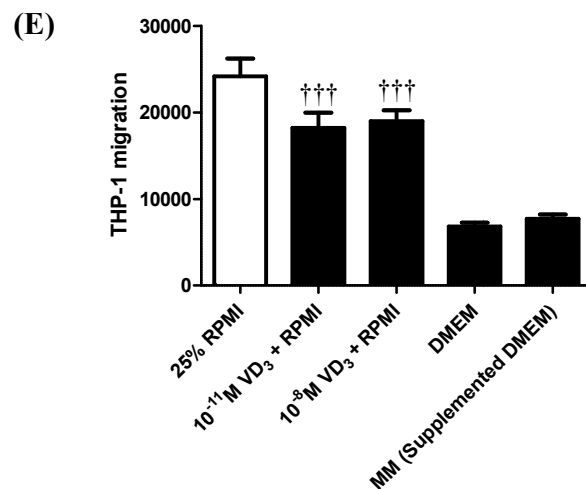
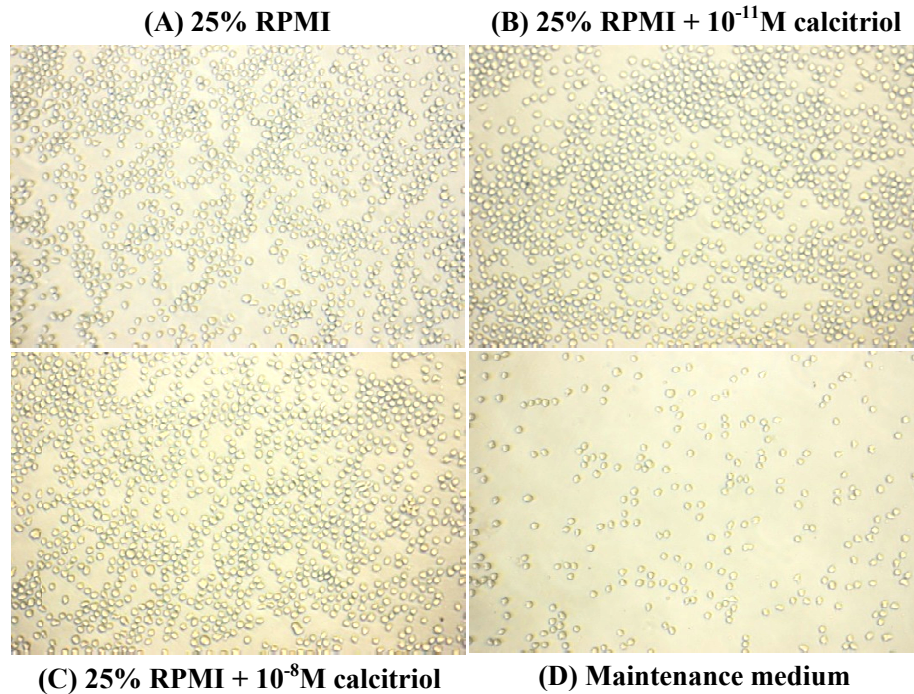
### **4.6.2 Effects of calcitriol supplementation on THP-1 cell migration by adipocytes stimulated with MC medium**

The medium collected from adipocytes incubated with 25% RPMI or 25% MC medium was used for the THP-1 migration assay. As shown in Figure 4.13, THP-1 monocyte migration was significantly increased in the medium of MC incubated adipocytes compared to adipocytes incubated with 25% RPMI. Low dose ( $10^{-11}$ M) calcitriol supplementation of adipocytes incubated with 25% MC medium did not alter THP-1 cell migration (Figure 4.13E). There was a significant increase of THP-1 cell migration in the high dose group ( $10^{-8}$ M;  $P = 0.002$ ).

#### **4.6.3 Calcitriol supplementation does not decrease THP-1 monocyte migration by adipocytes stimulated with TNF- $\alpha$**

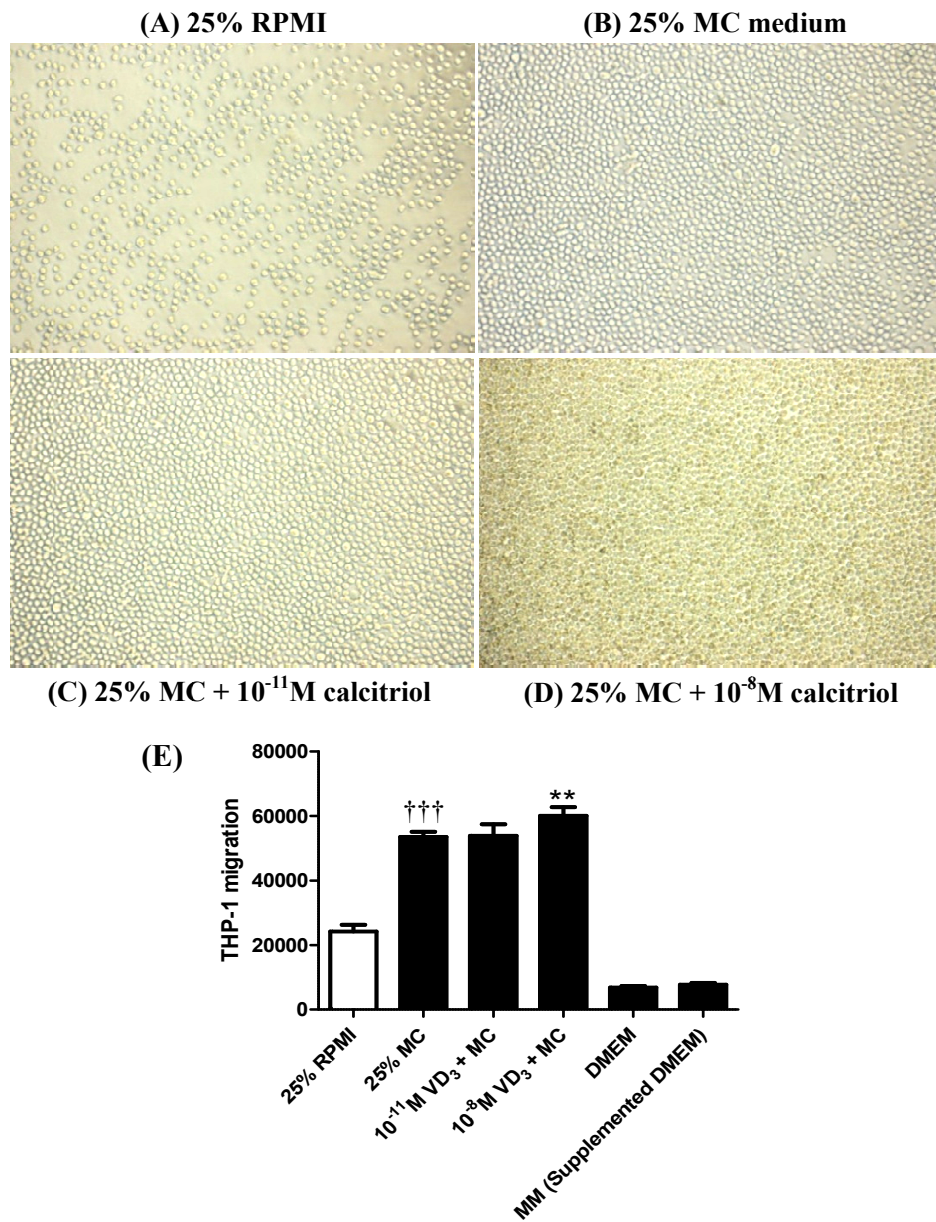
The medium collected from adipocytes incubated with and without 5ng/ml TNF- $\alpha$  in 25% RPMI medium was used for the THP-1 migration assay. According to Figure 4.14E, TNF- $\alpha$  significantly increased the THP-1 monocyte migration compared to controls. There was no significant effect of calcitriol supplementation on THP-1 cell migration in TNF- $\alpha$  stimulated adipocytes.

**Figure 4.12 THP-1 monocyte transmigration by the medium of calcitriol-supplemented adipocytes**



The figure shows THP-1 monocyte migration by the medium of adipocytes incubated in (A) 25% RPMI (B) 25% RPMI and  $10^{-11}$ M calcitriol (C) 25% RPMI and  $10^{-8}$ M calcitriol (D) supplemented DMEM (Maintenance medium). (E) shows the quantified results of transmigrated THP-1 monocytes. Cell medium collected after 24 hours in the studies described in section 4.2.1 was used for the transmigration assay. Results are given as means  $\pm$  SD for groups of 6.  $^{\dagger\dagger\dagger}P < 0.001$  vs controls (One-way ANOVA).

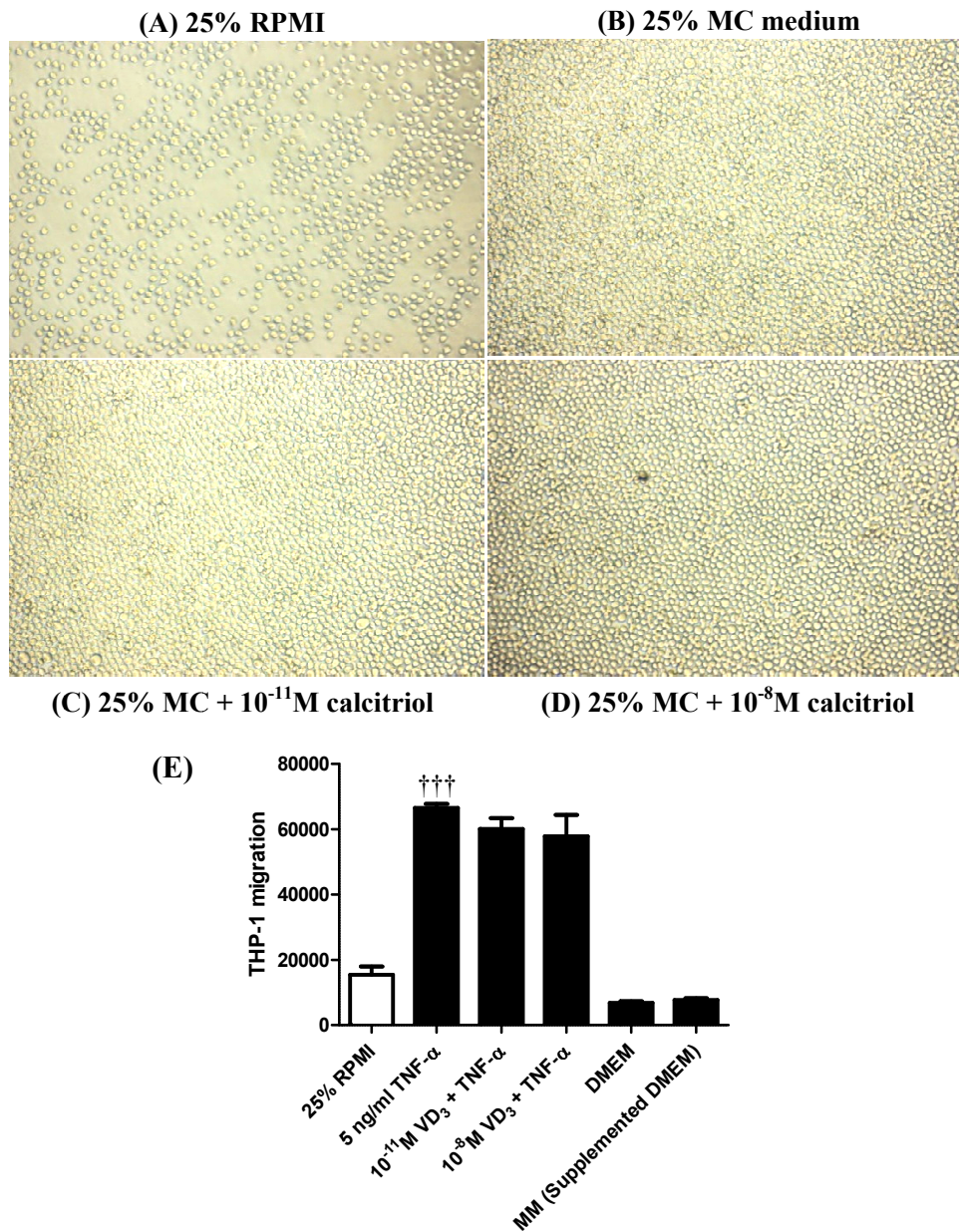
**Figure 4.13 THP-1 monocyte transmigration by the medium of adipocytes stimulated with MC medium**



The figure shows THP-1 monocyte migration by the medium of adipocytes incubated in (A) 25% RPMI (B) 25% MC medium (C) 25% MC medium and  $10^{-11}$ M calcitriol (D) 25% MC medium and  $10^{-8}$ M calcitriol. (E) shows the quantified results of transmigrated THP-1 monocytes. Cell medium collected after 24 hours in the studies described in section 4.2.3 was used for the transmigration assay. Results are given as means  $\pm$  SD for groups of 6. †††P < 0.001 vs unstimulated control, \*\*P < 0.01 vs unsupplemented control (One-way ANOVA).



**Figure 4.14 THP-1 monocyte transmigration by the medium of adipocytes stimulated with TNF- $\alpha$**



The figure shows THP-1 monocyte migration by the medium of adipocytes incubated in (A) 25% RPMI (B) 5 ng/ml TNF- $\alpha$  (C) TNF- $\alpha$  and 10<sup>-11</sup>M calcitriol (D) TNF- $\alpha$  and 10<sup>-8</sup>M calcitriol. (E) shows the quantified results of transmigrated THP-1 monocytes. Cell medium collected after 24 hours in the TNF- $\alpha$  studies described in section 4.2.3 was used for the transmigration assay. Results are given as means  $\pm$  SD for groups of 3-6. <sup>†††</sup>P < 0.001 vs unstimulated control (One-way ANOVA).

## **4.7 The effects of calcitriol on gene expression of VDR in human adipocytes**

### **4.7.1 Calcitriol enhances VDR gene transcription**

#### *4.7.1.1 Calcitriol increases basal VDR expression*

Figure 4.15 shows the level of VDR mRNA expression in MC medium and TNF- $\alpha$  stimulated adipocytes. Low dose calcitriol supplementation did not cause a difference in VDR gene expression levels. High dose calcitriol supplementation, however, induced a 2.3-fold increase in basal VDR expression (P = 0.043).

#### *4.7.1.2 Calcitriol further enhances VDR gene expression in adipocytes stimulated by 25% MC medium*

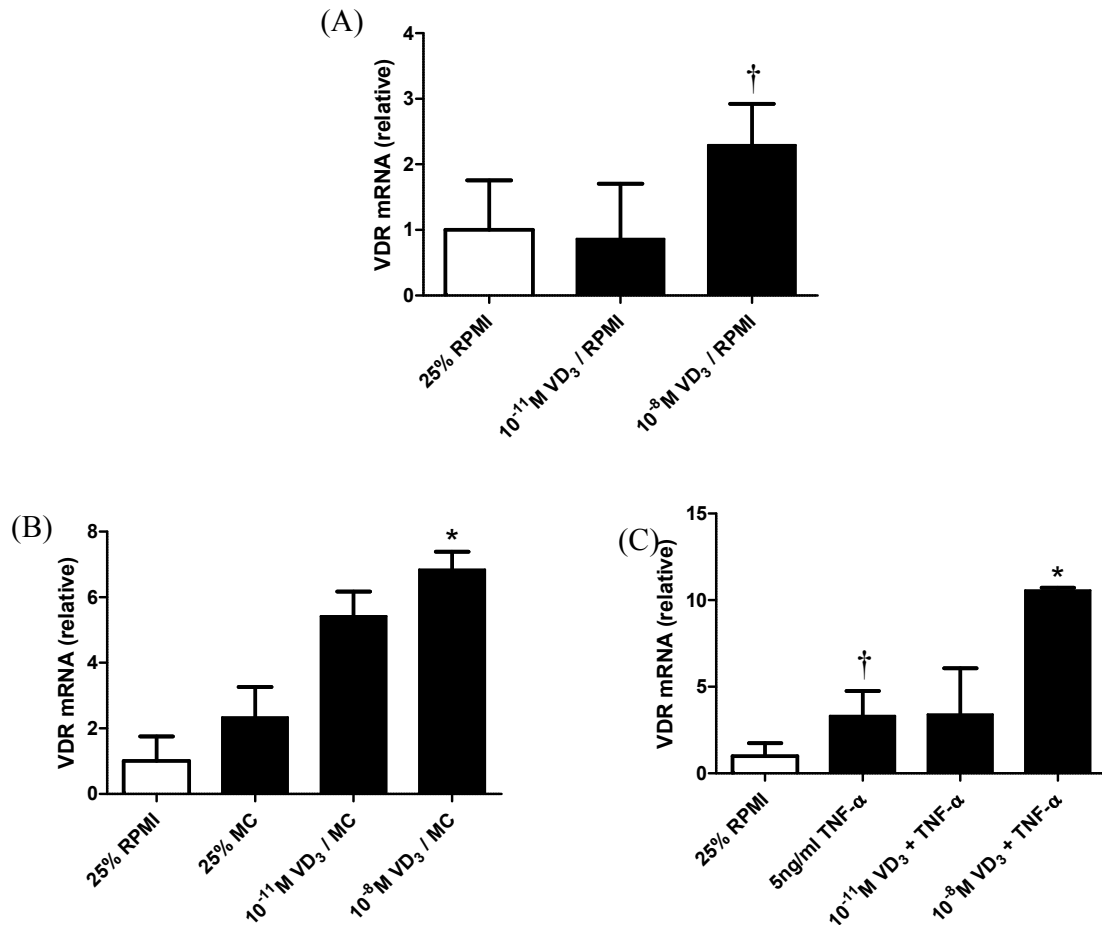
Figure 4.15 shows increased VDR gene expression in calcitriol-supplemented adipocytes stimulated with MC medium compared to unsupplemented, MC medium-stimulated adipocytes. There was a 2.9-fold increase in VDR gene expression with high dose calcitriol supplementation in 25% MC medium stimulated adipocytes (P = 0.012) compared to unsupplemented controls. Low dose calcitriol supplementation also increased VDR gene expression but this was not statistically significant.

#### *4.7.1.3 Calcitriol increases VDR gene expression in TNF- $\alpha$ stimulated adipocytes*

As shown in Figure 4.15, VDR gene expression was increased by TNF- $\alpha$ . Low dose calcitriol supplementation in adipocytes stimulated with TNF- $\alpha$  did not affect VDR gene

expression. In high dose supplementation however, a 3.2-fold increase in VDR gene expression was observed compared to unsupplemented TNF- $\alpha$ -stimulated controls (P = 0.034).

**Figure 4.15 VDR gene expression in MC medium and TNF- $\alpha$  stimulated adipocytes**

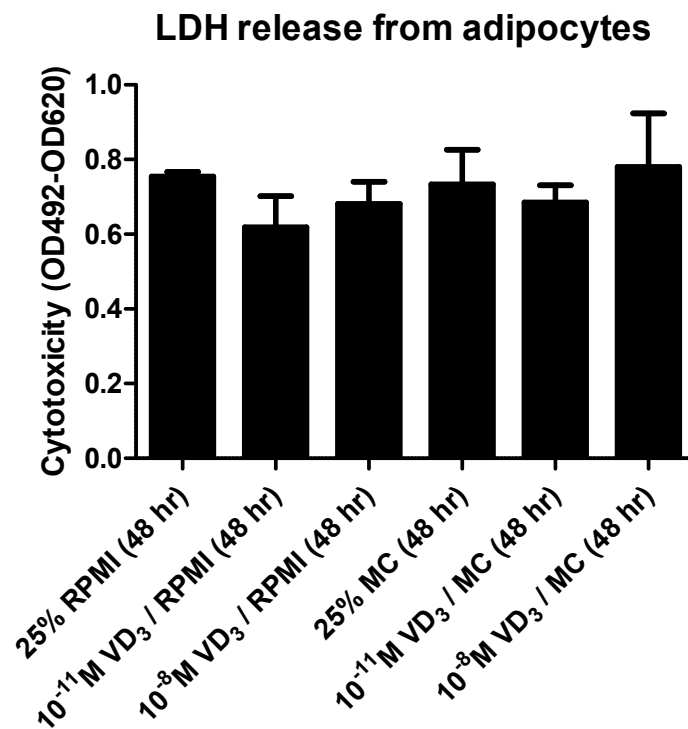


(A) Adipocytes incubated with calcitriol. (B) Adipocytes incubated with calcitriol stimulated with 25% MC medium. (C) Adipocytes incubated with calcitriol and stimulated with 5 ng/ml TNF- $\alpha$ . VDR gene expression was determined by real-time PCR and normalised to  $\beta$ -actin. Results are given as means  $\pm$  SD for groups of 6. \* $P$  < 0.05 vs un-supplemented, MC medium-stimulated controls. <sup>†</sup> $P$  < 0.05 vs unstimulated controls (One-way ANOVA).

## **4.8 Cytotoxicity assessment**

As shown in Figure 4.16, there were no significant differences in LDH release by adipocytes treated with MC medium in 48 hours. Therefore, neither macrophage-conditioned media nor calcitriol with DMSO induced cell cytotoxicity.

Figure 4.16 LDH release from human adipocytes



Cytotoxicity was determined by the measurement of lactate dehydrogenase released into cell culture medium by human adipocytes. Cell medium collected from calcitriol-treated adipocytes were tested for LDH release. Cell culture medium of adipocytes were treated with calcitriol in 25% RPMI or 25% MC medium and collected after 48 hours. Results are given as means  $\pm$  SD for groups of 4.

## **Chapter 5**

### **Discussion and conclusion**

## 5.1 Introduction

Adipose tissue is now considered to be a multifunctional endocrine organ secreting a wide range of protein factors collectively termed as adipokines (Trayhurn and Bing, 2006). These adipokines have considerable effects on lipid and glucose metabolism, the alternative complement system, the renin-angiotensin system as well as energy balance. There is now a growing number of adipokines found to be involved in inflammation and these particular adipokines have been known to increase in circulating levels in obesity (Trayhurn and Wood, 2005). The raised levels of acute-phase proteins and inflammatory cytokines found in the systemic circulation has led to the postulation that obesity is characterised by a state of low-level chronic inflammation (Xu *et al.*, 2003; Wellen and Hotamisligil, 2005). Medical dogma avers that excessive inflammation leads to lowered functionality of organs and the persistence of this inflammatory state promote the comorbid conditions associated with obesity, such as insulin resistance, Type 2 diabetes and cardiovascular disease.

A considerable amount of research has been conducted over recent years to elucidate the mechanistic links between adipokinic inflammation and obesity comorbidities (Hotamisligil *et al.*, 1996; Hirosumi *et al.*, 2002; Perseghin *et al.* 2003; Cai *et al.* 2005). Macrophage-infiltration in adipose tissue provides an important mechanistic link between the obese state and an increase in cytokine production which may form the basis of chronic inflammation associated with obesity comorbidities (Weisberg *et al.*, 2003). The vitamin D system is increasingly recognised to have a range of physiological functions



beyond calcium homeostasis and bone metabolism (Lin and White, 2004; Bikle, 2009). In particular, vitamin D<sub>3</sub> is a strong candidate for the promotion of anti-inflammatory activity, given its immunomodulatory effects in several cell types (Deluca and Cantorna, 2001; Wang *et al.*, 2004; Chen *et al.*, 2007). Vitamin D deficiency is also well-documented in obesity and chronic inflammation (Hyppönen and Power, 2007; Timms *et al.* 2002). It is therefore one of the primary aims of this study to contribute to current knowledge of vitamin D<sub>3</sub>, particularly its possible role in alleviating inflammation in adipocytes.

A simulated model of adipocyte inflammation was created by incubating adipocytes with macrophage-conditioned (MC) medium. This model was then used to study the efficacy of calcitriol supplementation in alleviating proinflammatory mediators expressed and released by human adipocytes. The potential involvement of NF- $\kappa$ B and MAPK signalling pathways was also studied.

## **5.2 Macrophage-produced factors induce inflammatory responses in human adipocytes**

Chapter 3 demonstrates that macrophage-secreted factors increase inflammatory mediators produced by human primary adipocytes. The LDH assay showed that there were no significant differences in LDH production between cells treated with MC medium and cells treated with RPMI medium. Therefore it was concluded that the MC medium did not have a cytotoxic effect on adipocytes and any changes to gene expression or protein release were not due to cytotoxicity in adipocytes. The results show that gene

expression of MCP-1, IL-6 and IL-1 $\beta$  in human primary adipocytes was extensively upregulated when exposed to macrophage-produced factors. The increase in MCP-1 and IL-6 gene expression was substantiated with corresponding data of increased MCP-1 and IL-6 production measured in the culture medium of adipocytes. The data strongly suggest that adipocytes are a major source of MCP-1 and IL-6 production in the presence of macrophage infiltration, substantiating the findings by Sartipy and Loskutoff (2003). The study also shows that expression of these proinflammatory genes are stimulated by TNF- $\alpha$ , a major cytokine produced by activated macrophages.

The drastic increase in MCP-1 produced by adipocytes stimulated by MC medium is consistent with the increase in macrophage infiltration in adipose tissue in obesity. MCP-1 fuels the paracrine loop between macrophages and adipocytes (Suganami *et al.*, 2005). Elevated levels of MCP-1 increase the diapedesis of monocytes and macrophages and promote monocyte differentiation into macrophages and foam cells (Tabata *et al.*, 2003). This effect was evident in the present study as the level of THP-1 monocyte migration was increased more than two-fold with macrophage-conditioned medium. Based on the present study and a previous study by Kanda *et al.* (2006), it is postulated that the THP-1 chemotactic activity in the transmigration study was mainly attributed to the MCP-1 content produced by stimulated adipocytes.

A large increase in MCP-1 by adipocytes has important implications in modulating adipose tissue function. Sartipy and Loskutoff (2003) demonstrated that recombinant MCP-1 significantly inhibited insulin-mediated glucose uptake in cells by approximately

30%. Sartipy and Loskutoff also showed in the same study that exposure of adipocytes to MCP-1 can reduce adiponin, lipoprotein lipase, GLUT-4, PPAR- $\gamma$ ,  $\alpha$ 2 and  $\beta$ 3-adrenergic receptor expression. This suggests that excessive MCP-1 production that can result from adipocyte and macrophage crosstalk may play a major role in the pathogenesis of common obesity comorbidities such as insulin resistance and dyslipidaemia.

The large increase in IL-6 produced by adipocytes stimulated with macrophage-secreted factors is an interesting key finding in this study. This study demonstrated a considerable increase in IL-6 levels produced by adipocytes stimulated with macrophage conditioned medium and TNF- $\alpha$ . The data also showed that IL-6 produced by adipocytes upon stimulation was considerably higher than that of IL-6 secreted by macrophages. This observation strongly suggests that most IL-6 found in adipose tissue in the occurrence of macrophage infiltration would be attributable to adipocytes, which is consistent with the observations in 3T3-L1 cells (Yamashita *et al.*, 2007). The results also suggest that the proportion of IL-6 produced by macrophages compared to adipocytes in WAT after stimulation with inflammatory mediators may be much lower than 50%, as proposed by Fantuzzi (2005). TNF- $\alpha$  stimulation of human adipocytes in this study did not elicit an IL-6 production as high as that of macrophage-conditioned medium, indicating that other moieties produced by macrophages in the macrophage-conditioned medium may be involved in IL-6 regulation in adipocytes. Adipose tissue is a major source of IL-6 production, accounting for 15-35% of circulating levels in the blood (Mohamed-Ali *et al.*, 1997). The results from the present study suggest that macrophage infiltration in adipose tissue could cause adipocytes to become a major source of IL-6 production.

NF- $\kappa$ B is a key transcription factor that plays a pivotal role in TNF- $\alpha$  induced inflammatory gene expression in adipocytes (Cawthorn and Sethi, 2008). p38 MAPK also regulates the expression of many cytokines and chemokines in non-fat cells, transducing the effects of TNF- $\alpha$  in defined phosphorylation cascades (Kiriakis, 1999; Rydén *et al.*, 2002). Although the role of p38 MAPK has been well studied in adipocyte differentiation and glucose metabolism, its role in the adipocyte inflammatory process is still unclear (Gehart *et al.*, 2010). It is evident that the activation of these two pathways is central to activating the gene expression of inflammatory mediators, including genes encoding TNF- $\alpha$  and IL-6. The current data together with studies carried out by Zhu *et al.* (2008) suggest that MCP-1 production is mediated by NF- $\kappa$ B. In the current study, I $\kappa$ B $\alpha$  was decreased and phosphorylated NF- $\kappa$ B p65 was increased in adipocytes stimulated by MC medium, suggesting that there was an increase in NF- $\kappa$ B activation. In addition, phosphorylated p38 MAPK was increased by stimulation with MC medium and this is consistent with an increase in p38 MAPK activation.

The relative expression of anti-inflammatory adipokines by adipocytes in the present study was also altered. Adiponectin and ZAG gene expression was downregulated by both macrophage-secreted factors and TNF- $\alpha$ . This is consistent with the recent findings by our group (Gao *et al.*, 2010). Substantiating the gene expression data, the present study showed that MC medium induced a decrease in adipocyte release of adiponectin and ZAG by adipocytes.

Recent studies by our group showed a three-fold increase in ZAG gene expression in adipocytes treated with rosiglitazone, indicating the involvement of PPAR- $\gamma$  action in regulating ZAG levels (Bao *et al.*, 2005). PPAR- $\gamma$  has been shown to regulate the transcription of many adipocyte-secreted proteins, including adiponectin and ZAG (Bao, 2005; Gao, 2010). The downregulation of ZAG and adiponectin suggests that a common pathway, presumably PPAR- $\gamma$  mediated, could be inhibited by NF- $\kappa$ B or MAPK activation.

Taken together, the secretion of proinflammatory adipokines by adipocytes stimulated with macrophage-derived factors provides a likely explanation for raised levels of inflammatory mediators, which is associated with increased macrophage infiltration in adipose tissue in obesity.

### **5.3 Calcitriol promotes anti-inflammatory activity in adipocytes**

This study has demonstrated that high dose calcitriol supplementation of adipocytes counteracted the increase in gene expression of MCP-1, IL-6 and IL-1 $\beta$  expression caused by macrophage medium stimulation. The data also showed a significant decrease in MCP-1 and IL-6 concentration in the medium of both MC medium stimulated adipocytes and unstimulated adipocytes, suggesting that calcitriol supplementation decreased the production of MCP-1 and IL-6. The analysis of LDH levels in cell culture medium showed that there were no significant differences between MC medium stimulated cells treated with calcitriol and control cells. Therefore any changes to the

gene expression or protein release were not due to cytotoxicity in adipocytes. Consistent with our results, a recent study has shown that calcitriol ( $10^{-7}$ M) reduced MCP-1 mRNA and protein release by human adipocytes stimulated by TNF- $\alpha$  (Lorente-Cebrián *et al.*, 2011).

Calcitriol supplementation also reduced the increase in MCP-1 and IL-6 gene expression caused by TNF- $\alpha$  stimulation in adipocytes. In addition, IL-6 release by adipocytes was lowered with calcitriol supplementation. The paralleled suppression of IL-6 production in both MC medium and TNF- $\alpha$  stimulated adipocytes with calcitriol treatment suggests that calcitriol reduces the proinflammatory effects induced by macrophage-derived factors in adipocytes. The results are consistent with the reduction in IL-6 production in 3T3-L1 adipocytes supplemented with vitamin D<sub>3</sub> and vitamin E (Lira *et al.*, 2011). *In vivo*, vitamin D<sub>3</sub> supplementation was shown to decrease serum IL-6 levels in clinical studies (Van den Berghe *et al.*, 2003). However, the inhibition of MCP-1 release was not observed in calcitriol-treated adipocytes withz TNF- $\alpha$  stimulation, suggesting that calcitriol-mediated inhibition of MCP-1 release by MC medium may not be mediated primarily by the effect of TNF- $\alpha$ .

The gene expression of anti-inflammatory adipokines in adipocytes was also significantly altered by calcitriol. Basal ZAG and adiponectin gene expression increased significantly in adipocytes with high dose calcitriol supplementation. High dose calcitriol supplementation in adipocytes also partially reversed the decrease in adiponectin and ZAG expression caused by MC medium stimulation. Adiponectin release was decreased

by calcitriol although there was no change in ZAG release levels. The results suggest that calcitriol also protects against the inhibitory effects of macrophage-derived factors by modulating the production of adiponectin and ZAG by human adipocytes.

These results led to the postulation that calcitriol may act on transcription factors and activation pathways leading to proinflammatory gene expression. Thus the effect of calcitriol supplementation on the expression of proinflammatory intracellular signalling molecules was subsequently explored. Calcitriol supplementation was able to increase I $\kappa$ B $\alpha$  levels in a dose-dependent manner, while decreasing the levels of phosphorylated NF- $\kappa$ B p65 and p38 MAPK with both low and high dose supplementation. The increase in I $\kappa$ B $\alpha$  and decrease in phosphorylated NF- $\kappa$ B p65 induced by high dose calcitriol is consistent with a stronger anti-inflammatory secretion profile observed in adipocytes supplemented with high doses of calcitriol. NF- $\kappa$ B activation is known to promote MCP-1 and IL-6 transcription in adipocytes (Zhu *et al.*, 2008; Ruan *et al.*, 2002). Similar effects of calcitriol on the inhibition of NF- $\kappa$ B have been reported in mouse embryonic fibroblasts (Chen *et al.*, 2011). Interestingly, calcitriol has also been shown to decrease NF- $\kappa$ B activation in mesangial cells caused by macrophage accumulation in kidney glomeruli and interstitium (Zhang *et al.*, 2007). Furthermore, it has been shown that the downregulation of MCP-1 production is also linked to the concurrent decrease of NF- $\kappa$ B and p38 MAPK (Fain and Madan, 2005).

Taken together, it appears that vitamin D<sub>3</sub> supplementation has an anti-inflammatory effect in adipocytes. The results of the study demonstrated that low dose calcitriol was

unable to effectively inhibit proinflammatory processes. A much more apparent anti-inflammatory effect in adipocytes was observed with high dose calcitriol supplementation. This suggests the involvement of an intracellular competitive inhibitory effect that may be mediated by calcitriol. The data also suggests that vitamin D<sub>3</sub> supplementation has beneficial effects in limiting the proinflammatory changes induced by macrophage-secreted factors. It is not known if calcitriol stimulates anti-inflammatory cytokines produced by macrophages and further studies will be needed.

Other interesting results include the detection of VDR gene expression in human adipocytes and the upregulation of VDR gene expression with high dose calcitriol supplementation. Interestingly, VDR gene expression was elevated in both MC medium and TNF- $\alpha$  stimulated adipocytes. These preliminary data suggest that VDR could be involved in the inflammatory response in adipocytes. Macrophages are known to produce both proinflammatory and anti-inflammatory cytokines (Opal and DePalo, 2000). Further studies, therefore, will be required to clarify the nature and regulation of VDR in adipocytes by macrophages.

In conclusion, the study suggests that increasing the calcitriol concentration available to adipocytes has potential benefits for the reduction of the inflammatory response that may arise from the macrophage and adipocyte crosstalk that occurs in obesity. This supports the notion that increasing the intake or synthesis of vitamin D may lower the inflammatory response by adipose tissue. The study is limited to observations of cells treated with calcitriol prior to inflammatory challenge, which suggests that the anti-



inflammatory effects seen may be a consequence of calcitriol availability at an early stage of adipocyte development. However, it is understood that adipocytes are renewed at an approximate rate of 10% annually for individuals of all ages and BMIs (Spalding *et al.*, 2008). This dynamic renewal of adipose tissue therefore presents opportunities for vitamin D pharmacotherapy of dysfunctional adipose tissue at the early stages of adipocyte development. However it is not known whether calcitriol will have anti-inflammatory effects on obese adipose tissue which may have had interactions with macrophages for a longer period of time. More studies will be required to observe the effects of calcitriol on adipose tissue in longer term obesity, as they may respond differently to macrophages as well as pharmacotherapy.

#### **5.4 Limitations of the study and future work**

The concentration of IL-1 $\beta$  in adipocyte culture medium could not be measured by IL-1 $\beta$  ELISA development kits we acquired. It is possible that the release of IL-1 $\beta$  by adipocytes may be lower than the detection limit of the assay. There is a general consensus that most IL-1 $\beta$  found in adipose tissue is produced by the stromal vascular cells, which include resident macrophages. Given the comparatively high amount of IL-1 $\beta$  produced by macrophages in 25% macrophage-conditioned medium used in the study, it was also not possible to effectively measure the differences in IL-1 $\beta$  production by adipocytes incubated in macrophage-conditioned medium.

While the macrophages in the macrophage conditioned medium did induce an overall proinflammatory effect on adipocytes, it is not known whether this emulated the

behaviour of macrophages in obesity. It is understood that macrophages associated with the lean phenotype are activated by the alternative pathway and may promote an anti-inflammatory effect. Adipose tissue macrophages recruited in obesity are also known to have unique properties compared to resident macrophages (Lumeng *et al.*, 2007). Future studies should include the use of macrophages with a resultant cytokine secretion profile that is representative of macrophages in obesity. The effects of calcitriol may also be investigated in macrophages, as calcitriol has been shown *in vitro* to alternatively activate macrophages and downregulate proinflammatory cytokine production.

TNF- $\alpha$  treated samples were not studied for adipokine expression and release due to the lack of time and resources for this dissertation. It is recommended that future work include studies on PPAR, C/EBP $\alpha$  and Akt detection to study the molecular mechanisms by which adiponectin and ZAG are regulated. Other possible signalling pathways that are VDR-related should be studied as well, such as the adenylate cyclase and PKC, of which upon activation increase and decrease VDR respectively.

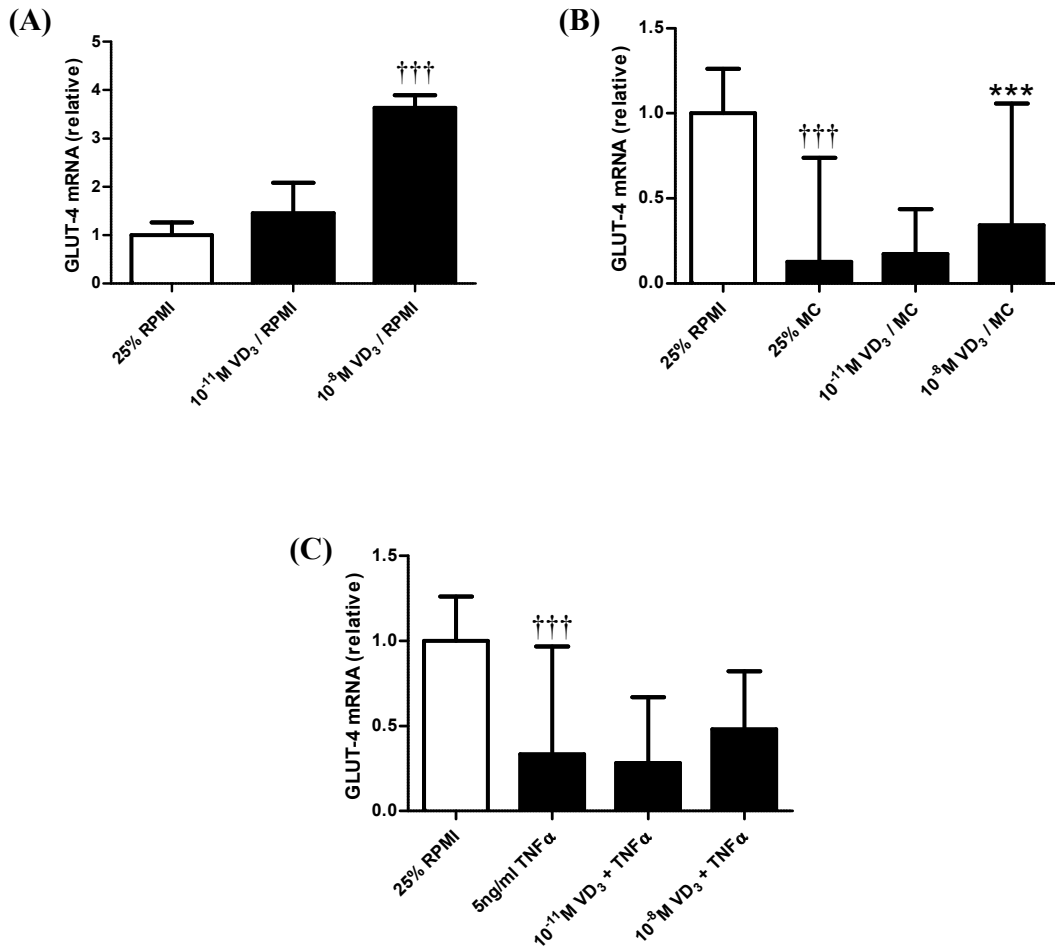
Because of its strong links to NF- $\kappa$ B and VDR signalling, as well as its role in glucose and lipid metabolism, PPARs have been identified as potential candidate genes to study for its role in inflammation and vitamin D action in adipocytes. The possible involvement of PPARs in inflammatory crosstalk between macrophages and adipocytes brings into question its role in insulin resistance and dyslipidaemia. The following section presents some pilot data on the effects of macrophage-secreted factors and vitamin D<sub>3</sub> on the indicators of glucose and lipid metabolism.

### *Calcitriol improves glucose metabolism*

The pilot data showed a modulation of glucose metabolism in adipocytes incubated with macrophage-produced factors. Adipocytes stimulated with 25% MC medium has a 7.9-fold decrease in GLUT-4 gene expression ( $P < 0.001$ ; Figure 5.1) TNF- $\alpha$  also induced a 3-fold decrease in GLUT-4 gene expression in adipocytes ( $P < 0.001$ ), strongly suggesting the cytokine's involvement in GLUT-4 regulation. Protein signalling studies also showed a decrease in GLUT-4 production (Figure 5.2). High dose calcitriol supplementation in a non-inflammatory environment increased GLUT-4 mRNA expression ( $P < 0.001$ ). High dose calcitriol supplementation was also able to effect a similar increase in an inflammatory environment provided by macrophage medium ( $P < 0.001$ ).

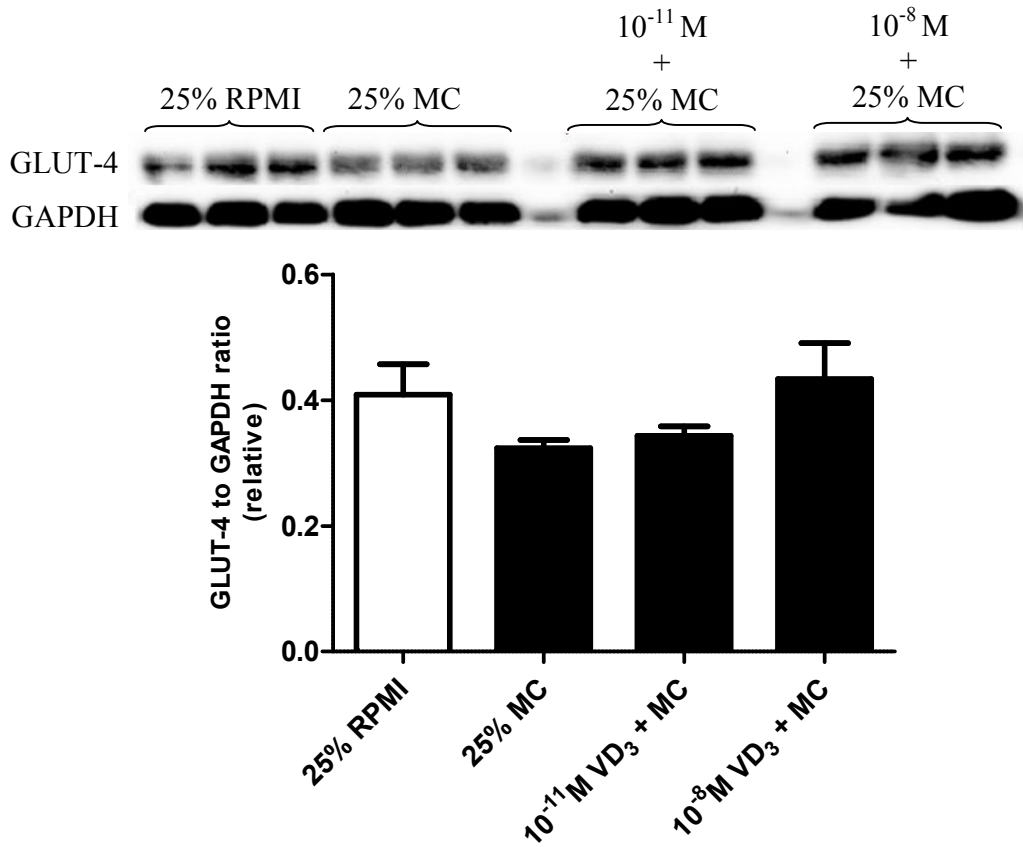
Expression of IR $\beta$  was slightly decreased with 25% MC medium incubation (Figure 5.3), which suggests a possible insulin/PI3K-dependent pathway that may be modulated by macrophage-secreted factors. Calcitriol supplementation did not appear to alter the levels of IR $\beta$ . It is postulated that proper insulin sensitivity experiments will need to be conducted to accurately determine the effect of macrophages on insulin sensitivity, which should include measurement of IRS-1 phosphorylation with insulin fasted specimens.

**Figure 5.1 GLUT-4 mRNA expression in calcitriol-supplemented adipocytes**



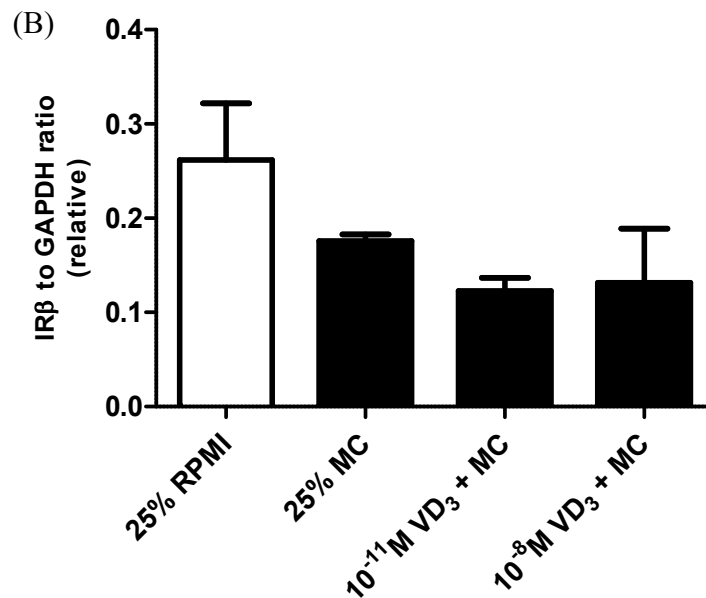
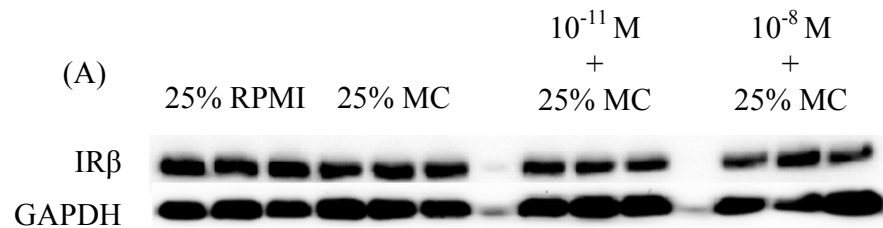
GLUT-4 mRNA expression of cells from calcitriol-treated groups incubated in conditioned outlined in sections 4.2.1 and 4.2.3. (A) GLUT-4 expression in calcitriol-treated cells incubated in RPMI. (B) GLUT-4 expression in calcitriol-treated cells incubated in 25% MC medium. (C) GLUT-4 expression in calcitriol-treated cells incubated with 5ng/ml TNF- $\alpha$ . Results are given as means  $\pm$  SD for groups of 6. (NT: non-treated.) \*\*\*P < 0.001 compared with untreated 25% MC controls. †††P < 0.001 compared with untreated 25% RPMI medium incubated controls (One-way ANOVA).

**Figure 5.2 GLUT-4 protein production in calcitriol-supplemented adipocytes**



GLUT-4 release from calcitriol-treated adipocytes incubated in 25% MC. Results are given as means  $\pm$  SD for groups of 3. NT, non-treated. All comparisons were not significantly different compared with untreated 25% RPMI medium incubated controls ( $P > 0.05$ , One-way ANOVA).

**Figure 5.3 IR $\beta$  expression in human primary adipocytes supplemented with calcitriol incubated with 25% MC medium**



IR $\beta$  expression in calcitriol-supplemented human primary adipocytes as outlined in Figure 4.9. (A) Western blots of protein lysates of control and 25% MC medium incubated adipocytes. (B) Densitometric analysis of blots was used for semi-quantitative analysis of IR $\beta$  levels. (Calcitriol: VD<sub>3</sub>) Data are means  $\pm$  SD for groups of 3, presented relative to controls and normalised to GAPDH levels. All comparisons assessed by One-way ANOVA.

## 5.5 Conclusion

Adipose tissue is now recognised as a major endocrine organ, as more adipokines are being uncovered and functions found for some of them. Consistent with previous studies, this study has shown that adipocytes play major roles in the inflammatory response by secreting large quantities of various proinflammatory adipokines in response to inflammatory stimuli by macrophage-conditioned medium and TNF- $\alpha$ . The results support the notion that adipose tissue has a key role in modulating inflammatory responses.

This study demonstrated that supplementation of adipocytes with the active form of vitamin D<sub>3</sub>, calcitriol, decreased the production of several proinflammatory mediators in human primary adipocytes. A high dose (10<sup>-8</sup>M) of calcitriol supplementation was able to decrease the basal production of the proinflammatory mediators MCP-1 and IL-6 by human primary adipocytes. High dose calcitriol supplementation was also able to decrease the gene expression of MCP-1, IL-6 and IL-1 $\beta$  in adipocytes stimulated with macrophage-conditioned medium. In agreement with the gene expression data, MCP-1 and IL-6 release was also decreased with calcitriol supplementation. High dose calcitriol led to a decrease in IL-6 release while had no effect on MCP-1 release from adipocytes stimulated with TNF- $\alpha$ , suggesting that the inhibitory effect of calcitriol may be elicited in concert with other factors produced by macrophages.

High dose calcitriol supplementation also led to a significant increase in basal gene expression of adiponectin and ZAG. Upon MC medium stimulation, high dose calcitriol supplementation partially reversed the inhibitory effects on adiponectin and ZAG gene expression. Calcitriol also partially restored the production of adiponectin by adipocytes although did not affect ZAG production. These data suggest that calcitriol promotes gene transcription of anti-inflammatory adipokines in human adipocytes.

As the production of the proinflammatory mediators plays a role in macrophage infiltration into adipose tissue, the medium of calcitriol-supplemented adipocytes was used to assess THP-1 monocyte migration. This study showed that calcitriol decreased the chemoattractant ability of adipocytes as both low dose ( $10^{-11}$ M) and high dose ( $10^{-8}$ M) calcitriol reduced THP-1 monocyte migration.

High dose calcitriol significantly increased NF- $\kappa$ B I $\kappa$ B $\alpha$  protein expression and decreased levels of phosphorylated p38 MAPK in adipocytes. It also showed an inhibitory effect on protein abundance of p38 MAPK, a known activator of inflammatory cytokine expression. This suggests that calcitriol has a significant effect on modulating intracellular signalling that mediate the transcription of proinflammatory genes.

Overall, macrophage-derived factors potently induced the inflammatory response in adipocytes; high dose calcitriol supplementation has a protective role by reducing the overproduction of proinflammatory mediators by human adipocytes. The study has also shown that the beneficial effect of calcitriol in adipocytes may be mediated via the inhibition of NF- $\kappa$ B and p38 MAPK signalling.



## **References**

AOUADI, M., TESZ, G. J., NICOLORO, S. M., WANG, M., CHOUINARD, M., SOTO, E., OSTROFF, G. R. & CZECH, M. P. 2009. Orally delivered siRNA targeting macrophage Map4k4 suppresses systemic inflammation. *Nature*, 458, 1180-1184.

ARNER, P. 1995. Differences in Lipolysis between Human Subcutaneous and Omental Adipose Tissues. *Annals of Medicine*, 27, 435-438.

BAO, Y., BING, C., HUNTER, L., JENKINS, J. R., WABITSCH, M. & TRAYHURN, P. 2005. Zinc- $\alpha$ 2-glycoprotein, a lipid mobilizing factor, is expressed and secreted by human (SGBS) adipocytes. *FEBS Lett*, 579, 41-47.

BASTARD, J. P., MAACHI, M., VAN NHIEU, J. T., JARDEL, C., BRUCKERT, E., GRIMALDI, A., ROBERT, J. J., CAPEAU, J. & HAINQUE, B. 2002. Adipose tissue IL-6 content correlates with resistance to insulin activation of glucose uptake both in vivo and in vitro. *J Clin Endocrinol Metab*, 87, 2084-9.

BEER 1852. Bestimmung der Absorption des rothen Lichts in farbigen Flüssigkeiten. *Annalen der Physik*, 162, 78-88.

BERG, A. H. & SCHERER, P. E. 2005. Adipose tissue, inflammation, and cardiovascular disease. *Circ Res*, 96, 939-949.

BIKLE, D. 2009. Nonclassic actions of vitamin D. *J Clin Endocrinol Metab*, 94, 26-34.

BING, C., BAO, Y., JENKINS, J., SANDERS, P., MANIERI, M., CINTI, S., TISDALE, M. J. & TRAYHURN, P. 2004. Zinc- $\alpha$ 2-glycoprotein, a lipid mobilizing factor, is expressed in adipocytes and is up-regulated in mice with cancer cachexia. *Proceedings of the National Academy of Sciences of the United States of America*, 101, 2500-2505.

BJORNTORP, P. & OSTMAN, J. 1971. Human adipose tissue dynamics and regulation. *Adv Metab Disord*, 5, 277-327.

BLANCHETTE-MACKIE, E. J., DWYER, N. K., BARBER, T., COXEY, R. A., TAKEDA, T., RONDINONE, C. M., THEODORAKIS, J. L., GREENBERG, A. S. & LONDOS, C. 1995. Perilipin is located on the surface layer of intracellular lipid droplets in adipocytes. *J Lipid Res*, 36, 1211-26.

BODEN, G. 2011. Obesity, insulin resistance and free fatty acids. *Curr Opin Endocrinol Diabetes Obes*, 18, 139-43.

BOTELLA-CARRETERO, J. I., ALVAREZ-BLASCO, F., VILLAFRUELA, J. J., BALSAL, J. A., VAZQUEZ, C. & ESCOBAR-MORREALE, H. F. 2007. Vitamin D deficiency is associated with the metabolic syndrome in morbid obesity. *Clin Nutr*, 26, 573-80.

BOURLIER, V. & BOULOUMIE, A. 2009. Role of macrophage tissue infiltration in obesity and insulin resistance. *Diabetes Metab*, 35, 251-260.

- BOYDEN, S. 1962. The chemotactic effect of mixtures of antibody and antigen on polymorphonuclear leucocytes. *J Exp Med*, 115, 453-66.
- CAI, D., YUAN, M., FRANTZ, D. F., MELENDEZ, P. A., HANSEN, L., LEE, J. & SHOELSON, S. E. 2005. Local and systemic insulin resistance resulting from hepatic activation of IKK-beta and NF-kappaB. *Nat Med*, 11, 183-90.
- CANCELLO, R., HENEGAR, C., VIGUERIE, N., TALEB, S., POITOU, C., ROUAULT, C., COUPAYE, M., PELLOUX, V., HUGOL, D., BOUILLOT, J. L., BOULOUMIE, A., BARBATELLI, G., CINTI, S., SVENSSON, P. A., BARSH, G. S., ZUCKER, J. D., BASDEVANT, A., LANGIN, D. & CLEMENT, K. 2005. Reduction of macrophage infiltration and chemoattractant gene expression changes in white adipose tissue of morbidly obese subjects after surgery-induced weight loss. *Diabetes*, 54, 2277-86.
- CARLBERG, C. 2003. Current understanding of the function of the nuclear vitamin D receptor in response to its natural and synthetic ligands. *Recent Results Cancer Res*, 164, 29-42.
- CARROLL, A. M., HAINES, L. R., PEARSON, T. W., BRENNAN, C., BREEN, E. P. & PORTER, R. K. 2004. Immunodetection of UCP1 in rat thymocytes. *Biochem Soc Trans*, 32, 1066-7.
- CAWTHORN, W. P. & SETHI, J. K. 2008. TNF-alpha and adipocyte biology. *FEBS Lett*, 582, 117-31.
- CEDERBERG, A., GRØNNING, L. M., AHRÉN, B., TASKÉN, K., CARLSSON, P. & ENERBÄCK, S. 2001. FOXC2 Is a Winged Helix Gene that Counteracts Obesity, Hypertriglyceridemia, and Diet-Induced Insulin Resistance. *Cell*, 106, 563-573.
- CHARRIERE, G., COUSIN, B., ARNAUD, E., ANDRE, M., BACOU, F., PENICAUD, L. & CASTEILLA, L. 2003. Preadipocyte conversion to macrophage. Evidence of plasticity. *J Biol Chem*, 278, 9850-5.
- CHEN, S., SIMS, G. P., CHEN, X. X., GU, Y. Y. & LIPSKY, P. E. 2007. Modulatory effects of 1,25-dihydroxyvitamin D3 on human B cell differentiation. *J Immunol*, 179, 1634-47.
- CHEN, Y., KONG, J., SUN, T., LI, G., SZETO, F. L., LIU, W., DEB, D. K., WANG, Y., ZHAO, Q., THADHANI, R. & LI, Y. C. 2011. 1,25-Dihydroxyvitamin D suppresses inflammation-induced expression of plasminogen activator inhibitor-1 by blocking nuclear factor-kappaB activation. *Arch Biochem Biophys*, 507, 241-7.
- CHIU, K. C., CHU, A., GO, V. L. W. & SAAD, M. F. 2004. Hypovitaminosis D is associated with insulin resistance and beta cell dysfunction. *Am J Clin Nutr*, 79, 820-825.
- CHOMCZYNSKI, P. & SACCHI, N. 2006. The single-step method of RNA isolation by

acid guanidinium thiocyanate-phenol-chloroform extraction: twenty-something years on. *Nat. Protocols*, 1, 581-585.

CINTI, S. 2009. Transdifferentiation properties of adipocytes in the adipose organ. *American Journal of Physiology - Endocrinology And Metabolism*, 297, E977-E986.

CLEMENT, K., VIGUERIE, N., POITOU, C., CARETTE, C., PELLOUX, V., CURAT, C. A., SICARD, A., ROME, S., BENIS, A., ZUCKER, J.-D., VIDAL, H., LAVILLE, M., BARSH, G. S., BASDEVANT, A., STICH, V., CANCELLO, R. & LANGIN, D. 2004. Weight loss regulates inflammation-related genes in white adipose tissue of obese subjects. *FASEB J*, 18, 1657-1669.

CONSTANT, V. A., GAGNON, A., LANDRY, A. & SORISKY, A. 2006. Macrophage-conditioned medium inhibits the differentiation of 3T3-L1 and human abdominal preadipocytes. *Diabetologia*, 49, 1402-11.

COPPACK, S. W. 2005. Adipose tissue changes in obesity. *Biochem Soc Trans*, 33, 1049-52.

COUSIN, B., MUNOZ, O., ANDRE, M., FONTANILLES, A. M., DANI, C., COUSIN, J. L., LAHARRAGUE, P., CASTEILLA, L. & PENICAUD, L. 1999. A role for preadipocytes as macrophage-like cells. *FASEB J*, 13, 305-12.

CURAT, C. A., MIRANVILLE, A., SENGENES, C., DIEHL, M., TONUS, C., BUSSE, R. & BOULOUMIE, A. 2004. From blood monocytes to adipose tissue-resident macrophages: induction of diapedesis by human mature adipocytes. *Diabetes*, 53, 1285-92.

DE MATTEIS, R., RICQUIER, D. & CINTI, S. 1998. TH-, NPY-, SP-, and CGRP-immunoreactive nerves in interscapular brown adipose tissue of adult rats acclimated at different temperatures: an immunohistochemical study. *Journal of Neurocytology*, 27, 877-886.

DELUCA, H. F. & CANTORNA, M. T. 2001. Vitamin D: its role and uses in immunology. *FASEB J*, 15, 2579-85.

DENG, T., SHAN, S., LI, P. P., SHEN, Z. F., LU, X. P., CHENG, J. & NING, Z. Q. 2006. Peroxisome proliferator-activated receptor-gamma transcriptionally up-regulates hormone-sensitive lipase via the involvement of specificity protein-1. *Endocrinology*, 147, 875-84.

DIEZ, J. J. & IGLESIAS, P. 2003. The role of the novel adipocyte-derived hormone adiponectin in human disease. *Eur J Endocrinol*, 148, 293-300.

DUNLOP, T. W., VAISANEN, S., FRANK, C., MOLNAR, F., SINKKONEN, L. & CARLBERG, C. 2005. The human peroxisome proliferator-activated receptor delta gene is a primary target of 1alpha,25-dihydroxyvitamin D3 and its nuclear receptor. *J Mol*

*Biol*, 349, 248-60.

EDENS, N. K., FRIED, S. K., KRAL, J. G., HIRSCH, J. & LEIBEL, R. L. 1993. In vitro lipid synthesis in human adipose tissue from three abdominal sites. *Am J Physiol*, 265, E374-9.

ENGVALL, E. & PERLMANN, P. 1971. Enzyme-linked immunosorbent assay (ELISA). Quantitative assay of immunoglobulin G. *Immunochemistry*, 8, 871-4.

FAGGIONI, R., FANTUZZI, G., FULLER, J., DINARELLO, C. A., FEINGOLD, K. R. & GRUNFELD, C. 1998. IL-1 beta mediates leptin induction during inflammation. *Am J Physiol*, 274, R204-8.

FAIN, J. N. 2006. Release of interleukins and other inflammatory cytokines by human adipose tissue is enhanced in obesity and primarily due to the nonfat cells. *Vitam Horm*, 74, 443-77.

FAIN, J. N. & MADAN, A. K. 2005. Regulation of monocyte chemoattractant protein 1 (MCP-1) release by explants of human visceral adipose tissue. *Int J Obes Relat Metab Disord*, 29, 1299-1307.

FANTUZZI, G. 2005. Adipose tissue, adipokines, and inflammation. *J Allergy Clin Immunol*, 115, 911-9; quiz 920.

FARNIER, C., KRIEF, S., BLACHE, M., DIOT-DUPUY, F., MORY, G., FERRE, P. & BAZIN, R. 2003. Adipocyte functions are modulated by cell size change: potential involvement of an integrin/ERK signalling pathway. *Int J Obes Relat Metab Disord*, 27, 1178-86.

FRAYN, K. N. 2002. Adipose tissue as a buffer for daily lipid flux. *Diabetologia*, 45, 1201-10.

FU, Y., LUO, N., KLEIN, R. L. & GARVEY, W. T. 2005. Adiponectin promotes adipocyte differentiation, insulin sensitivity, and lipid accumulation. *J Lipid Res*, 46, 1369-79.

FUJISAKA, S., USUI, I., BUKHARI, A., IKUTANI, M., OYA, T., KANATANI, Y., TSUNEYAMA, K., NAGAI, Y., TAKATSU, K., URAKAZE, M., KOBAYASHI, M. & TOBE, K. 2009. Regulatory Mechanisms for Adipose Tissue M1 and M2 Macrophages in Diet-Induced Obese Mice. *Diabetes*, 58, 2574-2582.

GAO, D. & BING, C. 2011. Macrophage-induced expression and release of matrix metalloproteinase 1 and 3 by human preadipocytes is mediated by IL-1 $\beta$  via activation of MAPK signaling. *Journal of Cellular Physiology*, 226, 2869-2880.

GAO, D., TRAYHURN, P. & BING, C. 2010. Macrophage-secreted factors inhibit ZAG expression and secretion by human adipocytes. *Molecular and Cellular Endocrinology*,

325, 135-142.

GEHART, H., KUMPF, S., ITTNER, A. & RICCI, R. 2010. MAPK signalling in cellular metabolism: stress or wellness? *EMBO Rep*, 11, 834-840.

GESTA, S., BEZY, O., MORI, M. A., MACOTELA, Y., LEE, K. Y. & KAHN, C. R. 2011. Mesodermal developmental gene Tbx15 impairs adipocyte differentiation and mitochondrial respiration. *Proc Natl Acad Sci U S A*, 108, 2771-6.

GIORDANO, A., FRONTINI, A., CASTELLUCCI, M. & CINTI, S. 2004. Presence and Distribution of Cholinergic Nerves in Rat Mediastinal Brown Adipose Tissue. *Journal of Histochemistry & Cytochemistry*, 52, 923-930.

GONG, F. Y., ZHANG, S. J., DENG, J. Y., ZHU, H. J., PAN, H., LI, N. S. & SHI, Y. F. 2009. Zinc-alpha2-glycoprotein is involved in regulation of body weight through inhibition of lipogenic enzymes in adipose tissue. *Int J Obes (Lond)*, 33, 1023-30.

GREENBERG, A. S., EGAN, J. J., WEK, S. A., GARTY, N. B., BLANCHETTE-MACKIE, E. J. & LONDOS, C. 1991. Perilipin, a major hormonally regulated adipocyte-specific phosphoprotein associated with the periphery of lipid storage droplets. *J Biol Chem*, 266, 11341-6.

HAMANN, A., BENECKE, H., LE MARCHAND-BRUSTEL, Y., SUSULIC, V. S., LOWELL, B. B. & FLIER, J. S. 1995. Characterization of insulin resistance and NIDDM in transgenic mice with reduced brown fat. *Diabetes*, 44, 1266-1273.

HAUSSLER, M. R., WHITFIELD, G. K., HAUSSLER, C. A., HSIEH, J. C., THOMPSON, P. D., SELZNICK, S. H., DOMINGUEZ, C. E. & JURUTKA, P. W. 1998. The nuclear vitamin D receptor: biological and molecular regulatory properties revealed. *J Bone Miner Res*, 13, 325-49.

HIRASAKA, K., KOHNO, S., GOTO, J., FUROCHI, H., MAWATARI, K., HARADA, N., HOSAKA, T., NAKAYA, Y., ISHIDOH, K., OBATA, T., EBINA, Y., GU, H., TAKEDA, S., KISHI, K. & NIKAWA, T. 2007. Deficiency of Cbl-b gene enhances infiltration and activation of macrophages in adipose tissue and causes peripheral insulin resistance in mice. *Diabetes*, 56, 2511-22.

HIROSUMI, J., TUNCMAN, G., CHANG, L., GORGUN, C. Z., UYSAL, K. T., MAEDA, K., KARIN, M. & HOTAMISLIGIL, G. S. 2002. A central role for JNK in obesity and insulin resistance. *Nature*, 420, 333-6.

HOFMANN, C., LORENZ, K., BRAITHWAITE, S. S., COLCA, J. R., PALAZUK, B. J., HOTAMISLIGIL, G. S. & SPIEGELMAN, B. M. 1994. Altered gene expression for tumor necrosis factor-alpha and its receptors during drug and dietary modulation of insulin resistance. *Endocrinology*, 134, 264-270.

HOLLAND, P. M., ABRAMSON, R. D., WATSON, R. & GELFAND, D. H. 1991.

- Detection of specific polymerase chain reaction product by utilizing the 5'---3' exonuclease activity of *Thermus aquaticus* DNA polymerase. *Proc Natl Acad Sci U S A*, 88, 7276-80.
- HONG, E. G., KO, H. J., CHO, Y. R., KIM, H. J., MA, Z., YU, T. Y., FRIEDLINE, R. H., KURT-JONES, E., FINBERG, R., FISCHER, M. A., GRANGER, E. L., NORBURY, C. C., HAUSCHKA, S. D., PHILBRICK, W. M., LEE, C. G., ELIAS, J. A. & KIM, J. K. 2009. Interleukin-10 prevents diet-induced insulin resistance by attenuating macrophage and cytokine response in skeletal muscle. *Diabetes*, 58, 2525-35.
- HOTAMISLIGIL, G. S. 2010. Endoplasmic reticulum stress and the inflammatory basis of metabolic disease. *Cell*, 140, 900-17.
- HOTAMISLIGIL, G. S., PERALDI, P., BUDAVARI, A., ELLIS, R., WHITE, M. F. & SPIEGELMAN, B. M. 1996. IRS-1-mediated inhibition of insulin receptor tyrosine kinase activity in TNF- $\alpha$ - and obesity-induced insulin resistance. *Science*, 271, 665-8.
- HOTAMISLIGIL, G. S., SHARGILL, N. S. & SPIEGELMAN, B. M. 1993. Adipose expression of tumor necrosis factor- $\alpha$ : direct role in obesity-linked insulin resistance. *Science*, 259, 87-91.
- HU, E., LIANG, P. & SPIEGELMAN, B. M. 1996. AdipoQ is a novel adipose-specific gene dysregulated in obesity. *J Biol Chem*, 271, 10697-10703.
- HULTIN, H., EDFELDT, K., SUNDBOM, M. & HELLMAN, P. 2010. Left-shifted relation between calcium and parathyroid hormone in obesity. *J Clin Endocrinol Metab*, 95, 3973-3981.
- HYPPÖNEN, E. & POWER, C. 2007. Hypovitaminosis D in British adults at age 45 y: nationwide cohort study of dietary and lifestyle predictors. *The American Journal of Clinical Nutrition*, 85, 860-868.
- INOUE, M., MATSUI, T., NISHIBU, A., NIHEI, Y., IWATSUKI, K. & KANEKO, F. 1998. Regulatory effects of 1 $\alpha$ ,25-dihydroxyvitamin D<sub>3</sub> on inflammatory responses in psoriasis. *Eur J Dermatol*, 8, 16-20.
- ISAIA, G., GIORGINO, R. & ADAMI, S. 2001. High prevalence of hypovitaminosis D in female type 2 diabetic population. *Diabetes Care*, 24, 1496-1496.
- ISHIBASHI, J. & SEALE, P. 2010. Beige Can Be Slimming. *Science*, 328, 1113-1114.
- ISSA, L. L., LEONG, G. M. & EISMAN, J. A. 1998. Molecular mechanism of vitamin D receptor action. *Inflamm Res*, 47, 451-475.
- JONES, G., STRUGNELL, S. A. & DELUCA, H. F. 1998. Current understanding of the molecular actions of vitamin D. *Physiol Rev*, 78, 1193-231.

- KANDA, H., TATEYA, S., TAMORI, Y., KOTANI, K., HIASA, K.-I., KITAZAWA, R., KITAZAWA, S., MIYACHI, H., MAEDA, S., EGASHIRA, K. & KASUGA, M. 2006. MCP-1 contributes to macrophage infiltration into adipose tissue, insulin resistance, and hepatic steatosis in obesity. *J Clin Invest*, 116, 1494-1505.
- KETTANEH, A., HEUDE, B., ROMON, M., OPPERT, J. M., BORYS, J. M., BALKAU, B., DUCIMETIERE, P. & CHARLES, M. A. 2007. High plasma leptin predicts an increase in subcutaneous adiposity in children and adults. *Eur J Clin Nutr*, 61, 719-726.
- KHANAL, R. C. & NEMERE, I. 2007. The ERp57/GRp58/1,25D3-MARRS receptor: multiple functional roles in diverse cell systems. *Curr Med Chem*, 14, 1087-93.
- KOPECKY, J., CLARKE, G., ENERBACK, S., SPIEGELMAN, B. & KOZAK, L. P. 1995. Expression of the mitochondrial uncoupling protein gene from the aP2 gene promoter prevents genetic obesity. *J Clin Invest*, 96, 2914-23.
- KOPECKY, J., ROSSMEISL, M., HODNY, Z., SYROVY, I., HORAKOVA, M. & KOLAROVA, P. 1996. Reduction of dietary obesity in aP2-Ucp transgenic mice: mechanism and adipose tissue morphology. *Am J Physiol*, 270, E776-86.
- KOSTELI, A., SUGARU, E., HAEMMERLE, G., MARTIN, J. F., LEI, J., ZECHNER, R. & FERRANTE, A. W. 2010. Weight loss and lipolysis promote a dynamic immune response in murine adipose tissue. *J Clin Invest*, 120, 3466-3479.
- KRUG, M. S. & BERGER, S. L. 1987. First-strand cDNA synthesis primed with oligo(dT). *Methods Enzymol*, 152, 316-25.
- KYRIAKIS, J. M. 1999. Activation of the AP-1 transcription factor by inflammatory cytokines of the TNF family. *Gene Expr*, 7, 217-31.
- LARGE, V., PERONI, O., LETEXIER, D., RAY, H. & BEYLOT, M. 2004. Metabolism of lipids in human white adipocyte. *Diabetes Metab*, 30, 294-309.
- LIAO, X., SHARMA, N., KAPADIA, F., ZHOU, G., LU, Y., HONG, H., PARUCHURI, K., MAHABELESWAR, G. H., DALMAS, E., VENTECLEF, N., FLASK, C. A., KIM, J., DOREIAN, B. W., LU, K. Q., KAESTNER, K. H., HAMIK, A., CLEMENT, K. & JAIN, M. K. 2011. Kruppel-like factor 4 regulates macrophage polarization. *J Clin Invest*, 121, 2736-49.
- LIN, R. & WHITE, J. H. 2004. The pleiotropic actions of vitamin D. *Bioessays*, 26, 21-28.
- LIRA, F. S., ROSA, J. C., CUNHA, C. A., RIBEIRO, E. B., DO NASCIMENTO, C. O., OYAMA, L. M. & MOTA, J. F. 2011. Supplementing alpha-tocopherol (vitamin E) and vitamin D3 in high fat diet decrease IL-6 production in murine epididymal adipose tissue and 3T3-L1 adipocytes following LPS stimulation. *Lipids Health Dis*, 10, 37.



- LIRA, F. S., ROSA, J. C., CUNHA, C. A., RIBEIRO, E. B., DO NASCIMENTO, C. O., OYAMA, L. M. & MOTA, J. F. 2011. Supplementing alpha-tocopherol (vitamin E) and vitamin D3 in high fat diet decrease IL-6 production in murine epididymal adipose tissue and 3T3-L1 adipocytes following LPS stimulation. *Lipids Health Dis*, 10, 37.
- LORENTE-CEBRIÁN, S., ERIKSSON, A., DUNLOP, T., MEJHERT, N., DAHLMAN, I., ÅSTRÖM, G., SJÖLIN, E., WÄHLÉN, K., CARLBERG, C., LAURENCIKIENE, J., HEDÉN, P., ARNER, P. & RYDÉN, M. Differential effects of 1 $\alpha$ ,25-dihydroxycholecalciferol on MCP-1 and adiponectin production in human white adipocytes. *European Journal of Nutrition*, 1-8.
- LOSKUTOFF, D. J. & SAMAD, F. 1998. The Adipocyte and Hemostatic Balance in Obesity : Studies of PAI-1. *Arteriosclerosis, Thrombosis, and Vascular Biology*, 18, 1-6.
- LOWELL, B. B. & FLIER, J. S. 1997. Brown adipose tissue, beta 3-adrenergic receptors, and obesity. *Annu Rev Med*, 48, 307-16.
- LOWELL, B. B., V, S. S., HAMANN, A., LAWITTS, J. A., HIMMS-HAGEN, J., BOYER, B. B., KOZAK, L. P. & FLIER, J. S. 1993. Development of obesity in transgenic mice after genetic ablation of brown adipose tissue. *Nature*, 366, 740-2.
- LUMENG, C. N., BODZIN, J. L. & SALTIEL, A. R. 2007. Obesity induces a phenotypic switch in adipose tissue macrophage polarization. *J Clin Invest*, 117, 175-84.
- LUMENG, C. N., DEYOUNG, S. M., BODZIN, J. L. & SALTIEL, A. R. 2007. Increased Inflammatory Properties of Adipose Tissue Macrophages Recruited During Diet-Induced Obesity. *Diabetes*, 56, 16-23.
- MAEDA, K., OKUBO, K., SHIMOMURA, I., FUNAHASHI, T., MATSUZAWA, Y. & MATSUBARA, K. 1996. cDNA cloning and expression of a novel adipose specific collagen-like factor, apM1 (AdiPose Most abundant Gene transcript 1). *Biochem Biophys Res Commun*, 221, 286-289.
- MAEDA, N., SHIMOMURA, I., KISHIDA, K., NISHIZAWA, H., MATSUDA, M., NAGARETANI, H., FURUYAMA, N., KONDO, H., TAKAHASHI, M., ARITA, Y., KOMURO, R., OUCHI, N., KIHARA, S., TOCHINO, Y., OKUTOMI, K., HORIE, M., TAKEDA, S., AOYAMA, T., FUNAHASHI, T. & MATSUZAWA, Y. 2002. Diet-induced insulin resistance in mice lacking adiponectin/ACRP30. *Nat Med*, 8, 731-7.
- MAESTRO, B., CAMPION, J., DAVILA, N. & CALLE, C. 2000. Stimulation by 1,25-dihydroxyvitamin D3 of insulin receptor expression and insulin responsiveness for glucose transport in U-937 human promonocytic cells. *Endocr J*, 47, 383-91.
- MAESTRO, B., MOLERO, S., BAJO, S., DAVILA, N. & CALLE, C. 2002. Transcriptional activation of the human insulin receptor gene by 1,25-dihydroxyvitamin D(3). *Cell Biochem Funct*, 20, 227-232.

- MALLOY, P. J., PIKE, J. W. & FELDMAN, D. 1999. The vitamin D receptor and the syndrome of hereditary 1,25-dihydroxyvitamin D-resistant rickets. *Endocr Rev*, 20, 156-88.
- MANGELSDORF, D. J., THUMMEL, C., BEATO, M., HERRLICH, P., SCHUTZ, G., UMESONO, K., BLUMBERG, B., KASTNER, P., MARK, M., CHAMBON, P. & EVANS, R. M. 1995. The nuclear receptor superfamily: the second decade. *Cell*, 83, 835-9.
- MARTINI, L. A. & WOOD, R. J. 2006. Vitamin D status and the metabolic syndrome. *Nutr Rev*, 64, 479-486.
- MATSUNUMA, A. & HORIUCHI, N. 2007. Leptin attenuates gene expression for renal 25-hydroxyvitamin D3-1 $\alpha$ -hydroxylase in mice via the long form of the leptin receptor. *Arch Biochem Biophys*, 463, 118-27.
- MOHAMED-ALI, V., GOODRICK, S., RAWESH, A., KATZ, D. R., MILES, J. M., YUDKIN, J. S., KLEIN, S. & COPPACK, S. W. 1997. Subcutaneous adipose tissue releases interleukin-6, but not tumor necrosis factor- $\alpha$ , in vivo. *J Clin Endocrinol Metab*, 82, 4196-4200.
- MORRISON, S. F. 2004. Central Pathways Controlling Brown Adipose Tissue Thermogenesis. *Physiology*, 19, 67-74.
- MORRISON, S. F., NAKAMURA, K. & MADDEN, C. J. 2008. Central control of thermogenesis in mammals. *Experimental Physiology*, 93, 773-797.
- MRACEK, T., DING, Q., TZANAVARI, T., KOS, K., PINKNEY, J., WILDING, J., TRAYHURN, P. & BING, C. 2010. The adipokine zinc- $\alpha$ 2-glycoprotein (ZAG) is downregulated with fat mass expansion in obesity. *Clin Endocrinol (Oxf)*, 72, 334-41.
- NAKAMURA, K. & MORRISON, S. F. 2008. A thermosensory pathway that controls body temperature. *Nat Neurosci*, 11, 62-71.
- NECHAD, M. 1986. Brown Adipose Tissue. *Structure and development of brown adipose tissue.*, 1-30.
- NGUYEN, M. T. A., SATOH, H., FAVELYUKIS, S., BABENDURE, J. L., IMAMURA, T., SBODIO, J. I., ZALEVSKY, J., DAHIYAT, B. I., CHI, N.-W. & OLEFSKY, J. M. 2005. JNK and Tumor Necrosis Factor- $\alpha$  Mediate Free Fatty Acid-induced Insulin Resistance in 3T3-L1 Adipocytes. *Journal of Biological Chemistry*, 280, 35361-35371.
- NONOGAKI, K., FULLER, G. M., FUENTES, N. L., MOSER, A. H., STAPRANS, I., GRUNFELD, C. & FEINGOLD, K. R. 1995. Interleukin-6 stimulates hepatic triglyceride secretion in rats. *Endocrinology*, 136, 2143-9.

- O'HARA, A., LIM, F. L., MAZZATTI, D. J. & TRAYHURN, P. 2009. Microarray analysis identifies matrix metalloproteinases (MMPs) as key genes whose expression is up-regulated in human adipocytes by macrophage-conditioned medium. *Pflugers Arch*, 458, 1103-14.
- OPAL, S. M. & DEPALO, V. A. 2000. Anti-Inflammatory Cytokines\*. *Chest*, 117, 1162-1172.
- OPAL, S. M. & HUBER, C. E. 2000. The role of interleukin-10 in critical illness. *Curr Opin Infect Dis*, 13, 221-226.
- OSTMAN, J., ARNER, P., ENGFELDT, P. & KAGER, L. 1979. Regional differences in the control of lipolysis in human adipose tissue. *Metabolism*, 28, 1198-205.
- OUCHI, N., KIHARA, S., FUNAHASHI, T., MATSUZAWA, Y. & WALSH, K. 2003. Obesity, adiponectin and vascular inflammatory disease. *Curr Opin Lipidol*, 14, 561-566.
- PARIKH, S. J., EDELMAN, M., UWAIFO, G. I., FREEDMAN, R. J., SEMEGA-JANNEH, M., REYNOLDS, J. & YANOVSKI, J. A. 2004. The relationship between obesity and serum 1,25-dihydroxy vitamin D concentrations in healthy adults. *J Clin Endocrinol Metab*, 89, 1196-9.
- PEDERSEN, M., BRUUNSGAARD, H., WEIS, N., HENDEL, H. W., ANDREASSEN, B. U., ELDRUP, E., DELA, F. & PEDERSEN, B. K. 2003. Circulating levels of TNF-alpha and IL-6-relation to truncal fat mass and muscle mass in healthy elderly individuals and in patients with type-2 diabetes. *Mech Ageing Dev*, 124, 495-502.
- PEINADO, J. R., JIMENEZ-GOMEZ, Y., PULIDO, M. R., ORTEGA-BELLIDO, M., DIAZ-LOPEZ, C., PADILLO, F. J., LOPEZ-MIRANDA, J., VAZQUEZ-MARTINEZ, R. & MALAGON, M. M. 2010. The stromal-vascular fraction of adipose tissue contributes to major differences between subcutaneous and visceral fat depots. *Proteomics*, 10, 3356-66.
- PERMANA, P. A., MENGE, C. & REAVEN, P. D. 2006. Macrophage-secreted factors induce adipocyte inflammation and insulin resistance. *Biochem Biophys Res Commun*, 341, 507-14.
- PERSEGHIN, G., PETERSEN, K. & SHULMAN, G. I. 2003. Cellular mechanism of insulin resistance: potential links with inflammation. *Int J Obes Relat Metab Disord*, 27 Suppl 3, S6-11.
- POITOU, C., DIVOUX, A., FATY, A., TORDJMAN, J., HUGOL, D., AISSAT, A., KEOPHIPHATH, M., HENEGAR, C., COMMANS, S. & CLEMENT, K. 2009. Role of serum amyloid a in adipocyte-macrophage cross talk and adipocyte cholesterol efflux. *J Clin Endocrinol Metab*, 94, 1810-7.
- PONCHEL, F., TOOMES, C., BRANSFIELD, K., LEONG, F. T., DOUGLAS, S. H.,

- FIELD, S. L., BELL, S. M., COMBARET, V., PUISIEUX, A., MIGHELL, A. J., ROBINSON, P. A., INGLEHEARN, C. F., ISAACS, J. D. & MARKHAM, A. F. 2003. Real-time PCR based on SYBR-Green I fluorescence: an alternative to the TaqMan assay for a relative quantification of gene rearrangements, gene amplifications and micro gene deletions. *BMC Biotechnol*, 3, 18.
- PRUNET-MARCASSUS, B., COUSIN, B., CATON, D., ANDRE, M., PENICAUD, L. & CASTEILLA, L. 2006. From heterogeneity to plasticity in adipose tissues: site-specific differences. *Exp Cell Res*, 312, 727-36.
- RATHER, L. J. 1971. Disturbance of function (functio laesa): the legendary fifth cardinal sign of inflammation, added by Galen to the four cardinal signs of Celsus. *Bull N Y Acad Med*, 47, 303-22.
- REBUFFE-SCRIVE, M., ANDERSSON, B., OLBE, L. & BJORNTORP, P. 1989. Metabolism of adipose tissue in intraabdominal depots of nonobese men and women. *Metabolism*, 38, 453-8.
- REYNISDOTTIR, S., DAUZATS, M., THORNE, A. & LANGIN, D. 1997. Comparison of hormone-sensitive lipase activity in visceral and subcutaneous human adipose tissue. *J Clin Endocrinol Metab*, 82, 4162-6.
- RIORDAN, N. H., ICHIM, T. E., MIN, W. P., WANG, H., SOLANO, F., LARA, F., ALFARO, M., RODRIGUEZ, J. P., HARMAN, R. J., PATEL, A. N., MURPHY, M. P., LEE, R. R. & MINEV, B. 2009. Non-expanded adipose stromal vascular fraction cell therapy for multiple sclerosis. *J Transl Med*, 7, 29.
- RODBELL, M., BIRNBAUMER, L. & POHL, S. L. 1970. Adenyl cyclase in fat cells. 3. Stimulation by secretin and the effects of trypsin on the receptors for lipolytic hormones. *J Biol Chem*, 245, 718-22.
- ROTTER, V., NAGAEV, I. & SMITH, U. 2003. Interleukin-6 (IL-6) Induces Insulin Resistance in 3T3-L1 Adipocytes and Is, Like IL-8 and Tumor Necrosis Factor- $\alpha$ , Overexpressed in Human Fat Cells from Insulin-resistant Subjects. *Journal of Biological Chemistry*, 278, 45777-45784.
- RUAN, H., HACOHEN, N., GOLUB, T. R., VAN PARIJS, L. & LODISH, H. F. 2002. Tumor Necrosis Factor- $\alpha$  Suppresses Adipocyte-Specific Genes and Activates Expression of Preadipocyte Genes in 3T3-L1 Adipocytes. *Diabetes*, 51, 1319-1336.
- RYDÉN, M., DICKER, A., VAN HARMELEN, V., HAUNER, H., BRUNNBERG, M., PERBECK, L., LÖNNQVIST, F. & ARNER, P. 2002. Mapping of Early Signaling Events in Tumor Necrosis Factor- $\alpha$ -mediated Lipolysis in Human Fat Cells. *Journal of Biological Chemistry*, 277, 1085-1091.
- SALANS, L. B., HORTON, E. S. & SIMS, E. A. 1971. Experimental obesity in man:

cellular character of the adipose tissue. *J Clin Invest*, 50, 1005-11.

SARTIPY, P. & LOSKUTOFF, D. J. 2003. Expression profiling identifies genes that continue to respond to insulin in adipocytes made insulin-resistant by treatment with tumor necrosis factor-alpha. *J Biol Chem*, 278, 52298-52306.

SAVERIO, C. 2006. The role of brown adipose tissue in human obesity. *Nutrition, Metabolism and Cardiovascular Diseases*, 16, 569-574.

SCHÄFER, M. K. H., EIDEN, L. E. & WEIHE, E. 1998. Cholinergic neurons and terminal fields revealed by immunohistochemistry for the vesicular acetylcholine transporter. II. The peripheral nervous system. *Neuroscience*, 84, 361-376.

SCHLEITHOFF, S. S., ZITTERMANN, A., TENDERICH, G., BERTHOLD, H. K., STEHLE, P. & KOERFER, R. 2006. Vitamin D supplementation improves cytokine profiles in patients with congestive heart failure: a double-blind, randomized, placebo-controlled trial. *Am J Clin Nutr*, 83, 754-9.

SEALE, P., KAJIMURA, S. & SPIEGELMAN, B. M. 2009. Transcriptional control of brown adipocyte development and physiological function--of mice and men. *Genes Dev*, 23, 788-97.

SEUFERT, J. 2004. Leptin effects on pancreatic beta-cell gene expression and function. *Diabetes*, 53 Suppl 1, 152-158.

SHAPIRO, A. L., VINUELA, E. & MAIZEL, J. V., JR. 1967. Molecular weight estimation of polypeptide chains by electrophoresis in SDS-polyacrylamide gels. *Biochem Biophys Res Commun*, 28, 815-20.

SMITH, P. K., KROHN, R. I., HERMANSON, G. T., MALLIA, A. K., GARTNER, F. H., PROVENZANO, M. D., FUJIMOTO, E. K., GOEKE, N. M., OLSON, B. J. & KLENK, D. C. 1985. Measurement of protein using bicinchoninic acid. *Analytical Biochemistry*, 150, 76-85.

SNIJDER, M. B., VAN DAM, R. M., VISSER, M., DEEG, D. J., DEKKER, J. M., BOUTER, L. M., SEIDELL, J. C. & LIPS, P. 2005. Adiposity in relation to vitamin D status and parathyroid hormone levels: a population-based study in older men and women. *J Clin Endocrinol Metab*, 90, 4119-23.

SONG, M. J., KIM, K. H., YOON, J. M. & KIM, J. B. 2006. Activation of Toll-like receptor 4 is associated with insulin resistance in adipocytes. *Biochem Biophys Res Commun*, 346, 739-45.

SPALDING, K. L., ARNER, E., WESTERMARK, P. O., BERNARD, S., BUCHHOLZ, B. A., BERGMANN, O., BLOMQVIST, L., HOFFSTEDT, J., NASLUND, E., BRITTON, T., CONCHA, H., HASSAN, M., RYDEN, M., FRISEN, J. & ARNER, P. 2008. Dynamics of fat cell turnover in humans. *Nature*, 453, 783-787.

- SUGANAMI, T., NISHIDA, J. & OGAWA, Y. 2005. A Paracrine Loop Between Adipocytes and Macrophages Aggravates Inflammatory Changes. *Arteriosclerosis, Thrombosis, and Vascular Biology*, 25, 2062-2068.
- SUGANAMI, T., TANIMOTO-KOYAMA, K., NISHIDA, J., ITOH, M., YUAN, X., MIZUARAI, S., KOTANI, H., YAMAOKA, S., MIYAKE, K., AOE, S., KAMEI, Y. & OGAWA, Y. 2007. Role of the Toll-like receptor 4/NF-kappaB pathway in saturated fatty acid-induced inflammatory changes in the interaction between adipocytes and macrophages. *Arterioscler Thromb Vasc Biol*, 27, 84-91.
- SUN, X. & ZEMEL, M. B. 2008. Calcitriol and calcium regulate cytokine production and adipocyte-macrophage cross-talk. *The Journal of Nutritional Biochemistry*, 19, 392-399.
- SUZAWA, M., TAKADA, I., YANAGISAWA, J., OHTAKE, F., OGAWA, S., YAMAUCHI, T., KADOWAKI, T., TAKEUCHI, Y., SHIBUYA, H., GOTOH, Y., MATSUMOTO, K. & KATO, S. 2003. Cytokines suppress adipogenesis and PPAR-[gamma] function through the TAK1/TAB1/NIK cascade. *Nat Cell Biol*, 5, 224-230.
- TABATA, T., MINE, S., KAWAHARA, C., OKADA, Y. & TANAKA, Y. 2003. Monocyte chemoattractant protein-1 induces scavenger receptor expression and monocyte differentiation into foam cells. *Biochem Biophys Res Commun*, 305, 380-5.
- TCHERNOF, A., BELANGER, C., MORISSET, A. S., RICHARD, C., MAILLOUX, J., LABERGE, P. & DUPONT, P. 2006. Regional differences in adipose tissue metabolism in women: minor effect of obesity and body fat distribution. *Diabetes*, 55, 1353-60.
- TIMMS, P. M., MANNAN, N., HITMAN, G. A., NOONAN, K., MILLS, P. G., SYNDERCOMBE-COURT, D., AGANNA, E., PRICE, C. P. & BOUCHER, B. J. 2002. Circulating MMP9, vitamin D and variation in the TIMP-1 response with VDR genotype: mechanisms for inflammatory damage in chronic disorders? *QJM*, 95, 787-796.
- TOWBIN, H., STAEHELIN, T. & GORDON, J. 1979. Electrophoretic transfer of proteins from polyacrylamide gels to nitrocellulose sheets: procedure and some applications. *Proc Natl Acad Sci U S A*, 76, 4350-4.
- TRAYHURN, P. 2007. Adipocyte biology. *Obes Rev*, 8 Suppl 1, 41-4.
- TRAYHURN, P. & BING, C. 2006. Appetite and energy balance signals from adipocytes. *Philosophical Transactions of the Royal Society B: Biological Sciences*, 361, 1237-1249.
- TRAYHURN, P., BING, C. & WOOD, I. S. 2006. Adipose Tissue and Adipokines—Energy Regulation from the Human Perspective. *The Journal of Nutrition*, 136, 1935S-1939S.
- TRAYHURN, P. & WOOD, I. S. 2005. Signalling role of adipose tissue: adipokines and

inflammation in obesity. *Biochem Soc Trans*, 33, 1078-81.

TRIPATHY, D., MOHANTY, P., DHINDSA, S., SYED, T., GHANIM, H., ALJADA, A. & DANDONA, P. 2003. Elevation of free fatty acids induces inflammation and impairs vascular reactivity in healthy subjects. *Diabetes*, 52, 2882-7.

TRUJILLO, M. E., SULLIVAN, S., HARTEN, I., SCHNEIDER, S. H., GREENBERG, A. S. & FRIED, S. K. 2004. Interleukin-6 regulates human adipose tissue lipid metabolism and leptin production in vitro. *J Clin Endocrinol Metab*, 89, 5577-82.

VAN DEN BERGHE, G., VAN ROOSBROECK, D., VANHOVE, P., WOUTERS, P. J., DE POURCQ, L. & BOUILLON, R. 2003. Bone Turnover in Prolonged Critical Illness: Effect of Vitamin D. *Journal of Clinical Endocrinology & Metabolism*, 88, 4623-4632.

VANDEN BERGHE, W., PLAISANCE, S., BOONE, E., DE BOSSCHER, K., SCHMITZ, M. L., FIERS, W. & HAEGEMAN, G. 1998. p38 and extracellular signal-regulated kinase mitogen-activated protein kinase pathways are required for nuclear factor-kappaB p65 transactivation mediated by tumor necrosis factor. *J Biol Chem*, 273, 3285-90.

VEGIOPOULOS, A., MÜLLER-DECKER, K., STRZODA, D., SCHMITT, I., CHICHELNITSKIY, E., OSTERTAG, A., DIAZ, M. B., ROZMAN, J., HRABE DE ANGELIS, M., NÜSING, R. M., MEYER, C. W., WAHLI, W., KLINGENSPOR, M. & HERZIG, S. 2010. Cyclooxygenase-2 Controls Energy Homeostasis in Mice by de Novo Recruitment of Brown Adipocytes. *Science*, 328, 1158-1161.

WALTERS, M. R. 1992. Newly identified actions of the vitamin D endocrine system. *Endocr Rev*, 13, 719-64.

WANG, B., JENKINS, J. R. & TRAYHURN, P. 2005. Expression and secretion of inflammation-related adipokines by human adipocytes differentiated in culture: integrated response to TNF-alpha. *Am J Physiol Endocrinol Metab*, 288, E731-40.

WANG, T. T., NESTEL, F. P., BOURDEAU, V., NAGAI, Y., WANG, Q., LIAO, J., TAVERA-MENDOZA, L., LIN, R., HANRAHAN, J. W., MADER, S. & WHITE, J. H. 2004. Cutting edge: 1,25-dihydroxyvitamin D3 is a direct inducer of antimicrobial peptide gene expression. *J Immunol*, 173, 2909-12.

WEISBERG, S. P., HUNTER, D., HUBER, R., LEMIEUX, J., SLAYMAKER, S., VADDI, K., CHARO, I., LEIBEL, R. L. & FERRANTE, A. W. 2006. CCR2 modulates inflammatory and metabolic effects of high-fat feeding. *J Clin Invest*, 116, 115-124.

WEISBERG, S. P., MCCANN, D., DESAI, M., ROSENBAUM, M., LEIBEL, R. L. & FERRANTE, A. W., JR. 2003. Obesity is associated with macrophage accumulation in adipose tissue. *J Clin Invest*, 112, 1796-808.

WELLEN, K. E. & HOTAMISLIGIL, G. S. 2003. Obesity-induced inflammatory

changes in adipose tissue. *J Clin Invest*, 112, 1785-1788.

WELLEN, K. E. & HOTAMISLIGIL, G. S. 2005. Inflammation, stress, and diabetes. *J Clin Invest*, 115, 1111-9.

WEN, H., GRIS, D., LEI, Y., JHA, S., ZHANG, L., HUANG, M. T., BRICKEY, W. J. & TING, J. P. 2011. Fatty acid-induced NLRP3-ASC inflammasome activation interferes with insulin signaling. *Nat Immunol*, 12, 408-15.

XU, H., BARNES, G. T., YANG, Q., TAN, G., YANG, D., CHOU, C. J., SOLE, J., NICHOLS, A., ROSS, J. S., TARTAGLIA, L. A. & CHEN, H. 2003. Chronic inflammation in fat plays a crucial role in the development of obesity-related insulin resistance. *J Clin Invest*, 112, 1821-1830.

YAMASHITA, A., SOGA, Y., IWAMOTO, Y., YOSHIZAWA, S., IWATA, H., KOKEGUCHI, S., TAKASHIBA, S. & NISHIMURA, F. 2007. Macrophage-adipocyte interaction: marked interleukin-6 production by lipopolysaccharide. *Obesity (Silver Spring)*, 15, 2549-52.

YEOP HAN, C., KARGI, A. Y., OMER, M., CHAN, C. K., WABITSCH, M., O'BRIEN, K. D., WIGHT, T. N. & CHAIT, A. 2010. Differential effect of saturated and unsaturated free fatty acids on the generation of monocyte adhesion and chemotactic factors by adipocytes: dissociation of adipocyte hypertrophy from inflammation. *Diabetes*, 59, 386-96.

ZEHNDER, D., BLAND, R., WILLIAMS, M. C., MCNINCH, R. W., HOWIE, A. J., STEWART, P. M. & HEWISON, M. 2001. Extrarenal expression of 25-hydroxyvitamin d(3)-1 alpha-hydroxylase. *J Clin Endocrinol Metab*, 86, 888-94.

ZEYDA, M., FARMER, D., TODORIC, J., ASZMANN, O., SPEISER, M., GYORI, G., ZLABINGER, G. J. & STULNIG, T. M. 2007. Human adipose tissue macrophages are of an anti-inflammatory phenotype but capable of excessive pro-inflammatory mediator production. *Int J Obes (Lond)*, 31, 1420-8.

ZEYDA, M. & STULNIG, T. M. 2007. Adipose tissue macrophages. *Immunol Lett*, 112, 61-67.

ZHANG, Z., YUAN, W., SUN, L., SZETO, F. L., WONG, K. E., LI, X., KONG, J. & LI, Y. C. 2007. 1,25-Dihydroxyvitamin D3 targeting of NF-[kappa]B suppresses high glucose-induced MCP-1 expression in mesangial cells. *Kidney Int*, 72, 193-201.

ZHONG, H., VOLL, R. E. & GHOSH, S. 1998. Phosphorylation of NF-kappa B p65 by PKA stimulates transcriptional activity by promoting a novel bivalent interaction with the coactivator CBP/p300. *Mol Cell*, 1, 661-71.

ZHU, J., YONG, W., WU, X., YU, Y., LV, J., LIU, C., MAO, X., ZHU, Y., XU, K. & HAN, X. 2008. Anti-inflammatory effect of resveratrol on TNF-alpha-induced MCP-1



expression in adipocytes. *Biochem Biophys Res Commun*, 369, 471-7.

ZIPPER, H., BRUNNER, H., BERNHAGEN, J. & VITZTHUM, F. 2004. Investigations on DNA intercalation and surface binding by SYBR Green I, its structure determination and methodological implications. *Nucleic Acids Res*, 32, e103.